FUNCTIONAL CHARACTERIZATION OF GENE PRODUCTS MEDIATING SH4-DOMAIN-DEPENDENT PROTEIN TARGETING

Referees:

Prof. Dr. Walter Nickel

Prof. Dr. Thomas Söllner

"Auch eine Enttäuschung, wenn sie nur gründlich und endgültig ist, bedeutet einen Schritt vorwärts."

Max Planck

DISSERTATION

submitted to the
Combined Faculties for the Natural Sciences and for Mathematics
of the Ruperto Carola University of Heidelberg, Germany
for the degree of Doctor of Natural Sciences

Presented by
Diplom Biologin
Tao Wang
Born in Tianjin, China

Oral examination

LIST OF PUBLICATIONS

Ritzerfeld, J., Remmele, S., Wang, T., Temmerman, K., Brügger, B., Wegehingel, S., Tournaviti, S., Strating, JR., Wieland, FT., Newmann, B., Ellenberg, J., Lawerenz, C., Hesser, J., Erfle,H., Pepperkok, R., Nickel, W. (2011). Phenotypic profiling of the human genome reveals gene products involved in plasma membrane targeting of SRC kinases Genome Res. 21:1955-1968.

Table of Contents

Summary

Src proteins are non-receptor tyrosine kinases, which are known to play crucial roles in regulating cell proliferation and differentiation. They localize at the cytoplasmic face of the plasma membrane mediated by a dual lipid modification of their N-terminal SH4 domains. Appreciable amounts of Src kinases are also found in intracellular compartments such as late endosomes, lysosomes and the Golgi apparatus. The lipid modifications of SH4 domains are both necessary and sufficient to mediate targeting of Src kinases to the inner leaflet of plasma membranes. However, the underlying mechanisms by which SH4-domain-containing proteins are transported to the plasma membrane are poorly understood. A genome-wide analysis to identify factors involved in SH4-domain-dependent protein targeting was carried out in a previous study of our laboratory by using an automated microscopy platform. We were able to identify proteins involved in lipid metabolism, intracellular transport and also cellular signaling processes. The goal of the current study was to validate and functionally characterize a subset of theses gene products. We were able to show that β-COP, a component of the heptameric coatomer complex, plays an important role in SH4-dependent protein transport. Likewise, we demonstrated a requirement for protein kinase C activity in correct targeting of SH4 proteins to the plasma membrane. Further, the findings on mevalonate pyrophosphate decarboxylase (MVD) corroborate the role of cholesterol-dependent membrane microdomains in the plasma-membrane targeting of SH4 proteins. Finally, we challenged the hypothesis that nedd8-activating enzyme 1 (NAE1) or a functional neddylation pathway is required for correct targeting of SH4-proteins. Employing both RNA interference and dominant negative constructs of components involved in the neddylation pathway as well as a pharmacological inhibitor of NAE1, we were able to confirm a role of NAE1 in the proper intracellular targeting of SH4-YES; however, a functional neddylation pathway is not essential for this process. Hence, NAE1 may have a distinct function other than neddylation in the transport of SH4 proteins. These findings pave the way for future investigations on the underlying molecular mechanism for the targeting of SH4-domain containing proteins to the inner leaflet of the plasma membrane.

Zusammenfassung

Src Kinasen spielen eine zentrale Rolle in intrazellulären Signaltransduktionsprozessen, und sind so an verschiedenen zellulären Prozessen, wie Zellproliferation und -differenzierung, beteiligt. Dabei ist ihre subzelluläre Lokalisierung für die funktionelle Interaktion mit anderen Proteinen von zentraler Bedeutung. Die stabile Assoziation mit Membranen wird durch eine N-terminale SH4-Domäne vermittelt, die über eine duale Lipidmodifikation an der zytoplasmatischen Seite der Plasmamembran verankert ist. Die erste Modifikation ist dabei eine Myristoylierung, welche eine transiente Interaktion mit intrazellulären Membrankompartimenten vermittelt und die Voraussetzung für eine darauffolgende Palmitoylierung ist. Diese zweite Modifikation bewirkt nicht nur eine stabile Membranverankerung, sondern begünstigt auch eine Anreicherung von SH4-domänenhaltigen Proteinen in cholesterinreichen Membranmikrodomänen. Diese Assoziation findet vermutlich schon auf der Ebene intrazellulärer Kompartimente, z.B. im Golgi-Apparat, statt und könnte für eine Sortierung zur Plasmamembran erforderlich sein. Der molekulare Mechanismus, der dem mikrodomänenabhängigen Transport von SH4-Proteinen vom Golgi-Apparat zur Plasmamembran zugrundeliegt ist jedoch nichtbekannt. In einer vorausgehenden Studie unseres Labors wurde eine genomweite Analyse durchgeführt um molekulare Komponenten zu ermitteln, die am SH4-abhängigen Transport zur Plasmamembran beteiligt sind. Hierbei wurden unter anderem Proteine identifiziert, die an der Lipidhomeostase, im intrazellulären Transport und an zellulären Signaltransduktionswegen beteiligt sind.
Ziel der vorliegenden Studie war es, die Rolle dieser Faktoren im intrazellulären Transport von acylierten Proteinen zu bestätigen und funktionell näher zu charakterisieren. Wir konnten zeigen, dass der heptamere Coatomer-Komplex, sowie die Aktivität der Proteinkinase C für eine erfolgreiche Sortierung von SH4-Proteinen zur Plasmamembran erforderlich ist. Darüber hinaus wurde eine potentielle Beteiligung von Membranmikrodomänen am SH4-abhängigen Transport durch die Beobachtung untermauert, dass Änderungen der zellulären Cholesterinmenge mit einer intrazellulären Anreicherung acylierter Proteine einhergehen. Abschließend untersuchten wir, ob Nedd8-activating enzyme 1 (NAE1), eine Komponente des zellulären Neddylierungsweges, sowie eine funktionelle Neddylierung für den Transport von SH4-Proteinen zur Plasmamembran erforderlich sind. Mithilfe von RNA Interferenz und dominant-negativen Mutanten von Komponenten des Neddylierungsweges, sowie eines spezifischen Inhibitors von NAE1 konnten wir bestätigen, dass NAE1 für eine erfolgreiche Sortierung der SH4-Domäne der Src Kinase Yes erforderlich ist. Eine funktionelle zelluläre Neddylierungsmachschinerie ist jedoch keine essentielle Voraussetzung für diesen Prozess. Diese Beobachtung deutet darauf hin, dass NAE1 eine weitere, bisher unbekannte Funktion in der Sortierung von Src Kinase besitzt, die unabhängig vom Prozess der Neddylierung ist.

1 Introduction

Cells are the fundamental units of life, building up all living organisms. The biological universe consists of two types of cells: 1) prokaryotic cells which consist of a single compartment surrounded by the plasma membrane and lack a defined nucleus. 2) eukaryotic cells containing a defined membrane-bound nucleus and internal membranes that enclose the organelles. These internal membranes further subdivide the cell into different compartments, which differ from each other in terms of such as acidity and protein compositions and also their functions. To maintain their diverse functions, cells need to enrich the proteins selectively in different compartments. The distribution of newly synthesized proteins is mediated by the biosynthetic/secretory pathway. Along the secretory pathway, the transport between different organelles is mediated by coated vesicles, which contain not only soluble and membrane-bound proteins but also lipids. For a long time proteins were considered as the key factor for trafficking events whereas lipid were regarded as a passive solvent. Introducing the lipid raft concept in 1997, it was postulated that the assemblies of cholesterol-sphingolipid-proteins so called lipid rafts are important for protein delivery to the cell surface in many cell types. Doubly acylated proteins like Src-family kinases with raft affinity are probably also transported in a lipid-raft dependent way to the plasma membrane. So far, our knowledge remains poor with regards to the underlying molecular mechanism.

1.1 PROTEIN SECRETION AND ENDOCYTOSIS

1.1.1 Classical protein secretion

Most eukaryotic secretory proteins travel through the highly specialized ER/Golgi system to reach the plasma membrane or the extracellular environment. The ER exists in two different forms; the rough ER and the smooth ER (Borgese et al., 1974; Jones and Fawcett, 1966). Rough ER contains membrane-bound ribosomes where proteins are synthesized and translocated into the ER. These proteins are destined for lysosomes, for export or for transport to the plasma membrane (Borgese et al., 1974; Jones and Fawcett,

1966; Rapoport, 1992). A signal sequence on the nascent protein directs ribosomes to the ER membrane when a protein is translated on ribosome with an ER signal sequence (Blobel and Dobberstein, 1975a; Blobel and Dobberstein, 1975b; Rapoport, 1992; Walter et al., 1984; Wei and Hendershot, 1996). The signal recognition particle (SRP) present in the cytosol binds to the ER signal sequence and the ribosome. Through this interaction, the polypeptide elongation is slowed down (Keenan et al., 2001). Following dissociation of SRP and SRP receptor the ribosome is transferred to the translocation channel (Gilmore et al., 1982; Gorlich et al., 1992), protein synthesis continues and the nascent polypeptide is threaded through the channel and into the lumen of the ER (Corsi and Schekman, 1996). During translocation the signal sequence is cleaved off by a signal peptidase and released from the translocation channel and then degraded to amino acids (Blobel and Dobberstein, 1975a; Blobel and Dobberstein, 1975b; Dalbey and Von Heijne, 1992). Within the ER, chaperones help the newly synthesized protein in reaching its proper folding (Wei and Hendershot, 1996). Further processing includes the building of disulfide bonds, N- and O-glycosylation, oligomerization, proteolytic cleavage and other post-translational modifications (Ma and Hendershot, 2004). Misfolded or misprocessed proteins may be retained in the ER and later transported to the cytosol for degradation by the proteasome (Nishikawa et al., 2005). Correctly folded polypeptides are package into vesicles and transported to the Golgi, an organelle consist of cis-, medial- and trans-cisternae (Glick, 2000). Proteins enter the Golgi at the cis compartment and exit at the trans compartment. After proteins that arrive in the trans-Golgi network, they are transported to the plasma membrane in vesicles and can be released into the extracellular space.

Concerning the intra-Golgi transport, two models exist: the first model “cisternal maturation” proposes that cargo remains in a given compartment and different enzymes arrive there to convert a cis cisterna into a medial one, a medial cisterna into a trans cisterna (Mellman and Simons, 1992; Mironov et al., 2005). Alternatively, the second model proposes that the cargo moves from one Golgi compartment to the next, encountering different enzymes in each subsequent compartment until it reaches trans cisterna (Mellman and Simons, 1992; Warren and Malhotra, 1998). This second model could use vesicles to transport cargo from one compartment to the next.

The COPII (coat containing complex II) machinery mediates cargo acquisition and is responsible for anterograde transport from the ER to the Golgi system (Barlowe, 1998; Lee et al., 2004; Rothman and Orci, 1992; Rothman and Warren, 1994). Small GTPase secretion-associated and Ras-related protein 1 (Sar1) initiates the recruitment of components and also the vesicle formation of COPII (Barlowe, 1998). Sar1-GTP recruits two cytosolic complexes the Sec23-Sec24 heterodimer and this complex interacts with cargo proteins via specific sorting signals (Matsuoka et al., 1998). This complex then recruits the Sec13-31 heterotetramer leading to polymerization and membrane deformation to form a COPII vesicle (Schekman and Orci, 1996). The exact nature of the interaction between Sec13-31 and Sec 23-24 is not known, however, Sec13-31 is probably providing a structural scaffold to crosslink Sec23-24 complexes, forming a coat lattice that propagates membrane curvature (Lee et al., 2004). After budding, the COPII vesicle sheds its coat, allowing its membrane to interact directly with the target membrane (Barlowe, 1998).

In addition to COPII-coated-vesicles, COPI (coat containing complex I) coated vesicles handle the retrograde transport from Golgi back to the ER and as well as both anterograde and retrograde transport within the Golgi stacks (Cosson and Letourneur, 1994; Letourneur et al., 1994; Nickel et al., 2002; Orci et al., 1997; Sonnichsen et al., 1996). COPI coat assembly is initiated by GDP-GTP exchange onto the small GTPase ADP-ribosylation factor 1 (Arf1) (Peyroche et al., 1996). Membrane-bound Arf1 recruits coatomer complex, which is consistent of seven subunits: the α/β′/ε complex and the β/γ/δ/ζ complex to the p24 family at the membrane (Bonifacino, 2004; Pavel et al., 1998). After the formation of a COPI-coated vesicle, the coat must be shed to allow for vesicle fusion with the target membrane (Beck et al., 2009). The uncoating step depends on GTP hydrolysis by Arf1, catalyzed by Arf1 GTPase-activating proteins (ArfGAPs) (Tanigawa et al., 1993). Membrane curvature might facilitate the recruitment of ArfGAPs and subsequent dissociation from the membrane (Goldberg, 1998; Goldberg, 1999). Brefeldin A, a fungal toxin which stabilizes the Arf in GDP-bound state and inhibits the recruitment of COPI on the Golgi membrane and further blocks the classical secretory pathway (Kirchhausen, 2000; Mossessova et al., 2003; Robineau et al., 2000; Schmid, 1997; Zhao et al., 1999).

Following vesicle formation the coat is released, SNARES (Soluble N-ethylamaleimide sensitive factor attachment protein receptor) (Bock et al., 2001; Clague, 1999; Rothman and Warren, 1994; Sollner and Rothman, 1996; Whyte and Munro, 2002) together with Rab family of GTPase and tethering factors ensure vesicle fusion with the target organelle (Novick and Zerial, 1997; Schimmoller et al., 1998b; Zerial and McBride, 2001b; Zhao et al., 1999). Cognate v- and t-SNAREs recognize and form a coiled-coil trans-SNARE complex that brings the membranes close and drives the fusion process (Hanson et al., 1997; Rothman and Warren, 1994; Sollner et al., 1993; Sollner and Rothman, 1996). Following the fusion event, the cis-SNARE complex is disassembled by the recruitment through SNAPs (soluble NSF attachment protein) of the ATPase NSF (N-thylmaleimide-sensitive fusion protein), which disassembles the SNAREpin and primes the membrane for another fusion event (Malsam et al., 2008; Zhao et al., 2007).

TGN acts as the main sorting station of proteins and lipids. Sophisticated sorting machinery mediates cargo delivery to the plasma membrane, endosomal compartments and specialized compartments in diverse cell types. Clathrin-coated vesicles mediate the transport between the TGN and endosomes (Le Borgne and Hoflack, 1998a; Le Borgne and Hoflack, 1998b). Transport to the plasma membrane is mediated by the formation of large pleiomorphic carriers (LPCs) that is microtubules-dependent for the transport to their final destination (De Matteis and Luini, 2008; Luini et al., 2005). Apart from post-translational modifications like glycosylation, the affinity of proteins to microdomains has an impact on sorting to the apical plasma membrane (Paladino et al., 2004; Schuck and Simons, 2004; Simons and van Meer, 1988). Sorting and transport machinery components and membrane material from the endosomal system and PM are recycled back to the TGN (De Matteis and Luini, 2008).

1.1.2 Endocytosis

Endocytic membrane traffic in mammalian cells has an important role in recycling membrane components, ligands and molecules to various intracellular destinations. There are several ways for internalizing molecules from the cell surface. Receptor-mediated endocytosis involving the internalization of receptors and their ligands by clathrin-coated pits is most well studied and is characterized by high selectivity served by specific

trafficking motifs. Tyrosine-based motif, dileucine-based motif, NPXY and mono-/multi-ubiquitination have been shown to direct clathrin-dependent endocytosis (Mousavi et al., 2004). Adaptor proteins (AP) recognize both, these motifs and clathrin, bring them together, and initiate the creation of clathrin coat pits. AP-2 has been found to associate with tyrosine-based and di-leucine-based motifs, as well as with NPXY motifs. Adaptor proteins like epsin and EGFR pathway substrate clone 15 (Eps15) have been shown to bind to the ubiquitin moiety of cargo proteins. Clathrin-coated pits are dispatched and, upon fission mediated by GTPase dynamin, form clathrin-coated vesicles (Conner and Schmid, 2003). Subsequently, they undergo homotypic fusion and further fuse with sorting endosomes. From sorting endosomes, the cargo protein can follow two distinct routes: either to be recycled back to the plasma membrane directly or indirectly through recycling endosomes and/or TGN; or to enter the degradation pathway leading to lysosomes as a final destination (Maxfield and McGraw, 2004). Endosomal recycling is controlled by small Rab GTPases that act as molecular switches mediating trafficking between the various endosomal compartments. Rab4, Rab5 and Rab7 as well as Rab11 have been localized to single endosomes where they segregate to distinct regions of the membrane and then define specific functional membrane domains (Sonnichsen et al., 2000). More specifically, Rab4 seems to have a role in recycling membrane from the sorting endosomes, which perhaps includes direct recycling to the plasma membrane. Rab5 mediates the homotypic fusion between endocytic vesicles and the fusion between endocytic vesicles and sorting endosomes. Rab11 plays a role in recycling *via* recycling endosomes. Rab7 takes part in the pathway leading to late endosomes (Schimmoller et al., 1998a; Somsel Rodman and Wandinger-Ness, 2000; Zerial and McBride, 2001a).

1.2 ACYLATION AND THEIR EFFECTS ON PROTEIN TARGETING

1.2.1 Acylation

1.2.1.1 N-Myristoylation

N-myristoylation describes the addition of myristate (C14:0) to a N-terminal glycine residue, which happens cotranslationally while the nascent polypeptide chain is still

attaching the ribosome (Deichaite et al., 1988). The consensus sequence for N-myristoyl transferase (NMT) protein substrate is: (M**G**XXXS/T). The initial methionine is cleaved cotranslationally by methionine amino-peptidase and myristate is linked to gly2 via an amide bond. Many N-myristoylated proteins are membrane associated and can be found either at the plasma membrane or at intracellular membranes in eukaryotic cells. A mutation of Gly2 to Ala prevents myristoylation and inhibits membrane binding showing the absolute requirement for Gly at the N-terminus. However myristoylation alone is in most cases not sufficient for a stable membrane binding (Deichaite et al., 1988). According to the two-signal model for membrane binding of myristoylated proteins, a second signal for membrane binding, either a polybasic cluster of amino acids or a palmitate moiety, is required (Figure 1) (Resh, 1994). For the first model 'myristate plus basic', myristate inserts hydrophobically into the lipid bilayer and basic amino acids interact electrostatically with the headgroups of acidic phospholipids. This mechanism mediates stable membrane association of the non-receptor tyrosine kinase Src (Silverman and Resh, 1992). With an exception of Src itself, the stable membrane association of the other Src family kinases are mediated by a `myristate + palmitate´ signal (Resh, 1994).

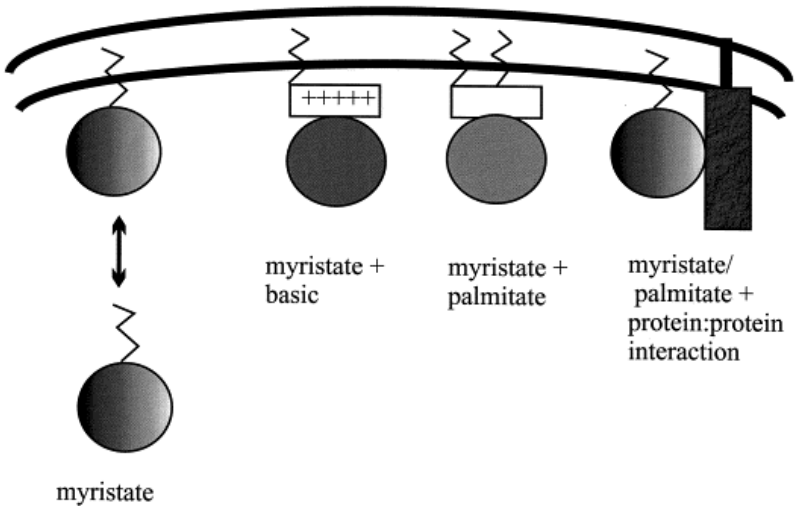

Figure 1 The two-signal model for membrane binding of myristoylated proteins. Membrane anchoring of myrisotylate proteins is stabilized by second membrane-binding signal, e.g. electrostatic interactions (myristate + basic) or a second acylation (myristate + palmitate) as well as interaction with membrane-bound proteins (myristate/palmitate + protein:protein interaction) (from Resh, 1990).

Since myristoylation alone is not sufficient for a stable membrane binding, myristoylation provides the opportunity of reversible membrane attachment. The MARCKS protein is a

protein kinase C (PKC) substrate and its membrane binding is regulated by a myristoyl electrostatic switch (McLaughlin and Aderem, 1995). Phosphorylation of MARCKS by PKC results in additional negative charges into the positively charged region. This leads to the reduction of the electrostatic interactions with acidic phospholipids and results in dissociation of MARCKS from the membrane and into the cytosol (Resh, 1999). Another potential example for a myristoyl-electrostatic switch is Src. The myristoylated SH4 domain of Src contains phosphorylation sites by PKC and PKA. Phosphorylation of either site reduces the partitioning of Src onto lipid bilayers. However, translocation of Src from the membrane to the cytosol upon phosphorylation has not been consistently demonstrated (Murray et al., 1998; Resh, 1994; Walker et al., 1993).

1.2.1.2 S-Palmitoylation

S-palmitoylation describes the reversible attachment of palmitate (C16:0) to cysteine residues via a labile thioester bond. Protein palmitoylation has been shown to have a role in protein-membrane interactions, protein trafficking and enzyme activity. However, the underlying molecular machinery for reversible palmitoylation of proteins is not well known so far. Compared to N-myristoylation no strict consensus sequence is needed for palmitoylation, however, palmitoylated cysteine residues share some characteristics like a) they are close to myristoylation or prenylation sites b) they are frequently located in cytoplasmic regions flanking transmembrane domains (Salaun et al., 2010). Studies from yeast showed that some palmitoylated yeast proteins display a marked dependence on a specific DHHC (aspartate-histidine-histidine-cysteine) protein. However those studies also reveal that some DDHC proteins have overlapping substrate specificities which is in accordance with studies in mammalian systems showing that specific substrates can be palmitoylated by more than one DHHC protein (Fang et al., 2006; Fukata et al., 2004; Greaves et al., 2010; Shmueli et al., 2010; Tsutsumi et al., 2009). There are about 23 putative S-palmitoyl transfereases in mammals. The large number of these DHHC proteins coupled with their localization to distinct membrane compartments (Ohno et al., 2006) suggests that the palmitoylation machinery is a highly regulated and coordinated system (Salaun et al., 2010).

The question whether palmitoylation of newly synthesized peripheral proteins is a Golgi-specific event is largely discussed. If it is so, specific palmitoylation at the Golgi might be an important prerequisite for the targeting to the plasma membrane. Recent studies took advantage of microinjection of semisynthetic N-Ras to study real-time spatiotemporal dynamics of palmitoylation (Rocks et al., 2010; Rocks et al., 2005). Immediately after microinjection, farnesylated N-Ras displayed a dispersed localization and followed by a rapid enrichment of the Cy3-labeled construct, which became apparent at the Golgi with plasma membrane staining visible at later time points (Rocks et al., 2010). The simplest explanation is that palmitoylation of the farnesylated N-Ras occurs at the Golgi, leading to accumulation at this compartment and further to the plasma membrane by anterograde transport (Rocks et al., 2010). Further, it was shown by using low temperature to block vesicular transport along the secretory pathway, Fyn, TC10, R-Ras and RhoB as well as Rap2C all displayed colocalization with a Golgi marker (Rocks et al., 2010). These observations imply that the Golgi may be a specialized reaction center for the palmitoylation of all newly synthesized peripheral proteins (Salaun et al., 2010). Rocks et al. (2010) argued against DHHC substrate specificity and suggested there was also not an essential DHHC recognition domain in the remainder of the Ras protein, meaning the major requirement for palmitoylation was a suitable cysteine residue in close membrane proximity. However, this idea is not consistent with previous studies on the feature of DHHC proteins and substrate proteins that contribute to the specificity of interaction (Greaves et al., 2010; Greaves et al., 2009a; Huang et al., 2009; Nadolski and Linder, 2009). Indeed, the depletion of a single DHHC protein ERF2 affected the palmitoylation of yeast Ras (Bartels et al., 1999; Roth et al., 2006). This inconsistency still needs to be further investigated.

Function of Palmitoylation

Palmitoylation often couples with other lipid modification to regulate membrane associations of soluble proteins. N-myristoylation or prenylation provides a degree of hydrophobicity leading to a transient membrane interaction due to single lipid modifications (Shahinian and Silvius, 1995). An additional palmitoylation, promotes and stabilizes membrane attachment (Shahinian and Silvius, 1995). Thus, at cellular level, the

access to membrane bound DHHC proteins is first facilitated by myristoylation or prenylation and in the following palmitoylation stabilizes membrane binding (Figure 2).

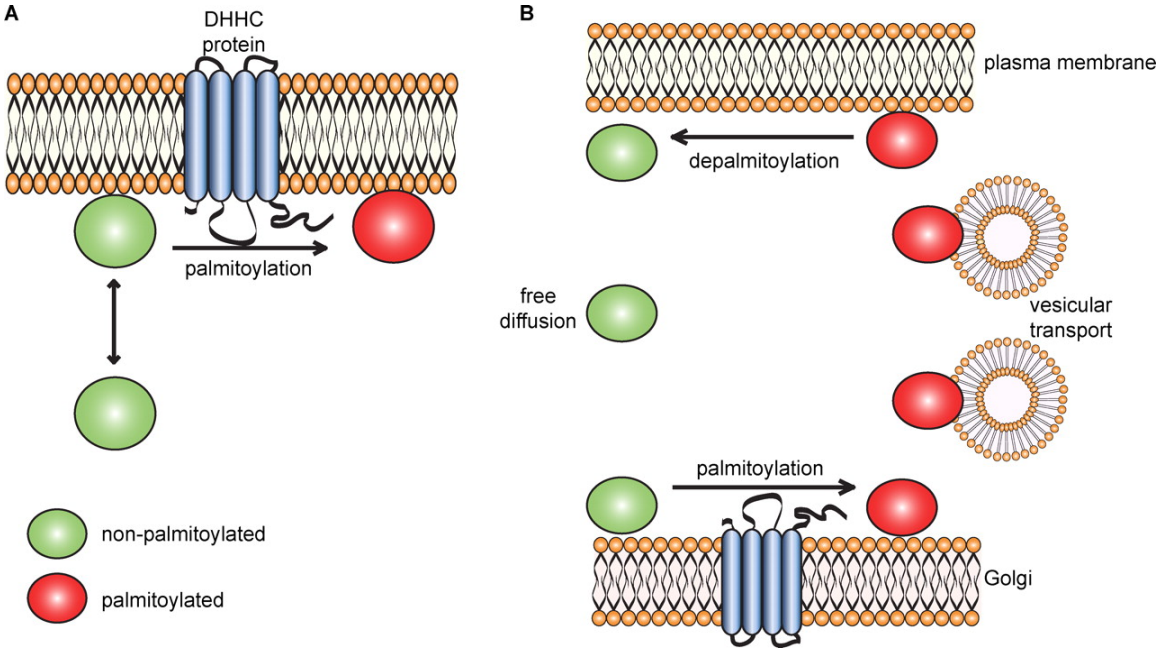

Figure 2 Regulation of membrane binding and trafficking of peripheral proteins by palmitoylation. (A) Proteins modified with single lipid groups (prenylation or N-myristoylation; green circles) have a weak membrane affinity that allows transient membrane interaction. Palmitoylation by membrane-bound DHHC proteins promotes stable membrane association by kinetic trapping. (B) Palmitoylation leads to a dramatic increase in membrane affinity by kinetic trapping. This increased membrane residency facilitates entry of palmitoylated proteins (red circles) into transport vesicles that deliver it to the plasma membrane. It is possible that palmitoylation also serves to move palmitoylated proteins into cholesterol-rich domains from which Golgi exit vesicles are formed (Salaun et al., 2010).

Therefore, a main function of palmitoylation is to stabilize the membrane attachment of soluble proteins, including farnesylated Ras and myristoylated Gα (Hancock et al., 1990; Linder et al., 1993; Parenti et al., 1993). Some soluble proteins are solely S-palmitoylated, and these proteins may use a weak membrane affinity for the transient membrane interaction before palmitoylation (Greaves et al., 2009a; Greaves et al., 2008; van Zanten et al., 2009).

Another central function of palmitoylation is the regulation of protein targeting to many distinct intracellular compartments (Greaves et al., 2009b; Linder and Deschenes, 2007), such as regulating of protein sorting on retention or anterograde transport of proteins at the ER-Golgi as well as protein cycling within the endosomal/lysosomal system (Greaves et al., 2009b; Linder and Deschenes, 2007). The underlying mechanism of palmitoylation

on protein sorting can be divided in two aspects. First, for some soluble proteins, palmitoylation may act as a passive sorting signal that provides an essential membrane anchor and in this way allow other protein domains to regulate further trafficking (Salaun et al., 2010). Second, palmitoylation may achieve active effects on protein sorting by driving partitioning of proteins into lipid-rafts (Levental et al., 2010b), or changing the orientation of proteins and protein-protein interactions (Hayashi et al., 2005; Lin et al., 2009) or regulating ubiquitination and thus modulating ubiquitination-dependent protein sorting (Valdez-Taubas and Pelham, 2005). Previous studies showed that the affinity to lipid rafts might facilitate the targeting of palmitoylated proteins from the Golgi to plasma membrane (Levental et al., 2010a; Melkonian et al., 1999). Further, it was proposed that lipid rafts might act as platforms for vesicle budding from the Golgi (Patterson et al., 2008).

Depalmitoylation

In contrast to the information available on palmitoylation, our current understanding of depalmitoylation is poor. Previous analysis of an N-Ras protein in which the palmitoyl group was attached by a noncleavable thioether linkage revealed a dispersed intracellular localization without Golgi enrichment (Rocks et al., 2005). It was suggested that this localization reflect a requirement for active regulation of palmitoylation/depalmitoylation cycling to achieve the correct localization of Ras. In comparison to the noncleavable thioether linkage, the palmitoylated protein with a cleavable thioester bond was therefore not expected to display any initial membrane targeting specificity. Despite this, the construct rapidly accumulated at the Golgi. This accumulation was suggested to follow on from binding of the farnesylated/palmitoylated protein to any membrane, depalmitoylation, and subsequent repalmitoylation at the Golgi. There were two main interpretations made from this behavior of farnesylated and palmitoylated N-Ras: 1) depalmitoylation must be very rapid to account for the speed of Golgi accumulation and 2) depalmitoylation must occur throughout the cell because if it was confined to a specific location, association of the farnesylated and palmitoylated protein with some membranes would be irreversible (Salaun et al., 2010). Meanwhile, a cycle of palmitoylation/depalmitoylation of H-Ras has been extensively analyzed (Ahearn et al.,

2011; Goodwin et al., 2005; Rocks et al., 2005; Roy et al., 2005). Acyl protein thioesterase 1 (APT1) is *bona fide* candidate depalmitoylating enzyme shown to mediate palmitate removal from H-Ras *in vitro* (Duncan and Gilman, 1998; Yeh et al., 1999). Despite APT1 being identified many years ago, its physiological importance of this protein as a thioesterase is not clear (Salaun et al., 2010). The recent description of a novel APT1 inhibitor (palmostatin B) provided an important tool to more characterize the function of APT1 in cellular palmitoylation dynamics (Dekker et al., 2010). Initial studies with palmostatin B suggests that it promotes a moderate increase in Ras palmitoylation and thus disrupts the intracellular localization of Ras (Salaun et al., 2010). A recent study showed that the prolyl isomerase (PI) FKBP12 binds to H-Ras in a palmitoylation-dependent fashion and promotes depalmitoylation in a dependent manner of cis-trans isomerization of a peptidyl-prolyl bond in proximity to the palmitoylated cysteines (Ahearn et al., 2011).

1.2.2 Lipid rafts

The lipid rafts concept

The lipid raft concept was introduced in 1997 by Simons and Ikonen. The term "lipid raft" was assigned to describe assemblies that were mainly generated by lipid-lipid interactions that lead to a phase separation of liquid- ordered (l_o) and liquid-disordered (l_d) phases within the membrane (Simons and Ikonen, 1997). In this work they postulated lipid rafts could function in membrane trafficking and signaling (Simons and Ikonen, 1997). In the liquid-ordered phase, sphingolipids associate laterally with one another probably via weak interactions between the carbohydrate heads of the glycosphingolipids. The saturated hydrocarbon chains in cell sphingolipids allows for cholesterol to be tightly intercalated filling voids created by interdigitating fatty acid chains (Figure 3). The inner leaflet is probably rich in phospholipids with saturated fatty acids and cholesterol; however, its characterization is still poorly understood.

A key issue ten years ago was the methodology used for the definition of a raft component. Raft constituents were defined as the insoluble fraction or detergent-resistant membrane (DRM) remaining after non-ionic detergent solubilisation at 4°C. This

criterion was often combined with the use of methyl-β-cyclodextrin to deplete cholesterol from cell membranes. This raised questions such as to whether rafts were a real physiological phenomenon (Munro, 2003; Shaw, 2006) because detergent solubilisation is an inherently artificial method giving different results depending on the concentration and type of detergent, duration of extraction and temperature (Lingwood and Simons, 2007; Simons and Gerl, 2010). Also cyclodextrin treatment led to side effects such as lateral protein immobilization (Kenworthy, 2008). There were claims that the lipid raft was at a technical impasse because a physical tool to study biological membrane was still lacking (Jacobson et al., 2007).

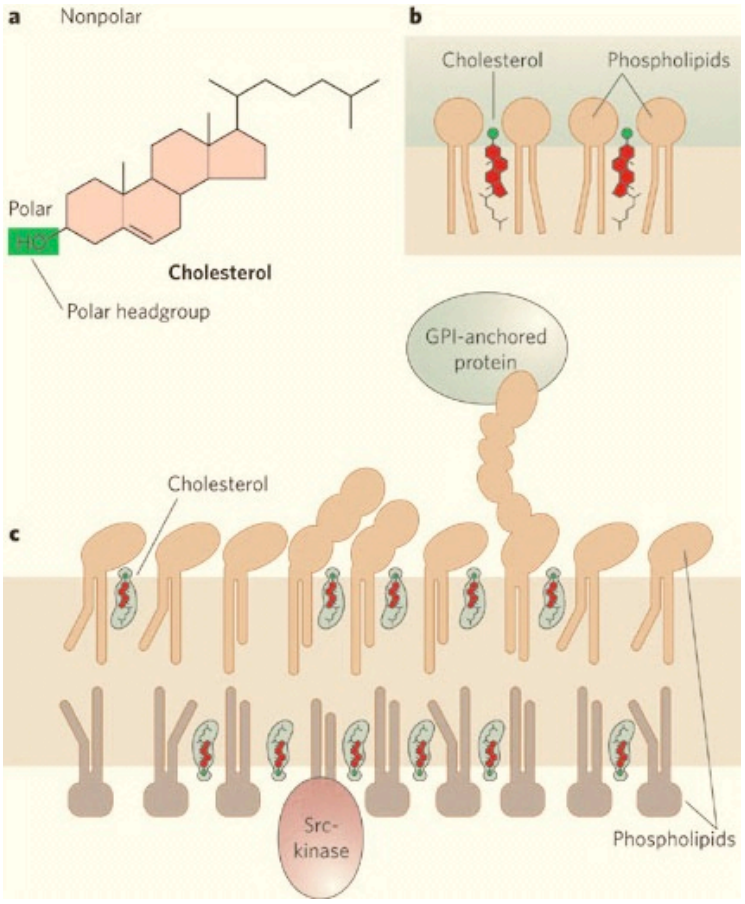

Figure 3 Model membrane containing lipid rafts. Cholesterol is important component of I_o phase membrane and fill interstitial spaces between lipids. Lipid rafts contains cholesterol and sphingolipid and specific proteins like GPI-anchored proteins in the outer leaflet and Src-kinase partition into the inner leaflet (Maxfield and Tabas, 2005).

So far the size of rafts and their lifetime has continued to be investigated, and the size seems to vary depending on the method employed to measure them while particularly the lifetime remains controversial (Jacobson et al., 2007). Currently, lipid rafts are viewed as dynamic nanoscale assemblies enriched in sphingolipid, cholesterol and GPI-anchored proteins (Hancock, 2006). This nanometer-size scale was later supported by viscous drag measures of antibody-bound raft proteins and electron microscopic observation of labeled raft antigens (Pralle et al., 2000). Novel microscopy techniques provided more data favoring the existence of nanoscale rafts in resting and activated cells (van Zanten et al., 2009). Though different techniques are yielding a range of values for different molecular constituents in different cell types, all data point to the existence of small, dynamic and selective cholesterol-dependent heterogeneity in the plasma membranes of living cells (Lingwood and Simons, 2010).

Lipid rafts in membrane trafficking

Since proteins associate with lipid rafts during apical transport, rafts could act as apical sorting platform (Simons and Ikonen, 1997). In polarized cells the sorting of many apical proteins may be governed by lipid-lipid and lipid-protein interactions instead of direct protein-protein interactions with apical sorting determinants in membrane anchors or extracellular domains that have not been identified (Schuck and Simons, 2004). Recent work has revealed the ability of individual rafts to cluster selectively into large domains and this finding led to a more comprehensive model for the role of lipid rafts in polarized sorting (Figure 4). Though the size and stability of rafts is controversial, there are indications that individual rafts can be induced to form large, stable clusters (Kusumi et al., 2004; Simons and Vaz, 2004). This clustering can be artificially initiated by antibody crosslinking but also occurs naturally for example when interactions between T-cell receptor and peptides bound to major histocompatibility complexes (MHC) on antigen-presenting cells trigger the clustering of lipid rafts during the formation of immunological synapses (Harder et al., 1998). As a consequence of lipid raft clustering, the affinity of transmembrane proteins to lipid rafts is further increased, whereas non-raft components are excluded (Schuck and Simons, 2004). Remarkably, antibody crosslinking of PLAP leads to clustering of the doubly acylated raft protein Fyn that resides on the inner leaflet

of the membrane. Thus, the crosslinking of one raft protein moves whole lipid rafts together in both membrane leaflets (Harder et al., 1998; Prior et al., 2003). The spontaneous curvature of lipid raft that results by lipid asymmetry between the inner and outer membrane leaflets could play a role in controlling the budding process (Huttner and Zimmerberg, 2001; Schuck and Simons, 2004). Therefore, raft clustering is a mechanism for the selective recruitment of proteins and lipids that have an affinity for liquid-ordered domains and meanwhile the efficient exclusion of non-raft proteins (Schuck and Simons, 2004).

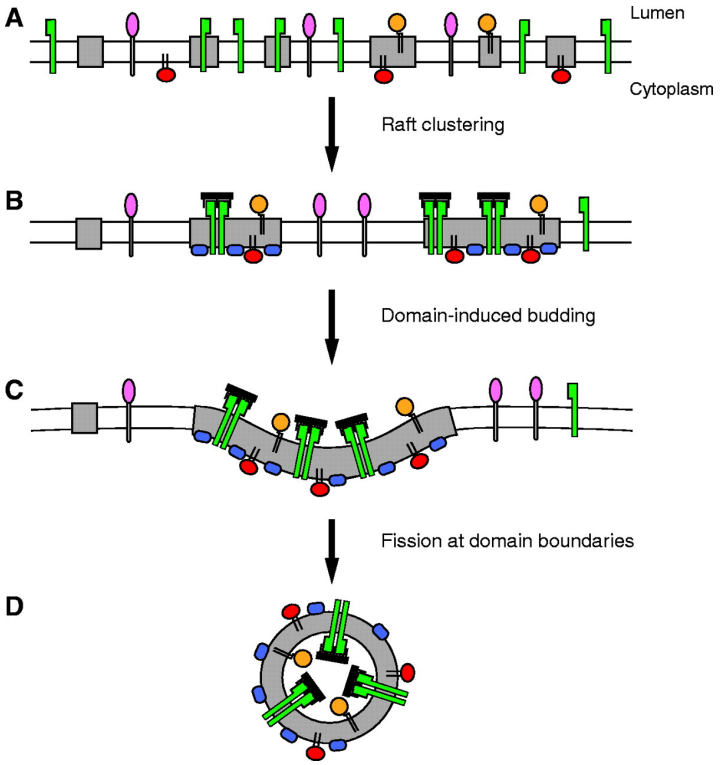

Figure 4 Raft clustering and domain-induced budding. A: GPI-anchored protein (gold) exclusively in rafts, a doubly acylated protein (red) mainly in rafts, a transmembrane protein (green) mainly out of rafts. B: When clustering is induced e.g. by the binding of annexin type (blue) to the cytoplasmic face of rafts, GPI-anchored and acylated protein partition into clustered rafts while weakly raft-associated transmembrane protein is driven into rafts by crosslinking a divalent interaction partner, e.g. a lectin (black). C: Growth of the clustered raft domain beyond size induces budding. D: Fission occurred at the domain boundaries (Schuck and Simons, 2004).

The yeast raft lipids, which are the cholesterol homologue ergosterol and sphingolipids, were recently shown to regulate the transport of detergent-resistant cargo to the plasma

membrane (Simons and Gerl, 2010). Immunoisolation and mass spectrometry analysis of TGN-derived vesicles showed that ergosterol and yeast sphingolipid were selectively enriched and the most abundant lipids in the transport vesicles (Klemm et al., 2009; Schuck and Simons, 2004). These were the first data giving direct experimental support to the hypothesis that raft cargo proteins are delivered from Golgi to the cell surface in a lipid raft carrier (Simons and Gerl, 2010). Bringing together apical sorting motifs mediate partitioning into newly formed raft clusters at the level of the Golgi which further promote formation of transport carriers by domain-induced budding (Schuck and Simons, 2004).

1.3 INTRACELLULAR TRANSPORT OF ACYLATED SH4 PROTEINS

1.3.1 Src Family Kinases

Src-family kinases, a family of non-receptor tyrosine kinases, includes at least eight highly homologous proteins: c-Src, Lyn, Fyn, c-Yes, c-Fgr, Hck, Lck and Blk (Thomas and Brugge, 1997). Src-family kinases are known to play roles in regulating cell proliferation and differentiation (Thomas and Brugge, 1997). Src, Lyn, Yes and Fyn are widely expressed in a variety of cell types, whereas Blk, Hck, Fgr and Lck are found primarily in hematopoietic cells (Bolen and Brugge, 1997; Thomas and Brugge, 1997).

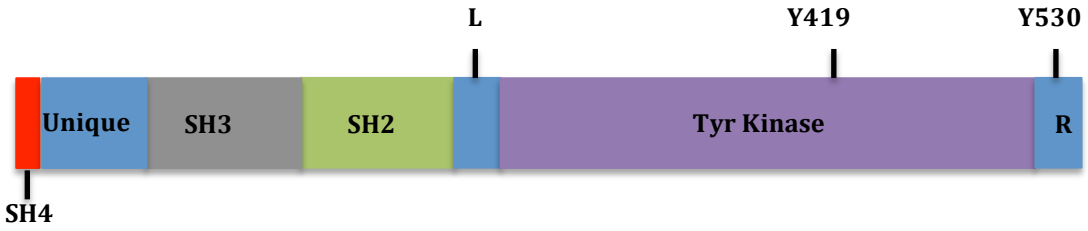

Figure 5 Schematic representation of Src domain structure. Src is composed of an N-terminal myristoylated SH4-domain, the unique region followed by SH3 and SH2 domain, a linker region (L) and a catalytic kinase domain that contains Y419 and a C-terminal regulatory domain (R) that contains Tyr530.

Src-family tyrosine kinases are composed of: (1) an N-terminal Src homology SH4 domain conferring membrane binding via one or several acylations (2) a poorly conserved domain, (3) an SH3 domain binding specific proline-rich sequences thus

mediating protein-protein interactions, (4) an SH2 domain, which can bind to specific sites of tyrosine phosphorylation, (5) an SH1 tyrosine kinase catalytic domain which contains an autophosphorylation site and mediates enzymatic activity (6) a C-terminal negative regulatory tail for autoinhibition of the kinase activity (Brown and Cooper, 1996) (Figure 5). It is generally thought that SFKs are predominantly located at the cytoplasmic face of plasma membrane by lipid modifications (Resh, 1994), however, appreciable fractions are also found at other intracellular locations, such as endosomes, secretory granules or phagosomes and the Golgi complex (Brown and Cooper, 1996; Kaplan et al., 1992; Kasahara et al., 2004; Mohn et al., 1995; Thomas and Brugge, 1997). Although distinct localizations of Src members have been implicated in their specific functions, the mechanism that underlies the targeting of SFKs to their specific locations remains to be elucidated.

Intracellular trafficking of Src, Lyn, Yes and Fyn

Early studies demonstrated that SFKs interact with membranes through their lipid acylation in the N-terminal SH4 domain (Blenis and Resh, 1993; Resh, 1993; Silverman et al., 1993). A recent study by Sato et al. (2009) showed that the differential trafficking of Src, Lyn, Yes and Fyn is specified by the state of palmitoylation in the SH4 domain. They demonstrated that Src as a nonpalmitoylated Src is rapidly exchanged between the plasma membrane and late endosomes/lysosomes. Lyn and Yes as monopalmitoylated SFKs are transported via the Golgi region along the secretory pathway, whereas a large fractions of Fyn, a dually palmitoylated SFK is directly targeted to the plasma membrane.

SRC	**M G S N K S K P K D A S Q R R R S L**
FYN	**M G C V Q C K D K E A T K L T E E R**
YES	**M G C I K S K E N K S P A I K Y R P**
LYN	**M G C I K S K G K D S L S D D G VD**

Figure 6 Primary sequences of the N-terminal 18 amino acids of SH4 domain of SFKs. Myristoylated glycines are highlighted in blue and palmitoylated cysteines are highlighted in green.

Src is one of two Src family kinases that are only myristoylated but not palmitoylated (Figure 6). A basic cluster of amino acids provides the second signal for membrane binding (Koegl et al., 1994; Resh, 1994; Shenoy-Scaria et al., 1994). Src is rapidly

exchanged between late endosomes or lysosomes and the plasma membrane, possibly through its cytosolic release (Kasahara et al., 2004). Src-containing endosomes are RhoB-positive at the perinuclear-recycling compartment, which participates in actin-dependent transport of Src to the plasma membrane (Sandilands et al., 2007).

Lyn and Yes are myristoylated and monopalmitoylated SFKs (Figure 6). Newly synthesized Lyn and Yes initially are at the cytoplasmic face the Golgi system, where palmitoylation probably happens. This provides entry into the secretory pathway to the plasma membrane (Kasahara et al., 2004). Lyn as a member of Src-family tyrosine kinases is widely expressed and has an important role in signal transduction at the cytoplasmic face of the plasma membrane (Tsukita et al., 1991). Incorporation of one or more palmitate moieties is reported to facilitate localization of Yes and Fyn to lipid rafts (Shenoy-Scaria et al., 1994). The transport of Lyn and Yes to the plasma membrane is blocked by low temperatures (19°) and dominant-negative Rab 11, indicating export via the TGN (Sato et al., 2009). Recently it was shown that newly synthesized Lyn accumulates on Golgi membranes and later will be transported along the secretory pathway in a Lyn kinase domain dependent manner to the plasma membrane (Obata et al., 2010). Moreover, it was demonstrated that the C-lobe of the Lyn kinase domain associates with long-chain acyl-CoA synthetase 3 (ACSL3) when Lyn positions in an open conformation, thereby initiating export from the Golgi (Obata et al., 2010). Ikeda et al. (2009) showed that besides N-terminal acylation, the kinase domain but not kinase activity of Lyn is also required for the targeting of newly synthesized Lyn to the Golgi, especially to the caveolin pool of the Golgi. Lack of Lyn kinase domain induces accumulation of Lyn on caveolin-negative Golgi membranes and thus inhibits the transport pathway to the plasma membrane (Ikeda et al., 2009).

After myristoylation and dual palmitoylation, newly synthesized Fyn is targeted directly to the plasma membrane (van't Hof and Resh, 1997). It was shown that Fyn interact with the plasma membranes 5 minutes after its biosynthesis and partition into membrane microdomains 10-20 minutes after membrane association (van't Hof and Resh, 1997). Further it was shown that palmitoylation of the SH4-domain of Fyn is sufficient to target

chimeric proteins to DRMs and plasma membrane (Wolven et al., 1997). The SH4 domain of Fyn contains two cysteine at position 3 and 6; deletion of cysteine 6 did not constrain membrane targeting however resulted in the export via the secretory pathway similar to the export of monoplamitoylated SFKs Yes and Lyn (Sato et al., 2009). Moreover, Fyn C3S/C6S that is no longer palmitoylated, behaves much more like Src by colocalization with RhoB endosomes while wild type Lyn is found to localize with Rho D endosomes (Sandilands et al., 2007). Liang et al. (2004) showed that methylation of its N-terminal domain lysine 7 and/or 9 is required for the functionality of Fyn that is dependent on the previous acylation.

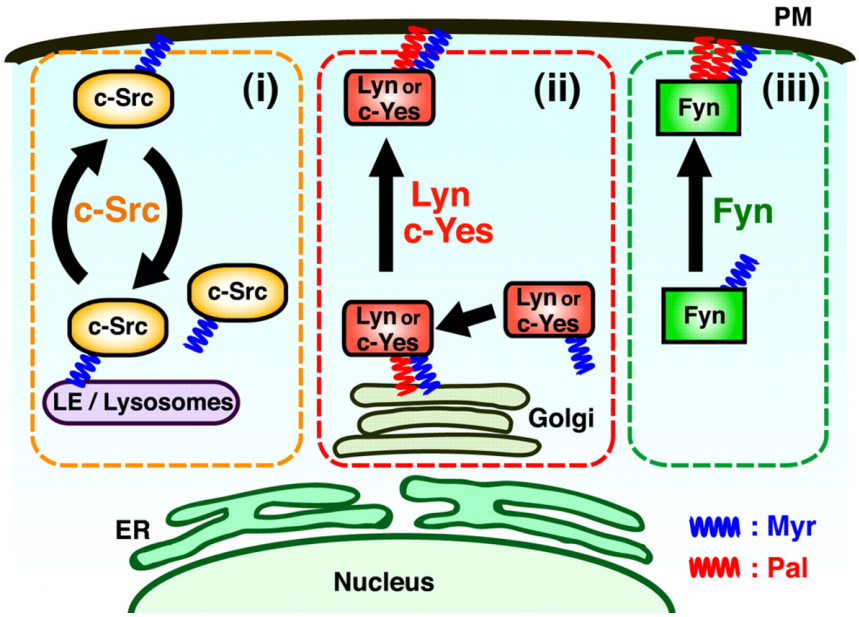

Figure 7: Schematic model of three major pathways for SFK targeting to the plasma membrane. (i) c-Src as an example for only myristoylated but not palmitoylated SFKs. The cycling of c-Src between late endosome/lysosomes and the plasma membrane is shown. (ii) Lyn or c-YES as for myristoylated and monoplamitoylated SFKs. The secretory pathway of Lyn/c-YES from Golgi apparatus to the plasma membrane is depicted. (iii) FYN as myristoylated and dually palmitoylated SRKs target direct to the plasma membrane (Sato et al., 2009).

1.3.2 Hydrophilic Acylated Surface Protein B (HASPB)

Hydrophilic Acylated Surface Proteins (HASPs) are members of Lm cDNA 16 gene family that encodes five genes located on a single choromosome in the Leishmania major genome. Gene B (HASPB) is a protein localizing to the surface of Leishmanina parasites only at infective stages (Pimenta et al., 1994). Deletion of the complete Lm cDNA locus

results in an increased sensitivity to complement-mediated lysis (McKean et al., 2001). HASPB is a predominantly hydrophilic molecule of 177 amino acids. Heterologous expression of HASPB in mammalian cells causes in externalization of the protein to the outer leaflet of the plasma membrane suggesting the underlying machinery required for export of HASPB is conserved among eukaryotes (Denny et al., 2000; Stegmayer et al., 2005). Export to the extracellular leaflet of the mammalian plasma membrane functions via direct translocation by an unknown mechanism (Stegmayer et al., 2005). Overexpression of SH4-HASPB in Chinese hamster ovary (CHO) cells results in a formation of highly dynamic non-apoptotic blebs of the plasma membrane (Tournaviti et al., 2007).

HASPB contains an N-terminal SH4 domain that undergoes dual acylation at glycine 2 for myristoylation and cystein 5 for palmitoylation (Denny et al., 2000). The 18 amino acids of SH4 domain is sufficient to target a reporter molecule such as GFP to the cell surface of parasites and mammalian cells (Denny et al., 2000; Stegmayer et al., 2005; Tournaviti et al., 2009). It was shown that incubation with brefeldin A, a drug causing a collapse of Golgi into the ER in mammalian cells does not interfere with the localization of HASPB at the plasma membrane in CHO cells (Denny et al., 2000). Based on these observations HAPSB has been termed an unconventional secretory protein (Denny et al., 2000). In accordance to these observations, HASPB does not contain a classical signal peptide and further it is not glycosylated, a modification that is cotranslational in the ER and continues in the Golgi (Denny et al., 2000). In addition, it was demonstrated that mutation of the glycine at position 2 results in abrogation of myristoylation and the subsequent palmitoylation and the intracellular translocation of HASPB mutant in both mammalian and parasitic cells (Denny et al., 2000). In contrast, mutation of the palmitoylation site results in accumulation of myristoylated HASPB at perinuclear membranes and its failure to partition into lipid rafts (Tournaviti et al., 2009), which seems to be the prerequisite for the targeting to the plasma membrane (Figure 8). Recent studies identified threonine 6 as a phosphorylation site of the SH4 domain of HASPB (SH4-HASPB) (Tournaviti et al., 2009). It was demonstrated that a threonine 6 to glutamate (T6E) exchange as a phosphorylation mimic resulted in a redistribution of SH4-HASPB from the plasma membrane to intracellular sites with a strong accumulation

in a perinuclear region (Tournaviti et al., 2009). In comparison, a threonine 6 to alanine (T6A) mutation did not disturb plasma membrane localization of SH4-HASPB (Tournaviti et al., 2009). The fact that both mutations (T6E and T6A) do not affect the partition of SH4-HASPB into DRMs indicates the regulation by a DRM-independent endocytic step (Tournaviti et al., 2009). Similar to the perinuclear accumulation of the phosphomimetic mutant, SH4-HASPB accumulates at perinuclear membranes when protein phosphatases PP1 and PP2A were downregulated by RNAi (Tournaviti et al., 2009). It was suggested that Sh4 proteins cycle back and forth between the plasma membrane and perinuclear compartments a process that is controlled by a regulatory cycle of phosphorylation and dephosphorylation (Tournaviti et al., 2009).

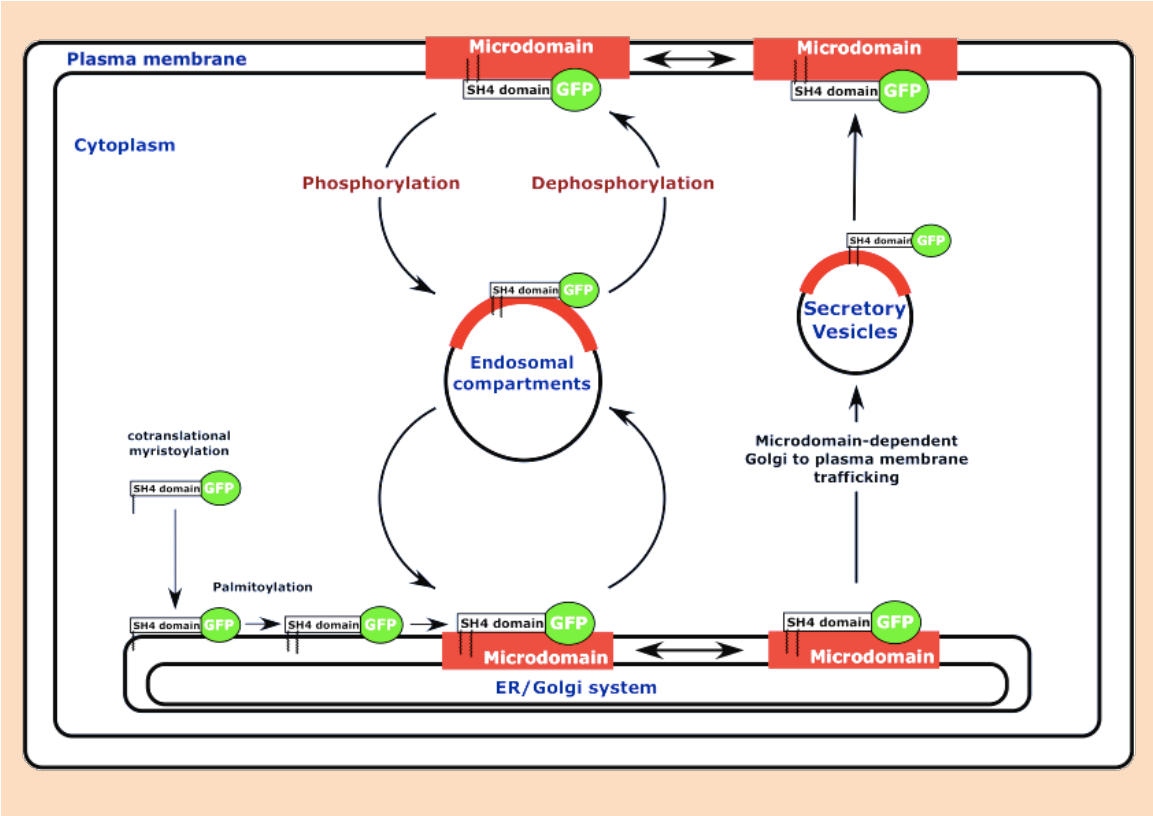

Figure 8 Schematic model of intracellular trafficking of acylated Src family kinases. SH4-domains interact with the ER/Golgi upon myristoylation where they are palmitoylated. Palmitoylated SH4-domains partition into microdomains and then are ready to be exported to the plasma membrane. A phosphorylation cycle regulates endocytosis and recycling without affecting microdomain association (modified from Nickel, 2005).

1.4 UBIQUITINATION RELATED POST-TRANSLATIONAL PROTEIN MODIFICATIONS

Ubiquitination is a prominent post-translational protein modification that regulates most cellular functions in eukaryotes (Glickman and Ciechanover, 2002; Haglund and Dikic, 2005; Weissman, 2001). Since the discovery of ubiquitin in the mid-1970s, an entire family of small proteins related to ubiquitin has resulted in the distribution of so called ubiquitin-like proteins or UBLs. All structurally characterized UBLs share the ubiquitin or β-grasp fold, even when their primary sequences are not detectably similar (Kerscher et al., 2006). Ubiquitin (Ub) and ubiquitin-like proteins (UBLs) share similar enzymatic mechanisms for their conjugation onto target proteins (Figure 9). The first step into a conjugation pathway requires an ATP-dependent activation through the formation of an adenylate intermediate in the nucleotide-binding pocket of their cognate E1 (activating enzyme) (Ciechanover et al., 1981; Haas et al., 1982). After this, the activated Ub/UBLs is transferred onto the catalytic cystein of E1 to form a high-energy thioester intermediate (Huang et al., 2007). Further, thioesterified Ub/UBLs will be transferred from E1 to E2 (the conjugating enzyme) catalytic cysteine with associated conformation changes, which requires a "fully loaded" E1 complex with two bound Ub/UBLs, one in adenylated form Ub/UBLs and the other linked via thioester bond Ub/UBLs (Huang et al., 2007). Finally, the Ub/UBLs is covalently transferred when a lysine side chain of the substrate is positioned in the way that it can destabilize the thioester linkage between Ub/UBLs and E2 and further promote the formation of a peptide bond. This step is usually assisted by E3s (ligases) that interact with protein substrates and activate E2 to facilitate this reaction.

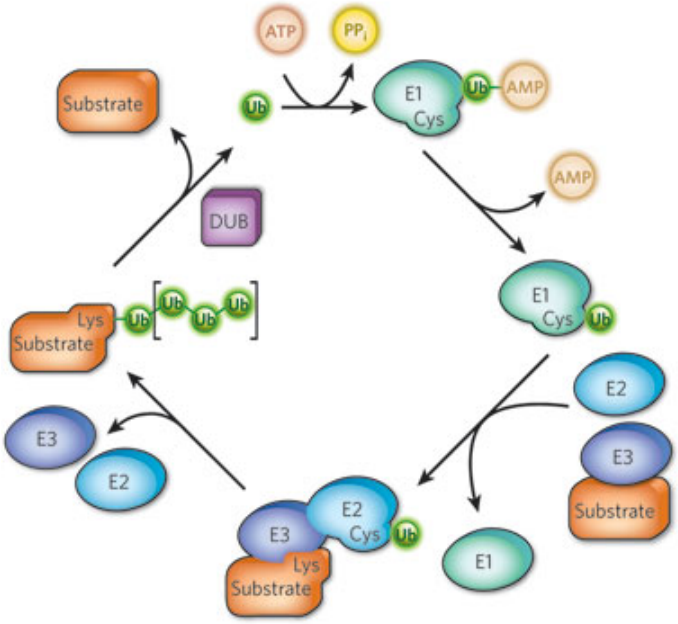

Figure 9 The basic principles of the ubiquitin-conjugation pathway. Three types of enzymes: E1, E2 and E3 participate in ubiquitination. E1 activates ubiquitin and E2 picks up the ubiquitin by transthiolation from E1 and conjugate it to substrates. E3 then ligates the ubiquitin to the substrates (Hochstrasser, 2009).

1.4.1 Ubiquitination

Ubiquitin is a highly conserved protein of eight kD that is conserved among eukaryotes but absent from bacteria and archaea. Classically, the best understood function of ubiquitin is the targeting of proteins for degradation by the proteasome where ubiquitin is attached in the form of a polyubiquitin chain to the substrate that is then recognized by specific receptors within the proteasome or by adaptor proteins that subsequently bind the proteasome (Elsasser et al., 2002; Young et al., 1998). Generally, ubiquitination also remodels the surface of substrate proteins and thereby potentially affects properties such as stability and activity (Pickart and Fushman, 2004), drives interaction with other proteins and plays roles in subcellular localization of their substrate (Mukhopadhyay and Riezman, 2007). Diverse forms of Ub modifications exist: 1) Monoubiquitination is the attachment of a single Ub to a protein; 2) Multiubiquitintion occurs when several Lys residues of the target protein are tagged with single Ub molecules; 3) Polyubiquitination describes a single Ub chain where the c-terminus of ubiquitin is bound to the previous ubiquitin via an isopeptide bond with an ε-amino group of a lysine residue (Hochstrasser, 2006). Monoubiquitination or multiubiquitination has been shown to be required for the

entry of certain cargo proteins into vesicles at the different stages of the secretory/endocytic pathway (Hicke, 2001) while polyubiquitination is mainly associated with proteasomal degradation although it certainly has a wide function (Pickart and Eddins, 2004). One of the nonproteasomal functions of ubiquitination was its implication in endocytosis in yeast (Hicke and Riezman, 1996; Kolling and Hollenberg, 1994), where monoubiquitination functions as an endocytic internalization signal (Terrell et al., 1998). However, this function is much less clear in mammalian cells.

1.4.2 Neddylation

Neddylation is a post-translational protein modification that is closely related to ubiquitination. While ubiquitination regulates a myriad of processes in eukaryotic cells, there are only limited substrates for neddylation discovered to date. NEDD8, a UBL protein, was originally identified in the embryonic mouse brain (Kumar et al., 1992). Further it was found that NEDD8 is highly conserved in most eukaryotes where it is expressed in most tissues indicating an important function in eukaryotic cells (Carrabino et al., 2004; Hori et al., 1999; Kumar et al., 1992). Indeed neddylation is essential for the viability of most model organisms including *Caenorhabditis elegans*, *Drosophila* and mouse with the exception of *S. cerevisiae* (Lammer et al., 1998; Liakopoulos et al., 1998) and deregulated neddylation might be involved in some human diseases such as neurodegenerative disorders and cancers (Chairatvit and Ngamkitidechakul, 2007; Salon et al., 2007).

Similar to ubiquitination, neddylation involves a three-step cascade (Figure 10). ATP-dependent NEDD8 activation is initiated by the NEDD8 E1 enzyme NAE1-UBA3, which creates a high-energy intermediate (Huang et al., 2004a). This is transferred to the NEDD8 E2 conjugation enzyme UBC12 (Huang et al., 2007) and finally, the conjugation to a lysine residue of a target protein is mediated with help of NEDD8 E3 ligase, which then ensures specific conjugation to its substrates. The NEDD8 E1 activity is carried out by a heterodimer of NAE1 and UBA3, which are homologous to the amino- and C-terminal domains of ubiquitin-activating enzyme, respectively (Liakopoulos et al., 1998; Osaka et al., 1998; Walden et al., 2003). The NAE1 binding site for UBA3 lies within

amino acid 443-479. Differently to ubiquitination, where ubiquitin can be transferred by multiple E2s, Ubc12 is the unique E2 for Neddylation (Liakopoulos et al., 1998). Indeed, despite of the high similarity between Ubiquitin and NEDD8, Ubc12 is exclusively loaded by NEDD8 and a covalent oxyester bond between the carboxyl-terminal glycine of NEDD8 and cysteine of UBC12 is formed (Leck et al., 2010). Protein neddylation is reversed by NEDD8 isopeptidases in a process known as deneddylation. Currently, the best-characterized NEDD8 isopeptidase is CSN5, a subunit of the COP9 signalsome (CSN), which deneddylates cullins (Schwechheimer, 2004; Wei and Deng, 2003). The CSN is conserved from yeast to humans (Schwechheimer, 2004; Wei and Deng, 2003) and essential for the viability in metazoans (Cope and Deshaies, 2003).

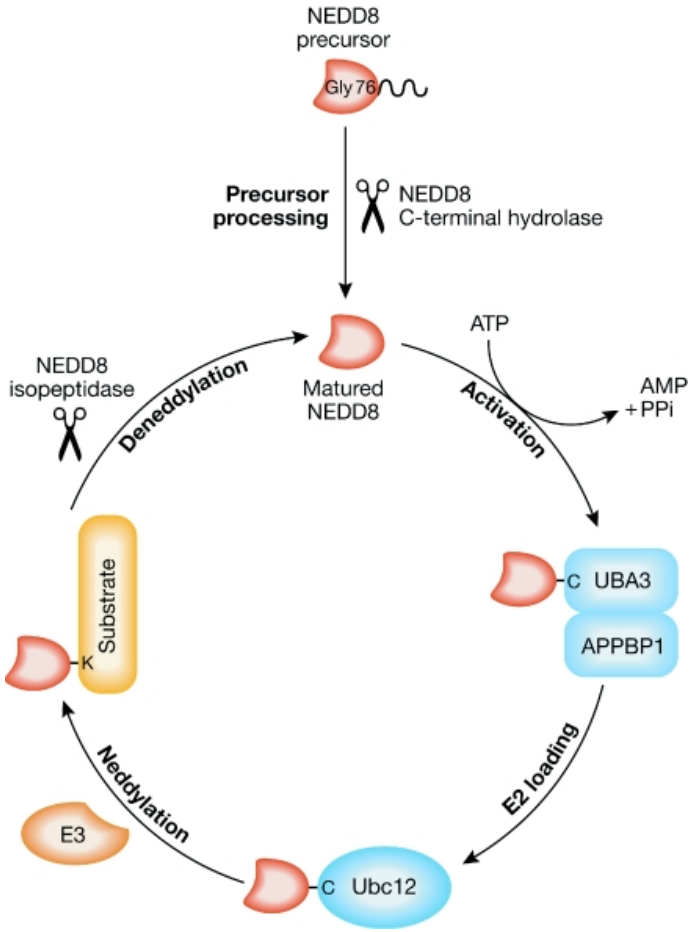

Figure 10 Schematic depiction of neddylation pathway. NEDD8 is activated by UBA3-APPBP1 (NAE1) heterodimer, further loaded onto the UBC12, conjugated to the substrate by E3 and recycled by an isopeptidase (from Rabut and Peter, 2008).

The first identified targets of NEDD8 were Cdc53 in *S. cerevisiae* (Liakopoulos et al., 1998) and CUL4A in human cells (Osaka et al., 1998), both of which are cullin family proteins. Cullins function as a part of the catalytic core of cullin-RING ubiquitin ligases (CRLs) (Petroski and Deshaies, 2005), which recruits charged ubiquitin E2s into the complex and catalyzes the ubiquitination of cullin substrates (Seol et al., 1999). Up to date, it is still unclear how many other proteins are modified by NEDD8 despite several proteomic approaches (Jones et al., 2008; Norman and Shiekhattar, 2006; Xirodimas et al., 2008). These studies confirmed that cullins are abundant NEDD8 substrates, however failed to identify other previously characterized neddylated proteins except p53 (Li et al., 2006).

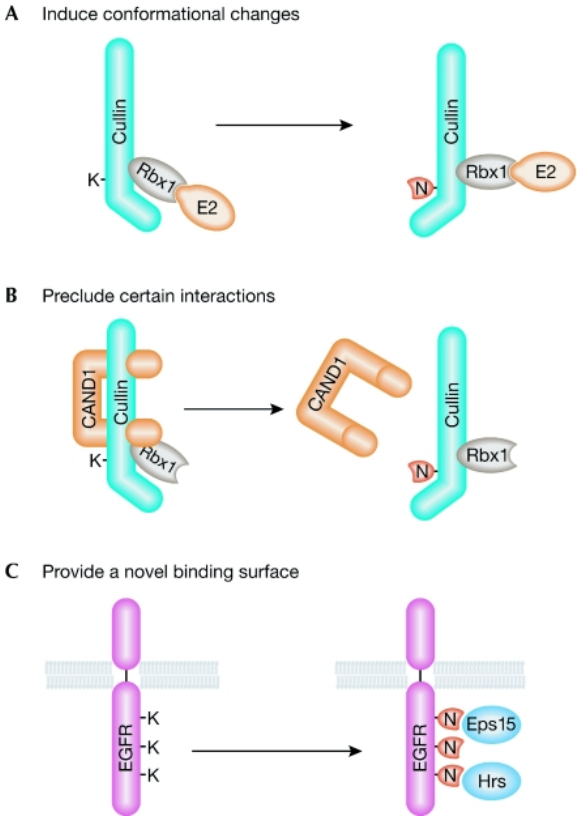

Figure 11 Examples of direct effects of neddylation. (A) Neddylation induces conformational changes. (B) Neddylation precludes association with certain partners or competes with other posttranslational modifications. (C) Neddylation provide a novel binding surface to recruit new partners (Rabut and Peter, 2008).

Neddylation of proteins modifies their three-dimensional surface and, hence, their biochemical properties (Rabut and Peter, 2008). The effects can be classified into three

categories which have subsequent consequences in subcellular localization or enzymatic activity (Figure 11) (Rabut and Peter, 2008). First, neddylation can induce conformational changes of its targets. Studies about cullins showed that the c-terminal domain of cullin forms a groove where Rbx1 is embedded and this conformation constrains the movement of Rbx1 and positions the E2 away from its ubiquitination substrates (Zheng et al., 2002). Neddylation of cullin induces a conformation switch in its C-terminal domain that frees the RING domain of Rbx1 thus allows it to adopt different orientations and to stimulate substrates of ubiquitination *in vitro* (Duda et al., 2008). As a second possibility, neddylation can preclude certain interactions (Rabut and Peter, 2008). Neddylation of cullin1 not only activates Rbx1 but also prevents it from binding to the cullin inhibitor CAND1 (Duda et al., 2008). Another example is that neddylation of EGFR can inhibit further ubiquitination since neddylation and ubiquitination modify overlapping lysines of EGFR (Oved et al., 2006). Finally, neddylation can stimulate the recruitment of NEDD8 interaction proteins. For example, neddylated EGFR likely provides a novel binding surface to recruit endocytic proteins such as Eps 14 or Hrs (Oved et al., 2006).

The amyloid precursor protein (APPs, 695-770 amino acids) is a ubiquitous membrane protein and its increased processing is believed play a role in Alzheimer´s disease(Muller and Kins, 2002). APP is a cell surface protein with a large extracellular amino-terminal domain, a single transmembrane segment and a short cytoplasmic tail. The cleavage of APP by α- and β-secretase yields a secreted form of APP and a C-terminal fragment (C83), and alternative cleavage by the β-secretase produces the C-terminal fragment (C99) which is further cleaved by γ-secretases to generate the amyloid peptide Aβ and the APP intracellular domain (AICD) fragment (C50) (Gu et al., 2001; Kerr and Small, 2005). In addition, APP was shown to be neddylated and functionally neddylation inhibits AICD-mediated transcriptional activation due to the inhibition of its interaction with the co-activator Fe65 and Tip60 (Lee et al., 2008). Further, it was proposed that the regulatory mechanisms by which AICD transcriptional activity might be regulated via covalent conjugation with NEDD8 (Lee et al., 2008).

1.5 AIM OF THIS STUDY

While it was known for nearly 20 years that SH4-domains direct targeting to the intracellular leaflet of the membrane and the targeting mechanism depends on lipid acylation of SH4 domain (Blenis and Resh, 1993), the underlying molecular mechanism of intracellular transport of SH4-domain containing proteins remains elusive. In a previous study from our laboratory, a genome wide RNAi screen was performed using an automated microscopy platform to identify gene products involved in intracellular targeting and transport of SH4 reporter proteins to the plasma membrane. All together 286 genes were identified in the primary genome wide screen.

The main goal of this study was to further validate a subset gene products identified during the primary screen and characterize in more detail their roles in the targeting of SH4-domain containing proteins to the plasma membrane. Among the identified gene products we found factors involved in lipid metabolism, intracellular transport and cellular signaling processes. We used complementary approaches to confirm the requirements of coatomer, PKCα and MVD in the plasma-membrane targeting of SH4-domain containing proteins. Further we focused our study on the hypothesis that NAE1 as a component of the neddylation pathway is involved in intracellular transport of SH4-reporter proteins. We applied RNAi-based downregulation, dominant negative constructs of components of the neddylation pathway; as well as a specific inhibitor against NAE1 to block cellular neddylation and characterized the effects on SH4-dependent transport.

2 MATERIAL AND METHOD

2.1 MATERIAL

2.1.1 Chemicals and consumables

Chemical/Consumable	Manufacturer
1 kb DNA standard	New England Biolabs, Frankfurt
2-bromopalmitate	Sigma-Aldrich Chemie GmbH, Steinheim
Acetic acid (CH_3COOH)	Carl Roth GmbH, Karlsruhe
30% acrylamide 4K solution 37,5:1 Rotiphorese	Carl Roth GmbH, Karlsruhe
Agar	Becton Dickinson, Le Pont de Claix
Agarose	Invitrogen Ltd., Paisely
Ammoniumperoxodisulphate (APS)	Carl Roth GmbH, Karlsruhe
Ammonium sulfate $(NH_4)_2SO_4$	Acros organics, New Jersey
Ampicillin	Gerbu Biotechnik GmbH, Gaiberg
NuPage Antioxidant	Invitrogen Ltd., Paisely
Aqua ad iniectabilia	Braun AG, Melsungen
Bovine serum albumin (BSA)	Carl Roth GmbH, Karlsruhe
Bromphenol blue	Serva Electrophoresis GmbH, Mannheim
buffer 4 for restriction enzymes	New England Biolabs Inc. Frankfurt
Calcium chloride Dihydrate	J.T. Baker, Deventer
Cell culture dishes (x cm, 10 cm, 15 cm)	Corning Incorporated
Cell Dissociation Buffer (CDB)	Invitrogen Ltd. Paisley
Cell scraper	Corning Incorporated
Centrifuge tubes polyclear 25 x 89 mm	Konrad Beraneck, Weinheim
Centrifuge tubes polyclear 14 x 89 mm	Konrad Beraneck, Weinheim
Centrifuge tubes polyclear 11 x 60 mm	Konrad Beraneck, Weinheim
Chloramphenicole	Carl Roth GmbH, Karlsruhe
Chloroquine	Sigma-Aldrich Chemie GmbH, Steinheim
Collagen R	Serva Electrophoresis GmbH, Heidelberg
Complete Protease Inhibitor Cocktail tablets EDTA-free	Roche Diagnostics, Mannheim
Coomassie Brilliant blue R250	SERVA Electrophoresis GmbH
Coomassie G-250	Carl Roth GmbH, Karlsruhe

CryoTubes Cryo S	Greiner bio-one
Diethylaminoethyldextran (DEAE-dextran)	Sigma Aldrich Chemie GmbH, Steinheim
Dimethyl sulphoxide (DMSO)	Merck KGaA, Darmstadt
Disodiumhydrogenphosphate (Na_2HPO_4)	AppliChem, Darmstadt
Dithiothreitol (DTT)	Gerbu Biotechnik GmbH, Gaiberg
Doxicycline	Clontech, Heidelberg
Eppendorf tubes 1,5 ml	Sarstedt, Nümbrecht
Ethanol p.a.	Merck KGaA, Darmstadt
Ethidium bromide	Carl Roth GmbH, Karlsruhe
Ethylenediaminetetraacetate-disodium (EDTA)	SERVA Electrophoresis GmbH
Falcon tubes 15, 50 ml	Greiner bio-one
Fetal Calf Serum (FCS)	PerBio
Filter tubes 45 µm for FACS	Falcon
Formaldehyde solution 37%	J.T. Baker, Deventer
L-Glutamine	Biochrom KG, Berlin
Glycerol	J.T. Baker, Deventer
Glycine	Applichem, Darmstadt
HisTrap HP 1ml	GE Healthcare
Hydrochloric acid (HCL)	VWR Prolabo
Imidazole	Merck KGaA, Darmstadt
Isopropyl-ß-D-thiogalactopyranoside (IPTG)	Gerbu Biotechnik GmbH, Gaiberg
Kanamycine	Gerbu Biotechnik GmbH, Gaiberg
Magnesium chloride ($MgCl_2$)	J.T. Baker, Deventer
D-MEM	Biochrom AG, Berlin
ß-mercaptoethanol	Merck KGaA, Darmstadt
N-morpholinoethanesulfonic acid (MES)	SERVA Electrophoresis GmbH
NuPage MES buffer 20 x	Invitrogen Ltd., Paisely
Methanol	Merck KGaA, Darmstadt
Midi Gel Adapter for Criterion TM Cell	Invitrogen Ltd., Paisely
Milk powder	Carl Roth GmbH, Karlsruhe
needle 27 gauge x 3/4 0,4 mm x 19 mm	BD, Drogneda, Ireland
Neubauer Chamber	W.Schreck, Hofheim
Nonidet P 40	Roche Diagnosics, Mannheim
NuPAGE Novex Midi Gels 4-12% Bis-Tris	Invitrogen Ltd., Paisely

Odyssey protein marker Precision Plus Protein All Blue Standards	BioRad Laboratories GmbH, München
Optiprep 60%	Sigma-Aldrich Chemie GmbH, Steinheim
Ortho-Phosphoric Acid H_3PO_4	Grüssing, Filsum
Paraformaldehyde	Riedel de Haën, Seelze
Penicillin/Streptomycin	Biochrom AG, Berlin
Petri dishes, glass 20 cm	Carl Roth GmbH, Karlsruhe
Phenylmethylsulfonyl Fluoride (PMSF)	Roche Diagnostics, Mannheim
Pipets 5,10 and 25 ml	Corning Incorporated
Pipet tips	Greiner bio-one
Potassium chloride (KCl)	AppliChem, Darmstadt
Potassium dihydrogenphosphate (KH_2PO_4)	GERBU GmbH, Gaiberg
Propan-2-ol p.a.	Merck KGaA, Darmstadt
Propidium iodide (PI)	Molecular probes
PVDF membrane Immobilon^{TM} FL	Millipore
D (+)-Saccharose	Carl Roth GmbH, Karlsruhe
silver nitrate $AgNO_3$	Sigma-Aldrich Chemie GmbH, Steinheim
silver nitrate solution, 0.1 mol/l $AgNO_3$	Grüssing, Filsum
Sodium acetate CH_3COONa	Grüssing, Filsum
Sodium carbonate anhydrous Na_2CO_3	AppliChem, Darmstadt
Sodium chloride (NaCl)	AppliChem, Darmstadt
Sodium dodecyl sulphate pellets (SDS)	Carl Roth GmbH, Karlsruhe
Sodium hydrogen carbonate ($NaHCO_3$)	J.T. Baker, Deventer
Sodium hydroxide (NaOH)	J.T. Baker, Deventer
Sodium Thiosulfate $Na_2S_2O_3$	J.T. Baker, Deventer
Superdex 75 HiLoad 16/60	GE Healthcare
Syringe, 1ml	Becton Dickinson, Le Pont de Claix
N,N, N`N´-tetramethylethylendiamine (TEMED)	Carl Roth GmbH, Karlsruhe
Tris[hydroxymethyl]aminoethane	Carl Roth GmbH, Karlsruhe
Triton X-100	Roche Diagnostics, Mannheim
Trypsin	Biochrom KG, Berlin
Tryptone	Becton Dickinson, Le Pont de Claix
Tween-20	Carol Roth GmbH, Karlsruhe
Whatman 3 mm paper	Whatman AG

Yeast extract	Becton Dickinson, Le Pont de Claix

2.1.2 Technical devices

Technical device	**Manufacturer**
Agarose gel chamber	BioRad Laboratories GmbH, München
Centrifuge: Centrifuge 5417R	Eppendorf AG, Hamburg
Centrifuge: Centrifuge 5415 C	Eppendorf AG, Hamburg
Centrifuge: Centrifuge 5804R	Eppendorf AG, Hamburg
Centrifuge: Optima L80-XP Ultracentrifuge	Beckman Instrument GmbH, München
Centrifuge: Sorvall RC 12 BP	Thermo Scientific
Criterion™ Cell Midi Gel System	BioRad
CryoBox	Nalgene
FACSAria cell sorter	Becton Dickinson, Le Pont de Claix
Fluorescence platereader Spectra MAX Gemini XS	Molecular Devices
Freezer : -86°C Freezer	Thermo Electron Corporation
Gel Doc 2000 System	BioRad Laboratories GmbH, München
Incubator (bacterial cells)	Haraeus, Hanau
Incubator (eukaryotic cells) : Steri-Cycle CO_2 Incubator HEPA Class 100	Thermo Scientific
Incubator shaker innova 4200	New Brunswick Scientific, Edison NJ
Laserscan microscope LSM-510	Zeiss, Göttingen
Magnetic stirrer	Heidolph
Microwave	Panasonic
Mini-Protean 3 III Gel System	BioRad Laboratories GmbH, München
Mini-Trans-Blot Blotsystem	BioRad Laboratories GmbH, München
Nanodrop ND-1000 Spectrophotometer	Technologies, Inc.
NuPage gel system	Invitrogen Ltd., Paisely
Odyssey imaging system	LI-COR Biosciences
pH-Meter 766 Calimatic	Knick GmbH
Pipetboy	IBS Integra Biosciences
Pipets P10, P20, P200, P1000, P10,000	Gilson
Power supply: Power Pac 200	BioRad Laboratories GmbH, München
Refrigerator: Premium	Liebherr

Resys Analytical ELISA Reader 2001	Anthos Analytical Apparatus Inc., Durham
Roto-Shake Genie	Scientific Industries GmbH, München
Scanner	EPSON Perfection 3200 Photo
Shaker: Promax 2020	Heidolph
Sonifier B-30	Branson Sonic Power Co.
Spinner flasks 2l	Techne, Camebridge
Sterile hood, Herasafe KS12	Thermo Scientific
Thermocycler primus 96 advanced	Peqlab Biotechnologie GmbH, Erlangen
Thermomixer 5436	Eppendorf AG, Hamburg
Thermomixer Comfort	Eppendorf AG, Hamburg
Vortex mixer Reax top	Heidolph
Water bath	Gesellschaft für Labortechnik GmbH, Burgwedel

2.1.3 Enzyme

Enzyme	**Manufacturer**
ECORI	New England Biolabs, Frankfurt
SalI	New England Biolabs, Frankfurt
SacII	New England Biolabs, Frankfurt
NheI	New England Biolabs, Frankfurt
XhoI	New England Biolabs, Frankfurt
T4 DNA Ligase	TaKaRa Biochemical, Berkeley

2.1.4 Kits

Kit	**Manufacturer**
BCA Protein Assay Kit	Pierce
MBS Mammalian Transfection Kit	Stratagene, La Jolla
NucleoBond PC 500 (Maxi)	Macherey-Nagel, Düren
NucleoSpin Plasmid (Mini)	Macherey-Nagel, Düren
QIAquick Gel Extraction Kit	QIAGEN GmbH, Hilden
QIAquick PCR Purification Kit	QIAGEN GmbH, Hilden
TaKaRa DNA Ligation Kit	TaKaRa Biochemical, Berkeley

2.1.5 Antibodies

Primary antibody	Manufacturer	Dilution in Western Blot
Mouse anti-HumanTransferin Receptor, monoclonal, Clone H68.4	ZYMED Laboratories	1: 500
Rabbit anti-Caveolin1, polyclonal, (N-20) SC-894	Santa Cruz	1: 1000
Rabbit anti-dsRED, polyclonal	Clontech	1:1000
Rabbit anti –GFP, polyclonal	AG Nickel, affinity purified	1:300
Mouse anti-GAPDH	Ambion	1:4000
Goat anti-MVD, polyclonal	Santa Cruz	1:1000
Rabbit anti-NEDD8, monoclonal	EPITOMICS	1:500
Mouse anti-PKC, monoclonal	Abcam	1:3000
Secondary antibody	**Manufacturer**	**Dilution in Western Blot**
Goat anti-mouse Alexa Fluor 680	Molecular Probes, Leiden	1:5000
Goat anti-rabbit Alexa Fluor 680	Molecular Probes, Leiden	1:5000

Table 1 Antibodies used in the current study

2.1.6 Plasmids

Plasmid	Application	Resistance	Origin
pIRES-dsRED	Cloning	Kanamycin	Clontech

Table 2 Plasmid used in the current study

2.1.7 Bacteria and media

Bacteria	Manufacturer
Subcloning Efficiency DH5α Chemically Competent *E.coli*	Invitrogen, Groningen

Table 3 Bacteria used in the current study

LB-Medium:	10 g	NaCl
	10 g	Tryptone
	5 g	Yeast Extract
	ad 1 l	H_2O MilliQ

For plate preparation, Agar was added with a final concentration of 16 g/l.

2.2 MOLECULAR BIOLOGICAL METHODS

2.2.1 PCR

PCR is a standard method for selective amplification of nucleic acid. DNA template defined by a forward and reverse primer was amplified in high amounts and could be used for further cloning to generate desired reporter constructs.

Following reaction mix was used for PCRs:

Sample reaction (total 50µl)

5 µl 10X Reaction Buffer

5 µl $MgCl_2$

0,5µl Taq

1µl dNTP

1µl Forward Primer

1µl Reverse Primer

1µl DNA template

35.5 µl H_2O

Thermal cycling program

Initial denaturation	95°C for 2 min	
Denaturation	95°C for 45 sec	
Primer-annealing	Tm of primers for 1 min	30 cycles
Elongation	72°C for 1 min	
Final elongation	72°C for 10 min	

Name	Sequence
NAE1 443-479 for	GGGGATCCGGCCAGGAGTATCTAACTATCAAG
NAE1 443-479 rev	GTAATGGTGAAAGATGATTATGTCTAGGTCGACCC
NEDD8 for	GGAATTCGCCACCATGGATTACAAGGATGACGACGATAAG
	CTAATTAAAGTGAAGACGCTGACCGGAAAGGAGATTG
NEDD8 rev	CGTCGACTCACTGCCTAAGTCCTCTCAGAGCCAACAC
UBA3 for	CGAATTCGCCACCATGGATTACAAGGATGACGACGATAAGGCTGTTGATGG
	TGGGTGTGGGGACAC
UBA3 rev	CGTCGACTTAAGAAGTAAAATGAAGTTTGAATAGTACAGTCTGTGGGGTGG
UBC12 for	CGAATTCGCCACCATGGATTACAAGGATGACGACGATAAG
	ATCAAGCTGTTCTCGCTGAAGCAGCAGA
UBC12 rev	CGTCGACCTATTTCAGGCAGCGCTCAAAGTAGGTGGAGC
Mouse NAE1 for	GAGATCTGCCTCCATGGATTACAAGGATGACGACGATAAG
	GCGCAGCCAGGGAAGATACTCAAGGA
Mouse NAE1 rev	CGTCGACCTACAACTGGAAAGTTGCAGAAGTTTGTGACATAC

Table 4 Primers used for cloning of DNA constructs

2.2.2 PCR purification

PCR products were purified by using PCR purification kit (QiaQuick PCR purification kit, Qiagen) following the manufacturer's manual. An appropriate volume of MilliQ H_2O was used for elution of the amplified DNA.

2.2.3 Restriction digest

Restriction endonuclease was used to perform the digestion of target vectors or PCR products for further cloning experiments. Restriction endonuclease is an enzyme which cuts double-stranded or single stranded DNA at specific recognition nucleotide sequences (restriction sites), which vary between four and eight nucleotides, resulting sticking or blunt ends. Depending on the enzyme and the quality of the DNA 1 to 5 U/µg DNA were used for a restriction digest.

Sample reaction (total volume 20 µl)

2 µl Digestion Buffer (New England Biolab)

5 µl DNA

0.5 µl Digestion enzyme

0.5 µl Digestion enzyme

12 µl H_2O

All the reactions were carried out at 37°C for at least 2 hours.

2.2.4 DNA dephosphorylation

Calf Intestinal Alkaline Phosphatase (CIP, New England Biolabs), an enzyme that can dephosphorylate the 5´phosphat group of DNA, was applied for preventing the self-ligation of digested vectors. The enzyme was used in a concentration of 1 U/µg DNA for 30 min at 37°C and subsequently inactivated at 70°C for 10 min.

2.2.5 Agarose gel electrophoresis

Agarose gel electrophoresis separates DNA and RNA fragments by their length. For visualization of the DNA, ethidiumbromide was added into the gel with a final concentration of 0-5 µg/ml. Agarose gels were documented using Gel Doc 2000 imaging system (Bio-Rad).

Fragment	Base pairs	DNA mass ng
1	10,002	42
2	8,001	42
3	6001	50
4	5001	42
5	4001	33
6	3001	125
7	2000	48
8	1500	36
9	1000	42
10a	517	42
10b	500	42

Table 5 DNA marker (1kb ladder from "New England Biolabs")

2.2.6 Gel extraction of DNA fragments

Digested DNA was separated on a 1% agarose gel by using agarose gel electrophoresis. After cutting out the desired bands, QIAquick Kits were employed for purification the

DNA by removing enzymes, salts, agarose, ethidium bromide, and other impurities from DNA samples following manufacturer's protocol.

2.2.7 Ligation of DNA fragments

The enzymatic recombination of DNA fragments was performed with T4 DNA-ligase (Promega). The 3´-Hydroxy-End with 5´-phosphat-End

Ligation into pGEMT vector

2 µl PCR products
1µl pGEMT Vector
5µl Ligase buffer
1µl T4-Ligase
1µl H_2O
Incubation at 16°C for 45 min

Ligation into pIRES-dsRED vector

The double-stranded oligonucleotides were inserted into the vector by ligation using the TaKaRa Ligation Kit (TaKaRa Biochemical). The appropriate amount of insert (1:1 molecular ratio vector to insert) can be calculated with the following equation:

$$\frac{\text{amount vector [ng]} \times \text{number of basepairs insert [bp]}}{\text{number of basepairs vector [bp]}} = \text{amount insert [ng]}$$

The ligation reaction was performed following the instructions of the manufacturer and incubation was carried out at 16°C for 2 h. For each ligation several reaction mixes were created, each containing a different molecular ratio of insert to vector (1:1, 3:1, 6:1).

A typical ligation reaction:		
	vector	x µl (at least 200 ng)
	insert	x µl
	solution I	10 µl
	H_20	ad 20 µl

2.2.8 DNA sequencing

Samples of 30 µl (50-100 ng/µl) were sent to GATC Biotechnology AG, Konstanz for sequencing. The sequencing procedure is according to the standard Sanger method (Sanger et al., 1977).

2.2.9 Bacterial transformation

Chemical competent DH5α cells were used for the bacterial transformation. Fifty µl competent cells were mixed with the ligation mix and incubated on ice for 20 minutes. Subsequently, the cells were heat-shocked for 45 seconds in a water bath at 42°C and immediately returned to iced for 2 minutes. 950 µl LB-medium was then added to the cells and incubated at 37°C for 1 hour at 450 rpm in a thermo block.

2.2.10 Isolation RNA from cultured cells

Isolation of RNA from cultured cells was carried out by using RNeasy Mini Kit (Qiagen). This kit allows the specific binding of RNA to a silica-based membrane. Following the manufacture's protocol, high-quality RNA is eluted from the membrane in 30-100 µl water.

2.2.11 Realtime-PCR

RNA isolated from cultured cells was used for the cDNA synthesis. Following steps were used for the synthesis of cDNA from RNA:

1µg RNA

2µl oligo dT primer (Promega)

ad 20µl H_2O

For annealing of oligo dT primer is annealed at 70°C for 10 minutes. Subsequently the reaction mix was placed on ice for at least 5 minutes.

Extension step:

6,4µl (25 mM) $MgCl_2$

8µl 5X reaction buffer

4µl (10 mM) dNTP mix

1µl Recombinant RNasin Ribonuclease Inhibitor

1µl ImPRom-II Reverse transcriptase

The reverse transcription reactions were first annealed at 25°C and then incubated at 42°C for 60 minutes and subsequently at 95°C for 5 minutes for the inhibition of reverse transcriptase.

Realtime PCR

TaqMan Gene Expression Assays (Applied Biosystems) were applied for the Realtime PCR. Predesigned gene specific probes were purchased for the performing quantitative gene expression studies. A reporter dye (FAM^{TM} dye) is linked to the 5´end of the probe. During PCR, the TaqMan MGB probe anneals specifically to a complementary sequence between the forward and reverse primer sites. When the probe is intact, the proximity of the reporter dye to the quencher dye results in suppression of the reporter fluorescence, primarily by Förster-type energy transfer. Only probes hybridized to the target will be cleaved by the DNA polymerase. Cleavage separates then the reporter dye from the quencher dye, which results in increased fluorescence by the reporter. Polymerization of the strand continues, but because the 3´end of the probe is blocked, no extension of the probe occurs during PCR. GAPDH was used for as an endogenous control.

10 µl TaqMan Gene Expression Assays (20X)

1.8µl Forward primer 10µM

1.8µl Reverse primer 10µM

1µl TaqMan MGB probe 5µM

4.4µl ddH_2O

1µl cDNA

---

total 20 µl

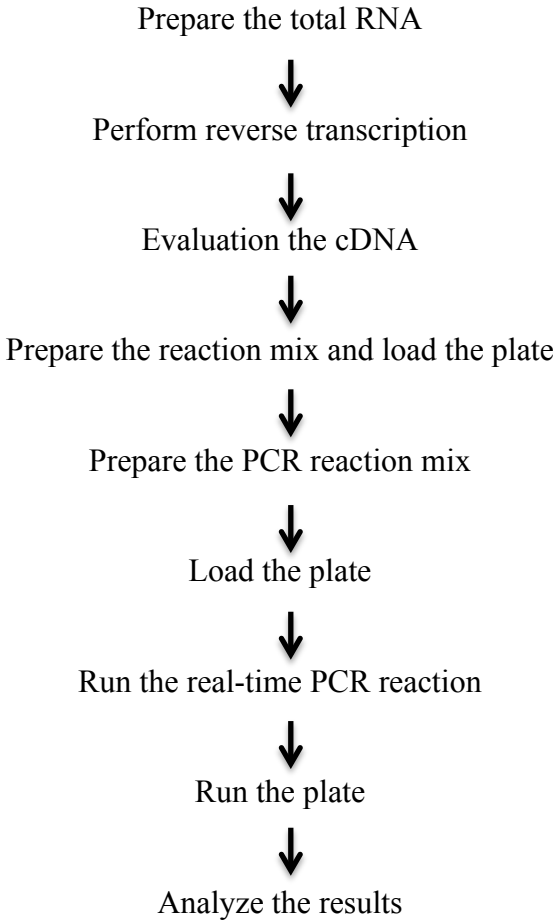

2.2.12 Plasmid transient transfection

FuGENE HD Transfection Reagent was used for plasmid transfection. For 6-well transfection, 2 µg DNA was diluted to a final volume of 50 µl Opti-MEM. 4 µg FuGENE HD was diluted to final volume of 50 µl Opti-MEM without allowing contact with the walls of plastic tube. Both pre-diluted reagents were then mixed and incubated for 20 minutes at room temperature. Thousand and four hundred µl Opti-MEM was then added to each well containing cells. The DNA-FuGENE HD complex were then added to the cells and incubated at 37°C in a CO_2 incubator at least 20 hours post-transfection.

2.3 EUKARYOTIC CELL CULTURE TECHNIQUES

2.3.1 Maintaining the cell lines

Cells were grown at 37°C in a CO_2-incubator at 100% humidity. New thawed cells were treated with mycoplasma Removal Agent (MP, Inc.) to avoid mycoplasma contamination. MRA was added in a 1:100 (0.5" g/ml) dilution to the medium and left on for 7 days.

PBS (Phosphate buffer saline):

140 mM	NaCl
2.7 mM	KCl
10 mM	Na_2HPO_4
1.8 mM	KH_2PO_4

2.3.2 Freezing of eukaryotic cells

After detaching cells by using Trypsin/EDTA, cells were suspended in growth medium and transferred to a 50 ml tube. The suspension was then centrifuged at 200 g for 3 minutes. Cells were then suspended in 2 ml freezing medium and transferred to cryo-vial (Greiner) at stored at -80°C. Frozen cryo-vials were removed to liquid nitrogen tanks for long-term storage.

Freezing medium:

20% (w/v)	FCS
10% (w/v)	DMSO
100 " g/ml	streptomycin/penicillin
plain DMEM	

2.3.3 Thawing of eukaryotic cells

Frozen cells were thawed at 37°C in a water bath and subsequently added to pre-warmed 20 ml complete medium. For removing DMSO in the medium, cells were centrifuged at 200 g for 3 minutes and suspended in complete medium. As the last step, cells were stored in a incubator at 37°C with 5% CO_2 for maximum 6 weeks.

2.3.4 Doxycycline-dependent protein expression

To induce the expression of reporter constructs by the retroviral expression vector pRev-TRE2 containing the doxycycline-responsive element, doxycycline (Clontech) was added to the complete medium in a final concentration of 1 g/ml.

2.4 SHORT INTERFERING RNA (siRNA) IN MAMMALIAN CELLS

2.4.1 Liquid-phase Transfection of Mammalian Cells with siRNAs

RNA interference is an RNA-dependent gene silencing process that is controlled by RNA-induced silencing complex (RISC). RNAi pathway is initiated by the enzyme Dicer, which cleaves long double-stranded RNA into 22 nucleotide small interfering RNAs. The siRNAs are incorporated into a multicomponent nuclease RISC. RISC then uses the unwound siRNA as a guide to substrate selection and in this way causing specific gene silencing.

For 6-well RNAi transfection

10 µl of a 20 µM stock was diluted in 175 µl Opti-MEM Reduced Serum Medium. 4 µl Oligofectamine was then diluted to a final volume of 15 µl. Subsequently the diluted oligonucleotides was combined with diluted oligofectamine and incubated for 20 minutes at room temperature. Growth medium from the cells were removed and washed once with medium without serum. Thousand and three hundred µl medium without serum was then added to each well containing cells. The siRNA-Oligofectamine complex were then added to the cells and incubated at 37°C in a CO_2 incubator at least 24 hours post-transfection.

2.4.2 Reverse Transfection of mammalian Cells with siRNAs

HeLa cells were seeded on coated 8-well plates or 384-well plates containing immobilized transfection reagent mix. For 48-60 hours knockdown time on siRNA-coated 8-well LabTek imaging chambers (Nunc), 4000 cells were seeded in 0,35 ml cultivation medium on each Labtek. Medium was replaced 36 hours post-transfection to prewarmed DMEM containing 1 µg/ml doxycycline. For 48 hours total knockdown time on 384 wells siRNA arras, 120 00ß cells were seeded in 3.5 ml cultivation medium on each plate.

2.4.3 Preparation of siRNA-coated 8-well Plates

For coating 8-well plates, 3 µM silencer select siRNA (Ambion) or 30 µM silencer siRNA (Ambion) was added to 6.5 µl of transfection mix and further incubated for 30 minutes at room temperature. 7.25 µl gelatin solution was added to yield a fian lvolume of 18.75 µl. 16 µl of 18.75 µl siRNA-containing transfection mix were then diluted with 800 µl H_2O. 100 µl diluted siRNA/TXFN/gelatin mix was transferred to each well on the 8-well plate. The solution was dried in a MiVac Concentrator (Genevac) at 50°C for 40 minutes. Caoted 8-well plates can be sotred at room temperature in the presence of drying pearls (Fluka) for several months.

Sucrose/Opti-Mem Solution:
1.37 g sucrose in 10 ml OptiMEM

0.2% gelatione solution:
0.2 g gelatin in 100 ml H_2O (heated to 56°C for 20 min, filter by 0.45 µm filter)

2.5 LIVE-CELL FLUORESCENCE MICROSCOPY

2.5.1 Widefield and Confocal Fluorescence Microscopy

30 minutes before imaging of live cells, prewarmed CO_2 independent medium (Invitrogen) was used containing 0.2 µg/ml Hoechst 33342 (Sigma) for staining cell nuclei. Axiovert 200M flurescence microscope (Zeiss) or a LSM 510 confocal microscope (Zeiss) was applied for the imaging.

2.5.2 Automated Widefield Fluorescence Microsocpy

For automated microscopy, prewarmed CO_2 independent medium (Invitrogen) was used containing 0.2 µg/ml Hoechst 33342 (Sigma) for staining cell nuclei, subsequently subjected to live-cell imaging on a Scan^R screening station (Olympus).

2.5.3 Image Quantification

We used Bodiy-Cer-Tx to identify the perinuclear area containing potential accumulation sites for reporter proteins. Further, we quantified the intracellular accumulation of reporter protein per cell. Z-stacks of cells were taken under identical parameters and exposure time. Only the stacks containing potential accumulation sites for reporter

proteins, which are marked by Bodipy-Cer in red, are considered for the calculation afterwards. For each stack, the intracellular accumulation site of reporter proteins was defined as Area of Interest (AOI). Integrated intensity of AOI and total signal of each slice was then measured using ImageJ. Afterwards, both values were summed up respectively and the percent of intracellular accumulation of reporter protein was calculated by the value of AOI divided by the total signal value.

2.6 BIOCHEMICAL METHODS

2.6.1 Determination of total protein concentration

Determination of protein concentration was carried out by using Pierce BCA Protein Assay Kit (Thermo Scientific). The Pierce BCA Protein Assay is a detergent-compatible formulation based on bicinchoninic acid (BCA) for the colorimetric detection and quantitation of total protein. The macromolecular structure of protein, the number of peptide bonds and the presence of four particular amino acids (cysteine, cystine, tryptophan and tyrosine) are reported to be responsible for color formation with BCA. Accordingly, protein concentrations generally are determined and reported with reference to standards or a common protein such as bovine serum albumin (BSA). A series of dilutions of know concentration are prepared from the protein and assayed alongside the unknown before the concentration of each unknown is determined based on the standard curve.

2.6.2 SDS-PAGE (sodium dodecyl sulphate polyacrylamide gel electrophoresis)

The purpose of this method is to separate proteins according to their size and not by other physical feature. The electrophoretic mobility of a protein depends not only on its length of a polypeptide chain or its molecular weight but also on posttranslational modifications. The anionic detergent SDS is for the denaturation of proteins and to apply a negative charge to each protein. Therefore, the proteins will move towards the positive charged electrode while the separation. SDS binds to proteins in proportion to their mass resulting in an approximately uniform mass to charge ratio for most proteins. Therefore it can be assumed that the migration distance of a protein is directly related to its size.

Sample preparation

Protein samples were boiled with 4X sample buffer at 95°C for 10 minutes. SDS-PAGE consists of acrylamide, bisacrylamide, SDS, Tris-Cl buffer with adjusted pH. Ammonium persulfate (APS) and TEMED were added when the gel was ready to be polymerized.

4x Sample buffer:	1.25 ml	0.5 M Tris-HCl, pH 6.8
	2.5 ml	Glycerol
	2.0 ml	10% (w/v) SDS
	0.2 ml	0.1% (w/v) Bromphenol blue
	0.5 ml	14.3 M ß-Mercaptoethanol
	3.55 ml	H_2O_{MilliQ}

SDS: (Sodiumdodecylsulfate) is an anionic detergent that denatures protein to polypeptides. When a protein mixed with SDS is heated at 95°C, SDS wraps the around the polypeptide backbone. It binds polypeptides in a constant weight ration of 1.4g/G of polypeptide. Intrinsic charges of polypeptides becomes negligible due to the negative charge contributed by SDS. As a result protein become negatively charged in proportion to its length.

β-mercaptoethanol: is used for the reduction of disulfide bridges in protein.

Preparation of Mini gels

Separation gel was poured between two glasses fixed in a casting frame and after polymerization stacking gel was poured on the top of separation gel. Subsequenetly, a plastic comb was inserted from the top to form the loading wells. After polymerization the gel was ready for analysis.

Electrophoresis was performed using the PROTEAN III system (BIO-RAD).Electrophoresis was performed at 200 volt for about 55 minutes.

Running buffer:	25 mM	Tris-HCl, pH 8.3
	192 mM	Glycine
	0.4% (w/v)	SDS

Substance	12% separation gel	4% stacking gel
H_2O	13.4 ml	12.2 ml
1.5 M Tris HCl pH 8.8	10	5
SDS 10%	400 µl	200 µl
Acrylamid/Bis 30% w/v	16 ml	2.66 ml
APS 10%	300 µl	200 µl
TEMED	30 µl	40 µl
Sum	40 ml	20 ml

Table 6 Gel solutions for 10 SDS-gels

Electrophoretic separation using Midi gels (NuPAGE-System)

4%-12% Bis-Tris gradient Midi gels (Invitrogen) were used to obtain a better resolution of protein bands in the low molecular weight range. These gels were used in combination with Midi Gel adaptors and the Criterion™ cell gel chamber (BioRad). After filling up with MES running buffer, 200 V was applied for approximately 45 min.

MES running buffer: 50 ml NuPage MES buffer 20 x
950 ml H_2O_{MilliQ}

In the upper buffer chamber, MES running buffer was supplemented with NuPage-antioxidant (150µl / 60 ml running buffer)

2.6.3 Western blot analysis

Proteins separated by SDS-PAGE were transferred to polyvinylidene fluoride (PVDF) membrane for immunodetection afterwards.

Transfer to PVDF-FL membrane

PVDF-FL membrane was activated by methanol for approximately 1 min and then transferred to blotting buffer. Sponges and Whatman paper were transferred into blotting buffer. The blotting apparatus was assembled as following order:

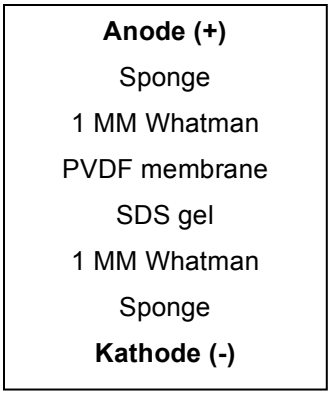

The western blot was carried out at a constant voltage of 100 V for 60 minutes.

Blotting buffer:	40 mM	Glycine
	25 mM	Tris Base
	20%	Methanol
	H_2O	ad 1x

2.6.4 Separation of detergent-resistant membranes (DRMs)

Preparation of cell lysates

Cells were washed twice with cool PBS. Subsequently, 1 ml of 0.5 mmol EDTA/PBS was added to the cells and incubated at 37°C for 10 min. Cells were scraped by cell-scraper and transferred in an eppendorf tube. After centrifugation at 400g for 3 min at 4°C, pellets were resuspended in 100 µl PBS containing 1% Triton-X-100 with Protease Inhibitor Cocktail (Roche). Cells were lysed during the 30 min-incubation time on ice. This cell suspension was further lysed with a 27-gauge needle 14 times. Lysate was then centrifuged at 800 g for 5 min at 4°C.

DRM preparation

45 µl cell lysate was homogenized with 90 µl of 60% Optiprep by intensive vortexting resulting in a 40% Optiprep resolution. This fraction was loaded in the bottom of SW 50.1 polyclear centrifuge tube (Beckman). A layer of 375 µl 28% Optiprep solution was loaded on the top of the last fraction. Finally, 90µl MBS 1% Triton X-100 were covered on the top of the gradient. By using SW 50.1 rotor (Beckman), the gradient was centrifuged at 100.000 g and 4°C for 3 hours. After centrifugation, 8 fractions of 45 µl

were taken starting from the top of gradient. 36 µl of each fraction was loaded on SDS-PAGE for further analysis.

MBS buffer:	20 mM	MES pH 6.5 (NaOH)
	150 mM	NaCl
	1% (w/v)	Triton X-100
	Roche Protease Inhibitor Cocktail without EDTA	

3 Results

Src proteins are non-receptor tyrosine kinases that play key roles in regulating cell proliferation, differentiation, migration and cell-shape changes (Brown and Cooper, 1996; Thomas and Brugge, 1997). Src-family tyrosine kinases are composed of: (1) an N-terminal Src homology SH4 domain conferring membrane binding via one or several acylations (2) a poorly conserved domain, (3) an SH3 domain binding specific proline-rich sequences and mediating protein-protein interactions, (4) an SH2 domain, which can bind to specific sites of tyrosine phosphorylation, (5) an SH1 tyrosine kinase catalytic domain which contains an autophosphorylation site and mediates enzymatic activity (6) a C-terminal negative regulatory tail for autoinhibition of the kinase activity (Brown and Cooper, 1996; Thomas and Brugge, 1997). The N-terminal SH4 domain modified by fatty acylation is responsible for membrane attachment and targeting to plasma membranes. However, the underlying molecular mechanism of the targeting of SH4-domain containing proteins remains elusive. In this work we aimed to validate the gene products identified in a previous genome wide RNAi screen and to further characterize their molecular functions of targeting SH4 proteins to plasma membranes. We validated several hits identified in the primary screen, namely COPB1, ARCN1, PRKCA, MVD and NAE1 by using microscopy-based RNAi screening and aimed to characterize their roles in trafficking of Sh4-domain-containing proteins in more detail. Further, we investigated the potential roles of NAE1 and cellular neddylation in SH4-domain-dependent trafficking to the plasma membrane.

3.1 VALIDATION AND CLASSIFICATION OF GENE PRODUCTS IDENTIFIED DURING PRIMARY SCREEN

In a previous study, a genome wide RNAi screen was performed using an automated microscopy platform to identify gene products involved in intracellular targeting and transport of SH4 reporter proteins to the plasma membrane. HeLa cells expressing fusion proteins of SH4-HASPB and SH4-YES in an inducible manner by doxycycline were used

to identify components of the transport machinery required for plasma membrane delivery of SH4-domain-containing proteins. To silence all around 22.000 genes of human genome, HeLa cells were reverse transfected with a genome-wide siRNA library consisting of more than 50.000 siRNAs by cultivation of cells on 384-spot siRNA arrays. Generated microscopy data were evaluated by applying a software-based image analysis module, which can detect and quantify intracellular retention of SH4 fusion proteins. All together 286 genes were identified in the primary screen by application of suitable score thresholds. In the current study, 286 genes were validated by automated microscopy-based screen. A subset of these was subjected to manual-based validation experiments enabling as to validate candidate genes with a particularly strong effect on SH4-dependent transport in a faster and more detailed approach.

3.1.1 Manual microscopy-based validation approach

We selected 12 candidate gene products identified in the primary screen that showed a strong intracellular retention of SH4 reporter proteins after respective siRNA treatments (Table 7). To validate these 12 candidate gene products, we used two independent siRNAs targeting different regions of each mRNA and subjected doxycycline-inducible HeLa cells expressing SH4-HASPB-GFP and SH4-YES-mCherry directly to wide field microscopy after siRNA treatments. With manual microscopy-based approach, we were able to image the cells at two different time-points, 48 hours and 60 hours post siRNA transfection. Manual microscopy-based validation was less time consuming compared to the complete validation screen of 286 gene products by using automated microscopy, which was done in parallel. We validated 5 gene products: NAE1, PHF5A, CCDC43 and GALTNL4 as well as MAK10 in the manual microscopy-based approach that showed a pronounced intracellular accumulation of SH4-proteins after respective siRNA treatments by manual inspection.

Gene Symbol	*Entrez Gene ID*	*RefSeq*	*siRNA ID*	*Antisense siRNA Sequence*
ANKRD20A	84210	NM_032250	s38654	UAUGAAAAUCCCGAUUUGGAG
ANKRD20A	84210	NM_032250	s226643	GUUGGUUCAAGUUGUUUUGCT
ARMC8	25852	NM_014154	s24623	AACCAAACAAGGUAAUGUCTT
ARMC8	25852	NM_014154	s24624	UAGUAGGUGAGCAAUAUUCTG
BIN3	55909	NM_018688	s31762	AAAGAUCUUGUGCAUUUCCGA
BIN3	55909	NM_018688	s31763	UAAGGGCUCGAUCACAGUCTT
CCDC43	124808	NM_144609	s42802	UUUCUGACCAUCGUUCCACAA
CCDC43	124808	NM_144609	s229298	UACGAUUUGUGCCUGCUUCTC
C9orf116	138162	NM_001048265	s44091	UACACGGAGACAGCCUUCUGG
C9orf116	138162	NM_001048265	s44092	UUACUGGUCCUGUACACGGAG
EIF4A3	9775	NM_014740	s18876	UUCACGAACCUGAAUAUCCAA
EIF4A3	9775	NM_014740	s18877	UGAUCUGCUUGAUUGCUCGTT
FAM3C	10447	NM_001040020	s20439	AUUAUUCUUAACACCACUCAT
FAM3C	10447	NM_001040020	s20440	UUUGUCUUAAUGCCCUUCCCA
GALNTL4	374378	NM_198516	s51535	UGCCGGUCCACAAUGAAGCAG
GALNTL4	374378	NM_198516	s51536	AAAGUUGUCAUAUUUGAUGTT
MAK10	60560	NM_024635	s34135	UUUACGUACUUUGCCGUCCAT
MAK10	60560	NM_024635	s34136	UGAACUGUAAGUAGUGCACTG
NAE1	8883	NM_001018159	s16975	UAUACGUUUUAGGUAUUCGTC
NAE1	8883	NM_001018159	s16976	UGGAGUAUGACUGUGGUCCTT
NKD1	85407	NM_033119	s39961	UUUCUCCUCUCGAUGUUCUCA
NKD1	85407	NM_033119	s39962	UUCUAUCCCGGCGAGAUCUAA
PHF5A	84844	NM_032758	s39505	ACUCCUUACAAUAAUAGGCAT
PHF5A	84844	NM_032758	s39506	AUAGGAGUCACAAAUCACACA

Table 7 Manual validation approach of selected gene products from primary genome wide RNAi screen

Manual validation approach of five gene products involved in SH4-dependent transport

For the manual validation approach, siRNAs were coated on the 8-well Lab-Teks and were subsequently reverse transfected into HeLa cells expressing SH4-HASPB-GFP and SH4-YES-mCherry for 36 or 48 hours before protein expression was induced by doxycycline for additional 12 hours. Subsequently, treated HeLa cells were subjected to live-cell wide field microscopy to determine the localization of both SH4 fusion proteins. We were able to validate 5 gene products including NAE1, PHF5A, CCDC43 and GALTNL4 as well as MAK10 that showed a clear intracellular accumulation of SH4-proteins after respective siRNAs treatments by manual inspection.

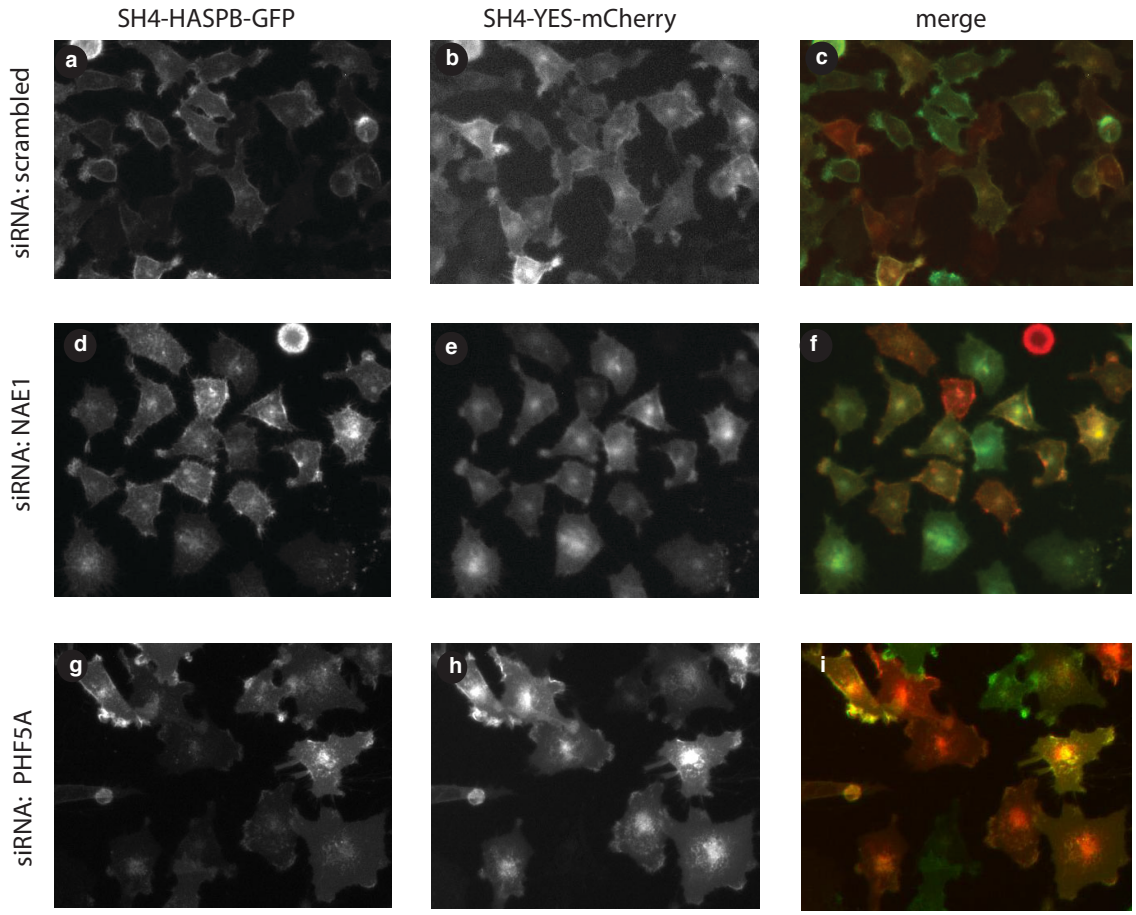

Figure 12 Characterization of NAE1 and PHF5A as components in SH4-dependent protein transport. HeLa cells expressing SH4-HASPB-GFP and SH4-YES-mCherry were reverse transfected with a scrambled siRNA (a-c) and a siRNA (s16975) against NAE1 (d-f) and a siRNA (s39506) against PHF5A. 48 hours post siRNA transfection cells were subjected to live-cell wide field microscopy to determine the localization of both SH4 fusion proteins by manual inspection (cutouts of 10X magnification images).

Figure 12 shows original wide-field microscopy data from the manual validation approach. HeLa SH4-HASPB-GFP and SH4-YES-mCherry cells were cultivated on siRNA-coated LAB-TEKs for 36 hours before protein expression was induced with doxycycline for additional 12 hours. Transfection of a siRNA direct against NAE1 results in a pronounced perinuclear retention of SH4-HASPB-GFP and SH4-YES-mCherry (Figure 12 d-f). NAE1 was first identified as a novel binding partner of the cytoplasmic domain of amyloid precursor protein (APP) and was thus called as APP binding protein 1 (APP-BP1) (Chow et al., 1996). The interaction of APP and NAE1 was shown to activate Rab5-dependent endocytosis in a neddylation-independent manner (Laifenfeld et al., 2007). In addition, NAE1 is involved in activation of the ubiquitin-like protein NEDD8

and participates in the neddylation pathway (Gong and Yeh, 1999). Similar to ubiquitination, ATP-dependent NEDD8 activation is initiated by NEDD8 E1 enzyme NAE1-UBA3. This heterodimer of NAE1 and UBA3 is homologous to the N- and C-terminal domains of ubiquitin-activating enzyme, respectively (Liakopoulos et al., 1998; Osaka et al., 1998; Walden et al., 2003). Another validated hit PHF5A is a nuclear protein, which is a subunit of the splicing factor 3b complex. Treatment against PHF5A also causes intracellular accumulation of SH4 reporter proteins as shown in Figure 12 g-i.

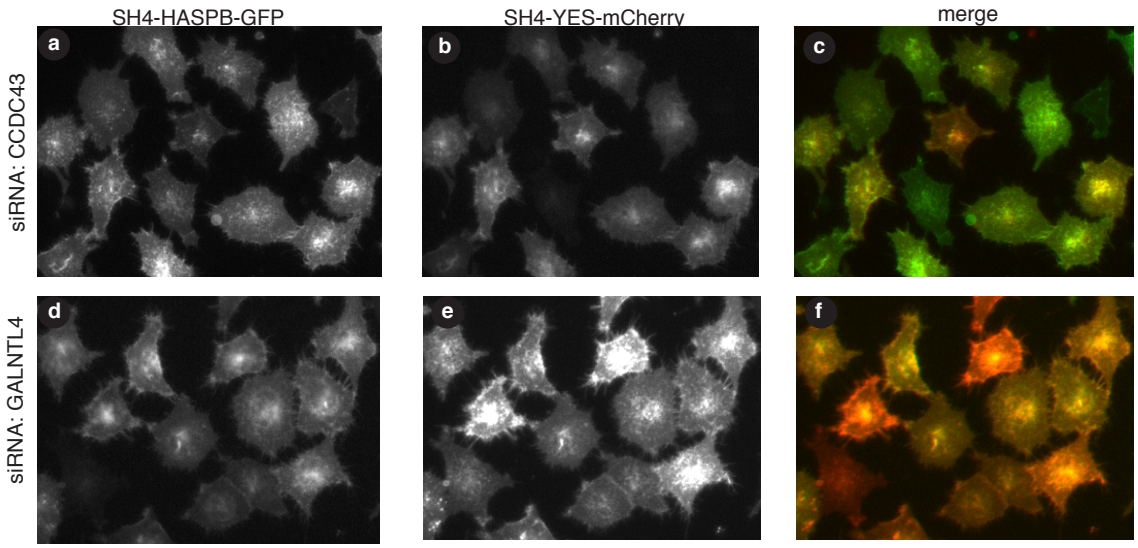

Figure 13 Characterization of CCDC43 and GALNTL4 as components in SH4-dependent protein transport. HeLa cells expressing SH4-HASPB-GFP and SH4-YES-mCherry were reverse transfected with a siRNA (s42802) against CCDC43 (a-c) and a siRNA (s34135) against GALTNTL4 (d-f). 48 hours post siRNA transfection cells were subjected to live-cell wide field microscopy to determine the localization of both SH4 fusion proteins by manual inspection (cutouts of 10X magnification images).

Figure 13 shows original widefield microscopy data from the manual validation approach. Treatment with a siRNA direct against coiled-coil domain containing 43 (CCDC43) results in a pronounced intracellular retention of both SH4-proteins. So far the molecular function of CCDC43 is still unknown. A similar phenotype can be observed after siRNA treatment against putative polypeptide N-acetylgalactosaminyltransferase-like protein 4 (GALNTL4), which is an integral membrane protein and localizes to Golgi apparatus. According to similarity analysis, GALNTL4 may catalyze the initial reaction in O-linked oligosaccharide biosynthesis, the transfer of an N-acetyl-D-galactosamine residue to a serine or threonine residue on the protein receptor.

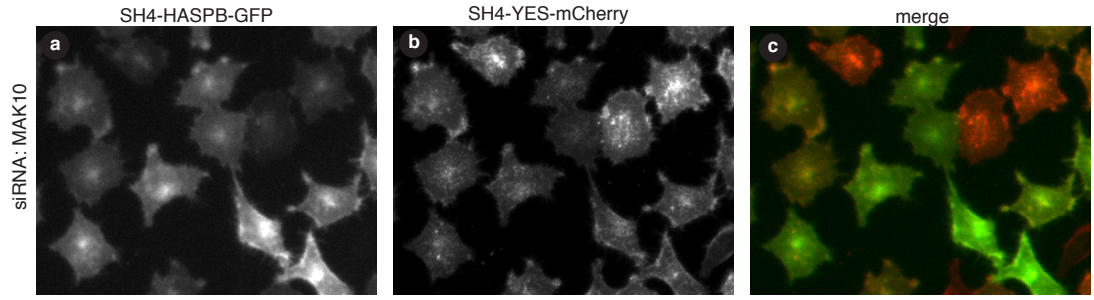

Figure 14 Characterization of MAK10 as a component in SH4-dependent protein transport. HeLa cells expressing SH4-HASPB-GFP and SH4-YES-mCherry were reverse transfected with a siRNA (s34135) against MAK10 (a-c). 48 hours post siRNA transfection cells were subjected to live-cell wide field microscopy to determine the localization of both SH4 fusion proteins by manual inspection (cutouts of 10X magnification images).

Figure 14 shows original wide-field microscopy data from the manual validation approach. Treatment with a siRNA direct against N-alpha-acetyltransferase 35, NatC auxiliary subunit (MAK10) results in a pronounced intracellular retention of both SH4-proteins. MAK10 is a component of the N-terminal acetyltransferase C (NatC) complex and may catalyze acetylation of N-terminal methionine residues according to similarity analysis.

3.1.2 Automated microscopy-based validation approach

All together 286 genes identified in the primary screen were subjected to an automated microscopy-based validation screen (Ritzerfeld et al., 2011). HeLa cells expressing SH4-HASPB-GFP and SH4-YES-mCherry were cultivated on siRNA-coated 96-well plates for 36 hours before protein expression for additional 12 hours. Subsequently the cells were subjected to automated fluorescence microscopy and further analyzed using the automated image analysis tool (Remmele et al., 2008). Table 8 and Table 9 show the comprehensive list of 54 gene products, which are validated to be involved in intracellular transport of SH4-proteins. Validated gene products were classified into different groups according to the function, subcellular localization and membrane association. Factors involved in protein transport, lipid homeostasis and protein modifications were identified in the validation screen (Ritzerfeld et al., 2011).

A software-based image analysis tool to detect and quantify intracellular retention of SH4 fusion proteins

The challenges of automated image analysis are how to correctly recognize and segment individual cells. The software must identify the cells, determine their shape and subsequently segment each cell into different subcellular compartments. For the recognition, stained cell nuclei are detected by an adaptive threshold approach based on the Hoechst channel images. Using cell nuclei as a seeding point, cells are identified and subdivided into three different compartments: membrane, cytoplasm and nucleus (Remmele et al., 2008). The three subcellular compartments are determined according to following rules: nucleus is defined in the region-growing approach; cell membrane is defined by a specific pixel width touching the cell boundary defined in the region-growing approach; cytoplasm is comprised of the residual area of the cell which is not attributed to the nucleus or the cell membrane (Remmle, et al., 2008). Cell boundaries were identified by a region-growing approach by two criteria: (1) when intensity difference of GFP fluorescence within and outside of the cells is large, (2) when the intensity of outer pixels is lower than the intensity threshold of a given cell (Figure 15 a). For classification of individual cells, intensity features from the cell as well as the three cellular compartments were extracted and used (Remmele et al., 2008; Ritzerfeld et al., 2011). Thus a perinuclear retention of SH4-reporter proteins in the Golgi region as an example would be classified as a hit because Golgi membranes result in an increased cytoplasmic intensity compared to nuclear and membrane-associated intensities.

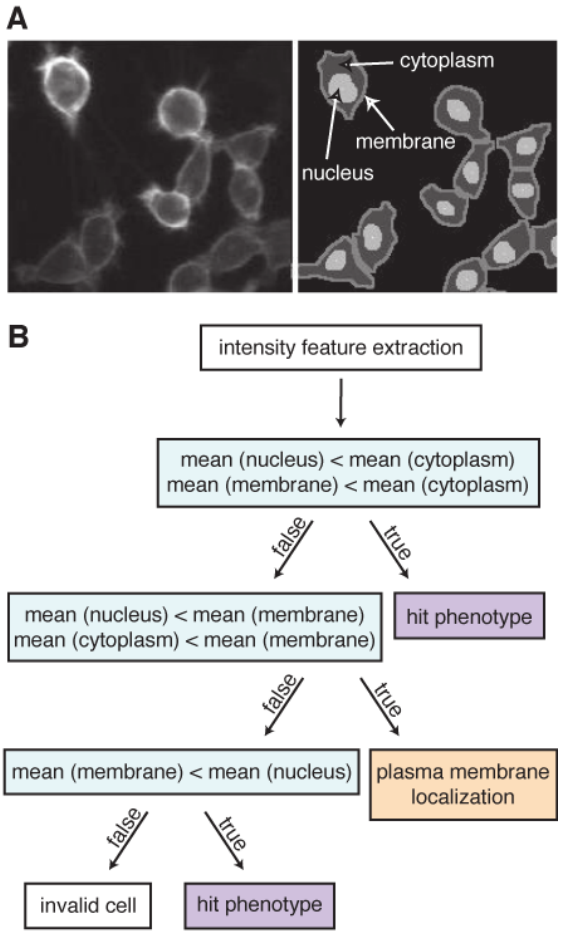

Figure 15 Cell segmentation and classification using an automated image analysis tool. (A) Individual cells were segmented into three different compartments: the plasma membrane, the cytoplasm and the nucleus. (B) Intensity features were extracted for the whole cell area and for each compartment and used for cell classification (Ritzerfeld et al., 2011).

Calculation of scores from classification results derived from the automated image analysis tool

We determined the percentage of cells displaying phenotypes and calculated the standard deviation of a complete array (all 384 spots on the same plate), which is used to determine a score for each experimental condition. These two values were used to calculate the distance of the respective spot´s percentage to the median in standard deviations of the same plate. This distance is expressed in scores. Scores above 2.5 and 3.5 for SH4-HASPB-GFP and SH4-YES-mCherry were used for primary screen, respectively. For the automated validation approach, median and standard deviation from all negative controls calculated on the same LabTek were used for the determination of

scores. Be regarding scores above 2 as hits for both SH4-reporter proteins, we were able to validate 54 gene products, whose downregulation had an impact on intracellular transport of SH4-domain-containing proteins (Table 8; Table 9).

Gene Symbol	Entrez Gene ID	RefSeq	siRNA ID	Antisense siRNA Sequence	SH4-HASPB-GFP	SH4-Yes-mCherry
Lipid Metabolism						
ACADVL	37	NM_000018	s208	AAACUGUUCAUUGACAAUCcc	3.4	6.1
MVD	4597	NM_002461	s224074	UUUUUAACUGGUCCUGGUGca		2.8
SMPDL3B	27293	NM_014474	s26101	UGCUAUGACGCGAUGAUGCtt	5.0	
SREBF2	6721	NM_004599	s28	UUUGACCUUUGCAUCAUCCaa	2.1	
Transport Factors						
COPA (α-COP)	1314	NM_004371	s3369	AAAGCGAGUUUUCUCAUCCtt	7.6	5.5
COPB1 (β-COP)	1315	NM_016451	s3371	UGGAUUAGCAUGACAGACCtt	7.0	4.2
			s3372	UCUUUGACUUUACAUCUCCtt	6.1	2.6
KIF20B	9585	NM_016195	s18420	UCGAUAUUCUUUAACUUGCtt	2.6	
			s18421	UGCUGAACUAAUACGUUUGgg	2.6	
RAN	5901	NM_006325	s11768	UUCUUGUAAGUAACUCUCGat		6.5
			s11769	UUUCCUGUCCUUAAUAUCCac		4.8
Protein Phosphorylation						
PRKCA (PKCα)	5578	NM_002737	s11093	UGCGGAUUUAGUGUGGAGCgg	4.3	3.3
PRKCB	5579	NM_212535	s11096	AAAUCGGUCAGUUUCAUCCgg	3.3	2.6
PTPRD	5789	NM_001040712	s11540	UACAUUCGCGUAUCUAUUCtt	2.4	
Other Protein Modifications						
ACY3	91703	NM_080658	s40752	UUCGCGAUUAAGCAGGUGCcc	2.8	3.2
GALNTL4	374378	NM_198516	s51536	AAAGUUGUCAUAUUUGAUGtt	2.7	
LIPT2	387787	XM_370636	s226411	AAUUGAGAAAUGACAAUCUat	5.0	5.3
NAA35	60560	NM_024635	s34135	UUUACGUACUUUGCCGUCCat	3.9	3.4
Membrane Receptors						
BAI3	577	NM_001704	s1878	UGGAUUGCUAAGCUCAUUCat	3.2	
CDH26	60437	NM_021810	s34067	AGCAGGAGUAGAGUGUAUGtt	3.1	2.8
IL7R	3575	XM_001127146	s7325	UGGUUAGUAAGAUAGGAUCca	2.5	3.5
ITGAV	3685	NM_002210	s7569	UAGGGUACACUUCAAGACCag	4.9	7.1
ITGB1	3688	NM_002211	s7575	AGCCGUGUAACAUUCCUCCag	4.4	3.2
			s7576	UAAUCGCAAAACCAACUGCtg	5.0	3.2
			s7574	UGCUGUUCCUUUGCUACGGtt	3.6	
LILRB5	10990	NM_006840	s21637	AAAAAGAAAGUGUCUAUCUga	2.4	
OR10V1	390201	NM_001005324	s52738	UCAGGGUCAGGUGAGAAUGga	2.9	2.5
TGFBR1	7046	NM_004612	s14073	AGUCUUUCAACGUAGUACCct		5.0

Table 8 Validated gene products with putative functions in the plasma-membrane targeting of SH4-proteins (part 1).

Gene Regulation and Expression						
EIF4A3	**9775**	**NM_014740**	s18876	UUCACGAACCUGAAUAUCCaa	3.3	3.9
			s18877	UGAUCUGCUUGAUUGCUCGtt	4.5	4.0
HNRNPA1	**3178**	**NM_002136**	s6710	UUAUCUGGUACCAUUAUUCaa		2.4
RPS26P35	**441377**	**XM_496991**	s54340	UCUUUAAGAACUCAGCUCCtt		3.4
RPL21P62	**442160**	**XM_001128707**	s54494	UAACUUGUUUGUUUACAACaa		2.8
RPS26P8	**644191**	**XM_930072**	s55596	UCACAUACAGUUUGGGAAGca		2.7
MBD3L2	**125997**	**NM_144614**	s42925	UGGAUUUCUCGUUUCUUCUgt	3.6	
RPL23AP82	**284942**	**NM_203302**	s49770	UCAGGACAAAUCAGGGUGGtg	3.2	2.3
PHF5A	**84844**	**NM_032758**	s39506	AUAGGAGUCACAAAUCACAca	4.2	3.5
POLR2F	**5435**	**NM_021974**	s224297	UGGCAGGUAACGGCGAAUGat	3.7	2.9
			s10809	UGUGGUGAUUCGCUUCUGGtt		2.7
PRPF8	**10594**	**NM_006445**	s20796	UCGUUGUUCACAUGUAGGGca	5.1	8.2
			s20797	AUGCGAUCAAUGUAUCUGCag	3.7	6.8
PRPF31	**26121**	**NM_015629**	s25122	UACUUAUCCCGGAUGAACUta		2.5
RPL18	**6141**	**NM_000979**	s194744	UAUAACUUGACCAACAGCCtc		3.7
			s194745	UAGGAUCCAGGGUUAGUUUtt		3.0
RPL21	**6144**	**NM_000982**	s12186	UAUCUCGGCUCUUAGAGUGct		3.0
			s12187	UAACAUUGUAGACUCUUCCag		2.9
RPS25P6	**401206**	**XM_937380**	s53508	UAAGUUAUUGAGCUUGUCCcg	3.8	3.8
SF3A1	**10291**	**NM_001005409**	s20117	UCAAUAUCCAGACCUGGUGcg		2.8
ZNF326	**284695**	**NM_182975**	s195972	UUCCAUUAAAGCCCUGAUAag		2.4
Others						
A2M	**2**	**NM_000014**	s819	UCGUUCUUAACCAUCACUGtg	3.2	2.9
ATP6AP2	**10159**	**NM_005765**	s19790	UUUCGGAAAACAACAGACCct		2.3
CACNA1S	**779**	**NM_000069**	s2297	UUCCGGUUUAUUUGGGUCCca		4.1
CHERP	**10523**	**NM_006387**	s20627	UUUGUUCUCUUCUCCGAGCct	2.8	3.1
DBH	**1621**	**NM_000787**	s3947	ACUGUGACCACCUUUCUCCca		2.7
CDC37P1	**390688**	**NM_001080829**	s52851	UCUUCAUCAUCGCUCAGUGtg		2.9
MAGEB1	**4112**	**NM_002363**	s8455	UUUAUACUUACGUAGAAUGaa	2.3	
SHC1	**6464**	**NM_003029**	s12811	AAAUGAGAUAGAUUGCAUGtg		4.0
SOBP	**55084**	**NM_018013**	s30136	AAGUAGUUCGCAGUUAUUCtt	3.4	3.5
TMEM126A	**84233**	**NM_032273**	s38695	AAUCCAGUAACUUAAGAUGtt		2.1
YAP1	**10413**	**NM_006106**	s20367	UGAUUUAAGAAGUAUCUCUga	2.2	
Unknown						
PATE2	**399967**	**NM_212555**	s53217	UAAUGAUACAUGCUCUGCCct	3.4	3.6
C12orf36	**283422**	**NM_182558**	s49233	UAGUGGAGCAUGAAGUGUCtt	3.0	
C16orf71	**146562**	**NM_139170**	s44876	UCUGGAAUCAGGGAGGUUUgg	3.2	
FAM108A1	**81926**	**NM_001130111**	s230886	UUAAUUUCCGUUUUCACGUat	2.2	

Table 9 Validated gene products with putative functions in the plasma-membrane targeting of SH4-proteins (part 2).

It is apparent from both manual and automated validation approaches a large number of gene products are identified as hits required for the intracellular trafficking of SH4 proteins. However, considering the knowledge on the hits, which is quite often limited, for example PHF5A is located in the nucleus or the function of CCDC43 is completely unknown, we decided to focus the current study on COPB1, PRKCA and MVD as well as NAE1.

3.2 ANALYSIS OF COATOMER AS A COMPONENT OF SH4-DOMAIN-DEPENDENT PROTEIN TARGETING

Previous studies on palmitoylation suggested that bulk palmitoylation occurs on the Golgi and this organelle provides directionality in the acylation cycle by allowing locally palmitoylated proteins to enter the secretory pathway from where they are targeted to the plasma membrane (Rocks et al., 2010). We tested the hypothesis that the general components of intracellular transport specifically the heterooligomeric coatomer complex might be required for correct targeting of SH4-proteins. siRNA-mediated down-regulation of the COPB1 gene consistently resulted in perinuclear retention of SH4-fusion proteins and knockdown of ARCN1 (COPD) caused a similar phenotype. Moreover, knockdown of coatomer subunits did not affect SH4-protein trafficking when HeLa cells were microinjected with recombinant coatomer. Thus, our observations propose that COPB1 as a component of a multi-protein complex plays an important role in SH4-dependent protein transport.

3.2.1 RNAi mediated down-regulation of coatomer subunits causes intracellular accumulation of SH4-proteins

The coatomer subunits COPB1 (β-COP) and COPA (α-COP) were identified and validated as essential components for the cellular targeting of SH4 fusion proteins to the plasma membrane.

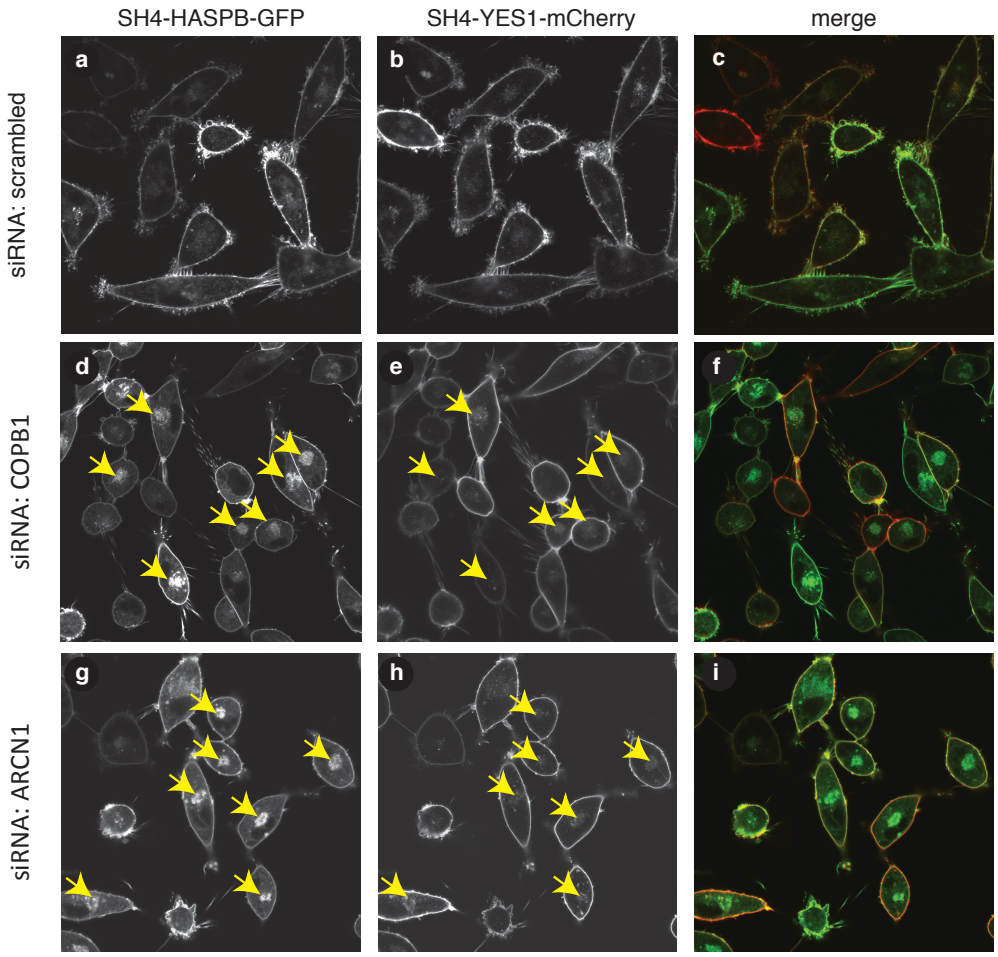

Figure 16 Knockdown of coatomer subunit COPB1 and COPD cause intracellular retention of SH4-proteins. HeLa cells expressing SH4-HASPB-GFP and SH4-YES-mCherry were transfected with a scrambled siRNA (a-c), a siRNA against COPB1 (d-f) and a siRNA against COPD. 48 hours post siRNA transfection cells were subjected to live-cell wide field microscopy to determine the localization of both SH4 fusion proteins.

Figure 16 shows that transfection of siRNA against coatomer subunits COPB1 (panel d-f) and COPD (panel g-i) cause a pronounced intracellular retention of SH4-proteins compared to the treatment with a scrambled siRNA (panel a-c). In following experiment, we took the advantage of the strong phenotype after treatment with siRNA against COPB1 and used it as positive control for the following investigations.

3.2.2 Determination of knockdown efficiencies of coatomer subunits on protein level

As mentioned in the previous section, we employed siRNA mediated knockdown against coatomer subunits to study the intracellular localization of SH4-proteins. Each siRNA was transfected for 48 hours followed by analysis of GFP, COPB1 and COPD on protein level.

A

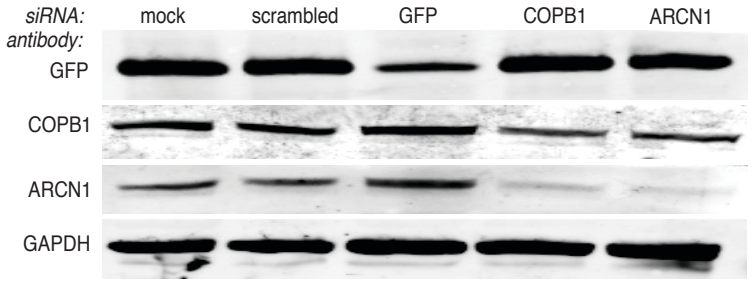

B

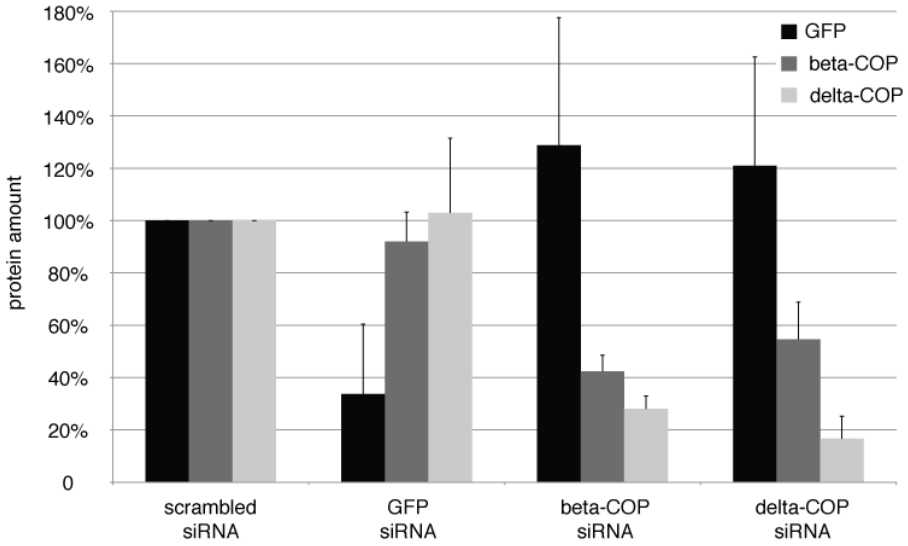

Figure 17 Determination of knockdown efficiencies of coatomer subunits on protein level. Sixty µg protein of total cell lysates of HeLa cells expressing SH4-HASPB-GFP and SH4-YES-mCherry were subjected to SDS-PAGE and Western blot (A). Antibodies against GFP, beta-COP, delta-COP and GAPDH were used for the detection on Western blot and further for the quantification of siRNA knockdown efficiencies on protein level (B).

Efficiencies of down-regulation of coatomer subunits COPB1 and COPD were determined at the protein level. GFP was down regulated as a positive control. Around 30%, 40% and 20% of GFP, COPB1 and COPD protein remained after down-regulation

with respective siRNAs (Figure 17). Downregulation of COPB1 caused also a loss of COPD and vice versa (Ritzerfeld et al., 2011).

3.2.3 Rescue experiment with recombinant coatomer

To address whether intracellular retention evoked by knockdown of coatomer subunits was indeed a result of depletion of the coatomer protein complex, we microinjected stable HeLa cells expressing SH4-HASPB-mCherry with recombinant coatomer before RNAi treatment against COPB1.

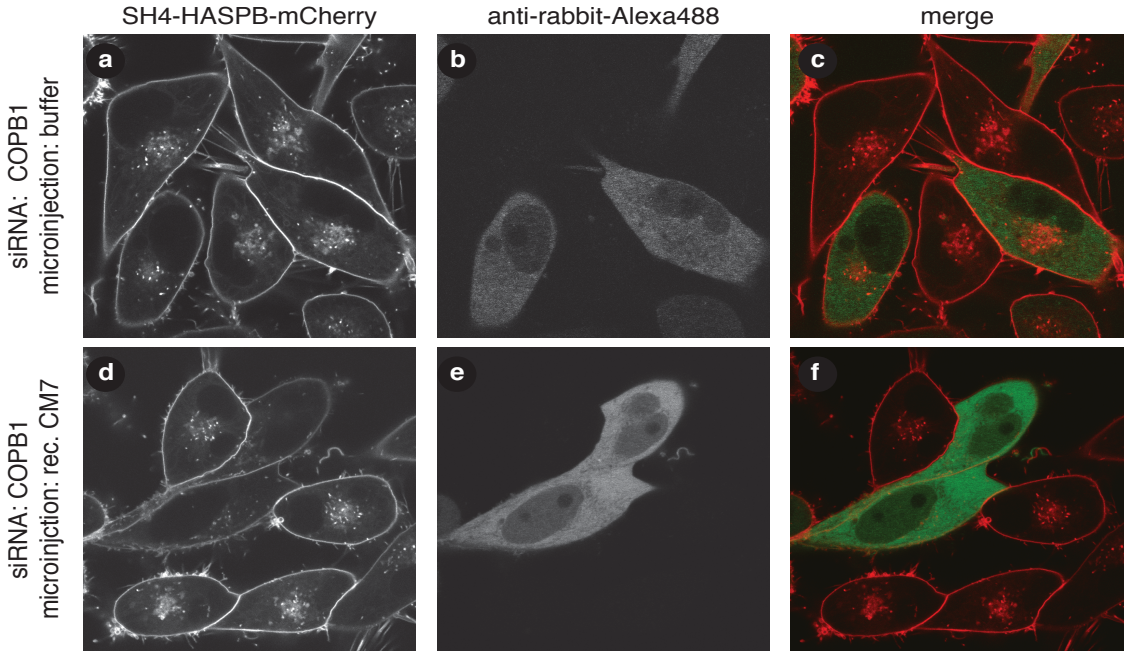

Figure 18 Rescue experiment by microinjection of recombinant coatomer. HeLa cells expressing SH4-HASPB-mCherry were microinjected with recombinant coatomer and an Alexa-488-labelled secondary antibody before transfection with a siRNA against COPB1. Post-transfection 30 hours, live-cell confocal microscopy was applied for the analysis of subcellular localization of the SH4 fusion protein.

As shown in Figure 18 d-f, the intracellular accumulation of SH4-HASPB-mCherry caused by silencing of COPB1 is prevented by microinjection of recombinant coatomer. Control cells microinjected with buffer upon knockdown of COPB1 show intracellular retention of SH4-HASPB-mCherry (Figure 18 a-c). These results demonstrate that coatomer is involved in proper targeting of SH4-HASPB to the plasma membrane (Ritzerfeld et. al., 2011).

3.3 ANALYSIS OF PROTEIN KINASE C ALPHA AS A COMPONENT OF SH4-DOMAIN-DEPENDENT PROTEIN TARGETING

Recent studies postulated that phosphorylation of SH4-domain-containing proteins such as SRC kinases can regulate endosomal recycling (Sandilands et al., 2004; Sandilands and Frame, 2008; Tournaviti et al., 2007). Remarkably, protein kinase C alpha (PRKCA) was identified as a gene product whose down-regulation caused perinuclear accumulation of SH4 fusion proteins. To test whether PKC activity is required for the correct targeting of SH4-proteins to the plasma membrane, HeLa cells were further treated with protein kinase c inhibitor GÖ 6983, which also resulted in a pronounced intracellular accumulation of SH4-proteins.

3.3.1 RNAi mediated down-regulation of PKCα causes intracellular accumulation of SH4-proteins

We employed siRNA treatment directed against PKCα to study the intracellular localization of SH4-proteins.

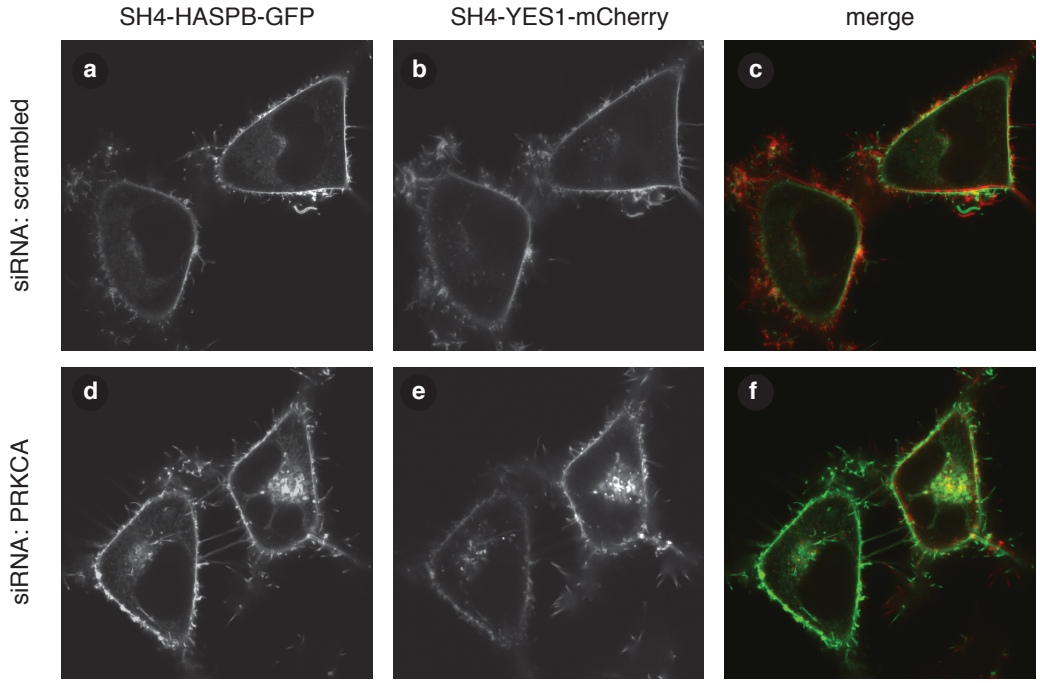

Figure 19 Characterization of PKCα as a component in SH4-dependent protein transport. HeLa cells expressing SH4-HASPB-GFP and SH4-YES-mCherry were transfected with a scrambled siRNA (a-c) and a siRNA against PRKCA (d-f)**.** 48 hours post siRNA transfection cells were subjected to live-cell wide field microscopy to determine the localization of both SH4 fusion proteins.

Figure 19 shows treatment of siRNA against PKCα causes a pronounced intracellular retention of SH4-proteins (panel d-f) compared to the treatment with a scrambled siRNA (panel a-c) (Ritzerfeld et al., 2011). PKCα belongs to PKC family; a family of serine/threonine kinases that are involved in a variety of cellular processes, such as cell adhesion and cell cycle checkpoint.

3.3.2 Determination of knockdown efficiency of PKCα on protein level and mRNA level

We employed siRNA mediated knockdown against PKCα to study the intracellular localization of SH4-proteins. Each siRNA was transfected for 48 hours followed by analysis of GFP and PKCα on protein as well as mRNA level by RT-qPCR.

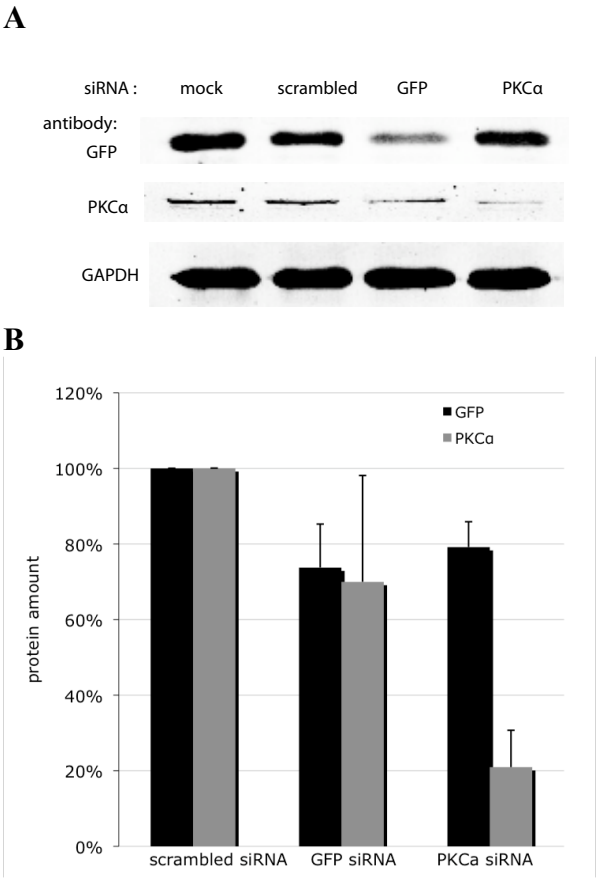

Figure 20 Determination of knockdown efficiencies of PKCα on protein level. Sixty µg protein of total cell lysates of HeLa cells expressing SH4-HASPB-GPP and SH4-YES-mCherry were loaded to SDS-PAGE and Western blot (A). Antibodies against GFP, PKCα and GAPDH were used for the detection on Western blot and further for the quantification of siRNA knockdown efficiencies on protein level (B).

Figure 20 showed GFP was down regulated as a positive control. Around 70% and 20% of GFP and PKCα protein remained after down-regulation with respective siRNAs

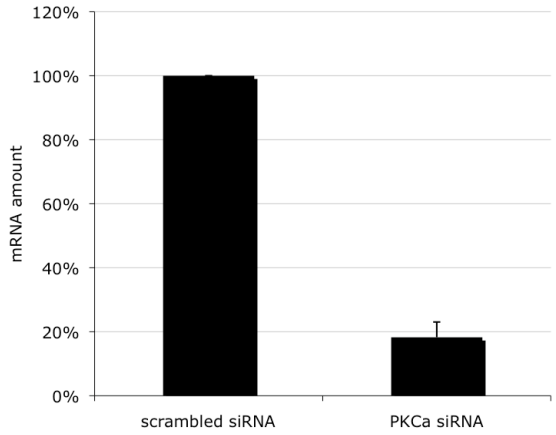

Figure 21 Determination of knockdown efficiency of PKCα on mRNA level. mRNA level of PKCα was quantified by Realtime-qPCR in HeLa cells expressing SH4-HASPB-GFP and SH4-YES-mCherry. Graphs indicate relative mRNA levels after 48h in cells treated with respective siRNAs.

Figure 21 shows the reduction of PKCα on mRNA level after treatment with siRNA against PKCα for 48 hours in HeLa cells expressing SH4-HASPB-GFP and SH4-YES-mCherry. Around 20% of PKCα on mRNA level remained in the cells after treatment with a siRNA directed against PKCα compared to the treatment with a scrambled siRNA.

3.3.3 Inhibitor GÖ 6983 of PKC causes a pronounced intracellular accumulation of SH4-proteins

In order to investigate whether the activity of PKC is required for targeting of SH4 proteins to the plasma membrane, we treated cells with the pharmacological inhibitor GÖ 6983 of protein kinase C and observed the intracellular localization of SH4 reporter proteins.

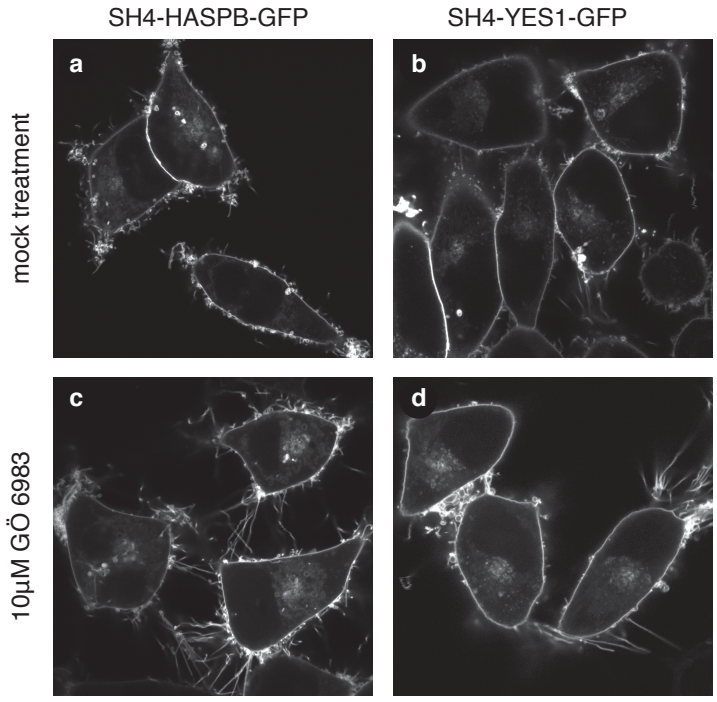

Figure 22 Incubation with inhibitor GÖ 6983 of PKC causes a pronounced intracellular accumulation of SH4-proteins. 10 µM inhibitor GÖ 6983 was incubated for 16 hours with HeLa cells expressing SH4-HASPB-GFP and SH4-YES-mCherry and subsequently analyzed by confocal microscopy.

As shown in Figure 22, incubation with GÖ 6983 for 16 hours results a pronounced intracellular accumulation of SH4 reporter proteins similar to the RNAi treatment against PKCα. These results indicate that activity of PKC is required for the correct targeting of SH4 reporter proteins to the plasma membrane (Ritzerfeld et al., 2011).

3.4 INVESTIGATION OF THE ROLE OF LIPID HOMEOSTASIS IN SH4-DOMAIN-DEPENDENT PROTEIN TARGETING

A task of the study was to identify enzymes that play key roles in lipid biosynthesis and homeostasis. Among the results, mevalonate pyrophosphate decarboxylase (MVD), a key factor of cholesterol biosynthesis that generates active isoprene was identified and validated in the automated validation approach. MVD is a cytosolic homodimer and plays a role in early steps of cholesterol biosynthesis where it catalyzes the conversion of mevalonate pyrophosphate into isopentenyl pyrophosphate and dehydrates its substrate under the consumption of ATP (Hogenboom et al., 2002; Hogenboom et al., 2003; Toth

and Huwyler, 1996). Downregulation of MVD indeed caused reduced cellular cholesterol levels that were concomitant with intracellular retention of SH4 proteins. Further, we conducted experiments to test the hypothesis that homeostasis of cholesterol as a raft lipid is required for the correct targeting of SH4 proteins to plasma membrane.

3.4.1 RNAi mediated down-regulation of MVD causes a pronounced intracellular accumulation of SH4-proteins

We employed siRNA treatment directly against MVD to study the intracellular localization of SH4-proteins.

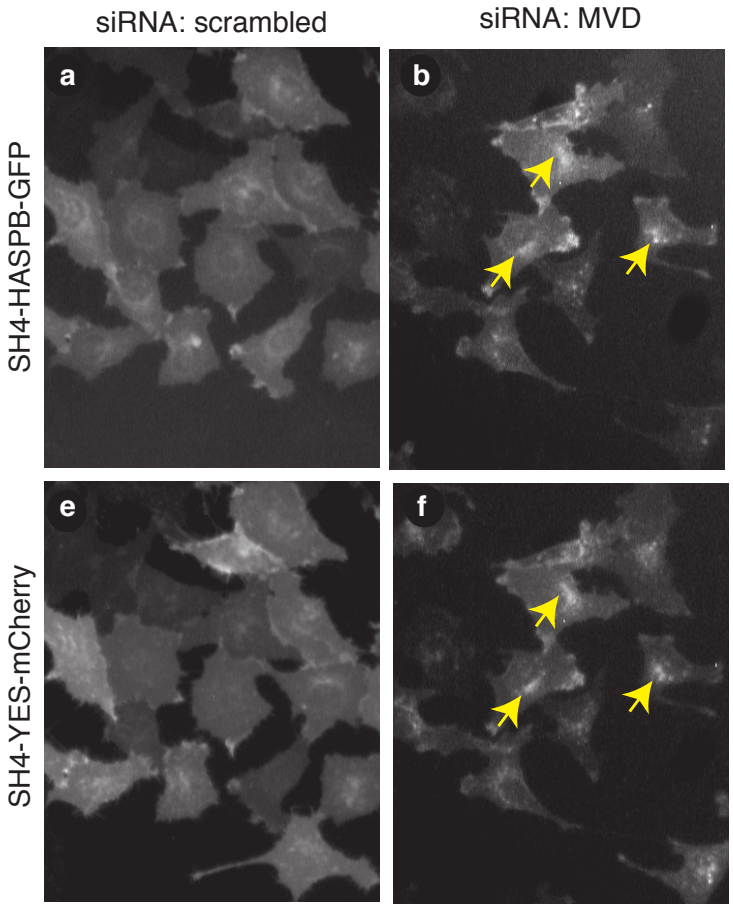

Figure 23 Characterization of MVD as a component in SH4-dependent protein transport. HeLa cells expressing SH4-HASPB-GFP and SH4-YES-mCherry were transfected with a scrambled siRNA (a,e) and a siRNA against MVD (b,f) and 48 hours post siRNA transfection cells were subjected to live-cell wide field microscopy to determine the localization of both SH4 fusion proteins.

Figure 23 shows siRNA treatment against MVD causes a pronounced intracellular retention of SH4-proteins (panel e-f) compared to the treatment with a scrambled siRNA (panel a-b) (Ritzerfeld et al., 2011). MVD is a cytosolic homodimer and plays a role in early steps of cholesterol biosynthesis where it catalyzes the conversion of mevalonate pyrophosphate into isopentenyl pyrophosphate and dehydrates its substrate under the consumption of ATP (Hogenboom et al., 2002; Hogenboom et al., 2003; Toth and Huwyler, 1996).

3.4.2 Determination of knockdown efficiency of MVD on protein and mRNA level

As mentioned in the previous section, we employed siRNA mediated knockdown against MVD to study the intracellular localization of SH4-proteins. Each siRNA was transfected for 48 hours followed by analysis of GFP and MVD on protein as well as mRNA level by RT-qPCR.

A

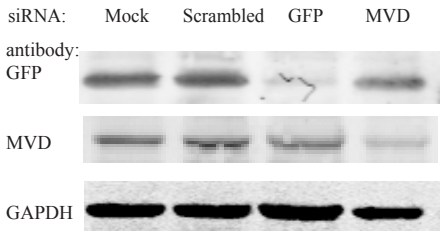

B

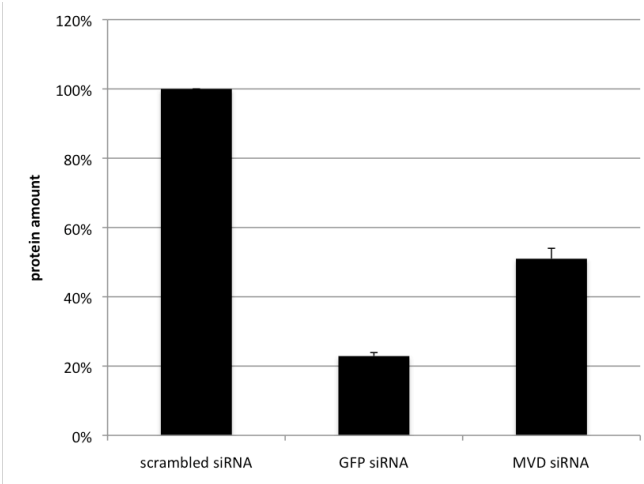

Figure 24 Determination of knockdown efficiency of MVD on protein level. Sixty µg protein of total cell lysates of HeLa cells expressing SH4-HASPB-GFP and SH4-YES-mCherry were subjected to SDS-PAGE and Western blot (A). Antibodies against GFP, MVD and GAPDH were used for the detection on Western blot and further for the quantification of siRNA knockdown efficiency on protein level (B).

Figure 24 shows the reduction of MVD on protein level after treatment with siRNA against MVD for 48 hours in HeLa cells expressing SH4-HASPB-GFP and SH4-YES-mCherry. Around 50% MVD on protein level remained in the cells compared to treatment with a scrambled siRNA. We used siRNA against GFP as a positive control and as shown in Figure 24 B the knockdown efficiency of GFP is around 20%.

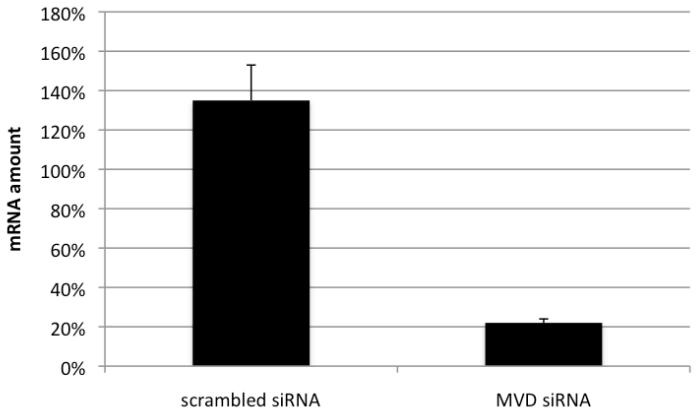

Figure 25 Determination of knockdown efficiency of MVD on mRNA level. mRNA level of MVD were quantified by Realtime-qPCR in HeLa cells expressing SH4-HASPB-GFP and SH4-YES-mCherry. Graphs indicate relative mRNA levels after 48h in cells treated with various siRNAs.

As shown in Figure 25 around 20% of MVD mRNA remained in the cells expressing SH4-HASPB-GFP and SH4-YES-mCherry 48 hours after treatment with a siRNA directed against MVD comparing to the treatment with a scrambled siRNA.

Together, these experiments indicate a requirement for MVD in correct targeting of SH4 reporter proteins to the plasma membrane. Further, our results also indicate that the turnover of MVD protein was a relative slow process since only 20% of MVD mRNA compared to around 50% MVD protein remained in the cell after 48 hours treatment with siRNA against MVD.

3.4.3 Role of cellular cholesterol levels in the SH4-domain dependent trafficking

Since we observed the knockdown of MVD caused intercellular retention of SH4 proteins and MVD is the enzyme involved in cholesterol synthesis, we further challenge the hypothesis that cholesterol homeostasis is essential for targeting of SH4-proteins to the plasma membrane.

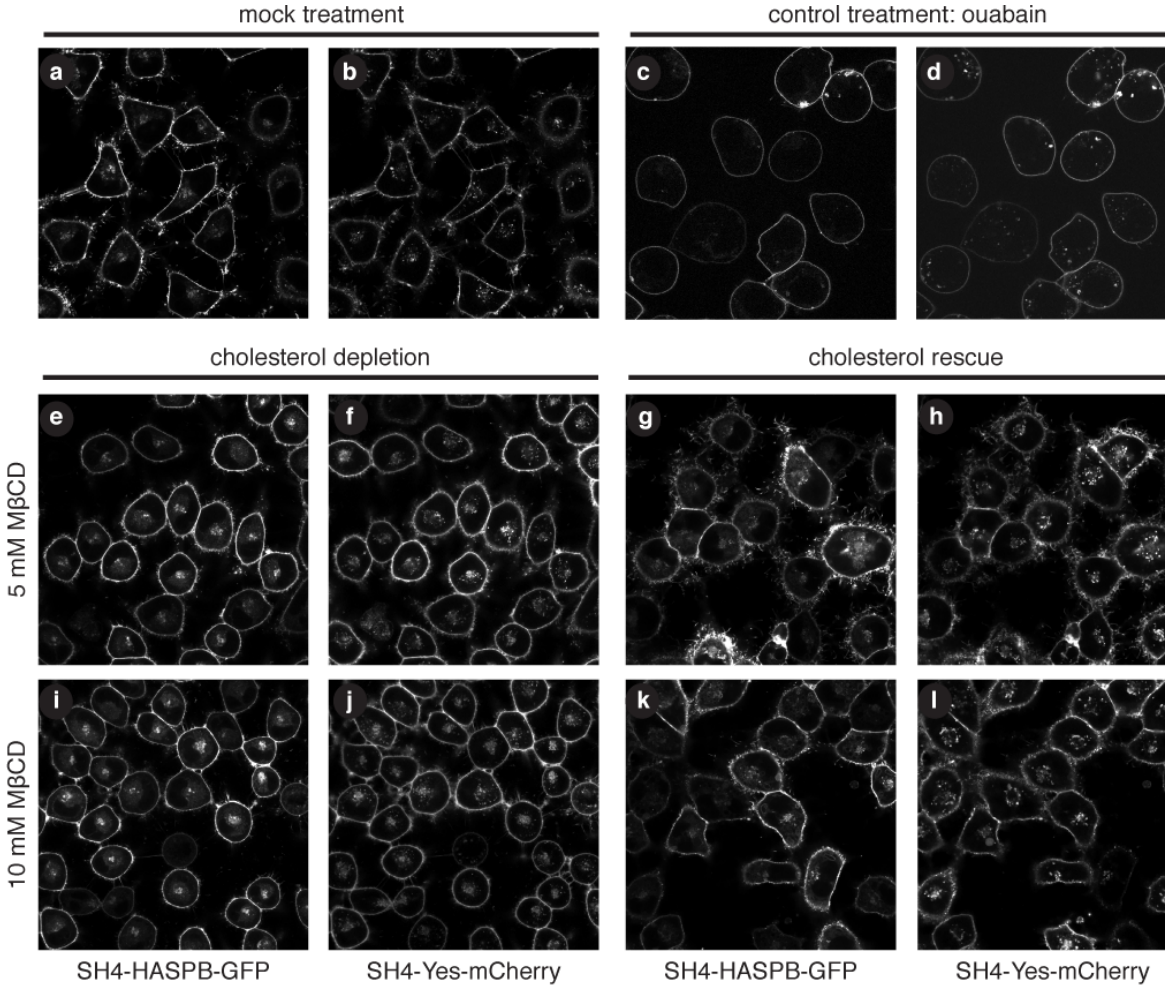

Figure 26 MβCD treatment causes intracellular retention of SH4 proteins. To deplete cholesterol level, cells were incubated for 1 hour in 5/10 mM methyl-β-cyclodextrin (MβCD). Subsequently, medium containing MβCD was removed and fresh medium containing water-soluble cholesterol was added to the cells for 1 hour. Further, live-cell confocal microscopy was applied directly after the treatment.

We employed MβCD to disrupt lipid rafts by removing cholesterol from membranes. After a one-hour treatment with MβCD, a pronounced intracellular accumulation of SH4 reporter proteins is observed by confocal microscopy (Figure 26). Further, to test whether

accumulation was indeed a direct result of cholesterol depletion, we incubated cells with water-soluble cholesterol for cholesterol replenishment. Water-soluble cholesterol is known to form soluble inclusion complexes between MβCD with cholesterol and thereby enhancing the solubility of cholesterol. This treatment resulted in a pronounced re-distribution of both SH4-HASPB-GFP and SH4-YES-mCherry. To test the possibility that the MβCD caused a pleiotropic effect on SH4 protein trafficking to the plasma membrane, we used oubain as a negative control, an unrelated inhibitor blocking the activity of NA^+/K^+ ATPase. There we also observed a mild morphology change of cells, however, compared to MβCD treatment, a perinuclear accumulation of SH4 reporter proteins is not observed (Figure 26).

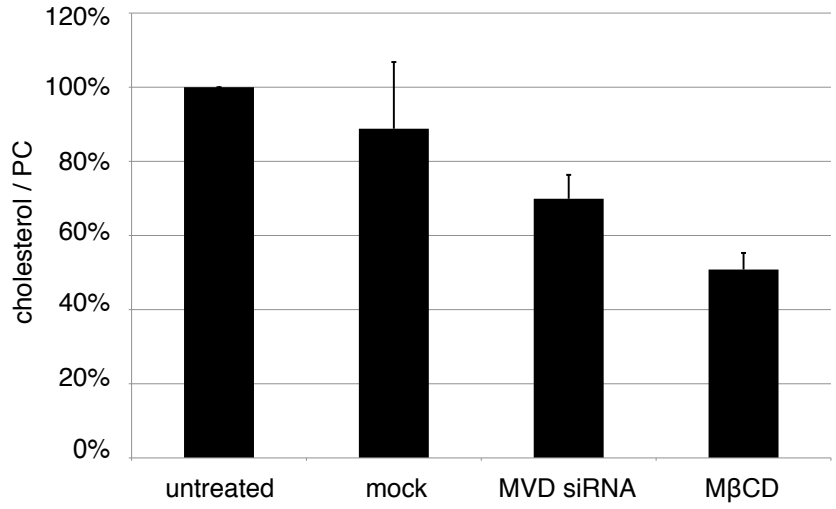

Figure 27 Determination of cellular cholesterol levels. Cholesterol / PC ratios were measured by using nano-electrospray ionosation mass spectrometry as described in Merz et al, 2011. Following treatment of cells with either a siRNA against MVD or treatment with MβCD, lipid analysis was performed from both whole cells and cellular membranes.

We measured the cellular cholesterol levels by nano-electrospray ionization mass spectrometry using phosphatidylcholine (PC) as a bulk lipid to normalize data (Ritzerfeld et al., 2011). Cholesterol levels were reduced to 70% after 48 hours treatment of a siRNA directed against MVD (Figure 27). One-hour incubation of 10 mM MβCD resulted in pronounced intracellular retention of SH4 proteins, concomitant with a 50% reduction of cellular cholesterol relative to PC.

Our combined results suggest interference with cellular cholesterol levels results in pronounced intracellular retention of SH4-proteins and further corroborate the role of cholesterol dependent lipid rafts in SH4-domain-dependent protein targeting to the plasma membrane (Ritzerfeld et al., 2011).

3.5 INVESTIGATION OF A POTENTIAL ROLE OF NAE1 IN SH4-DOMAIN-DEPENDENT PROTEIN TARGETING

In the manual validation approach, we found that the knockdown of NAE1 caused a pronounced intercellular retention of SH4 proteins (Figure 28). NAE1 was first identified as a novel binding partner of the cytoplasmic domain of amyloid precursor protein (APP) and thus called as APP binding protein1 (APP-BP1) (Chow et al., 1996). In addition, NAE1 is involved in activation of the ubiquitin-like protein NEDD8 and participates in the neddylation pathway (Gong and Yeh, 1999). Furthermore, NAE1 also binds and co-localizes with amyloid precursor protein (APP) in membrane lipid rafts (Chen et al., 2003). We challenged the hypothesis that not only NAE1 and but also a functional cellular neddylation pathway and its interacting partners are also involved in the SH4-protein targeting to the plasma membrane.

3.5.1 Validation analysis of siRNA treatments against NAE1 and its functional interaction partners NEDD8 and APP

To study molecular functions of NAE1 in plasma membrane targeting of SH4 protein, we treated HeLa cells expressing SH4-HASPB-GFP and SH4-YES-mCherry with respective siRNA against NAE1 and its functional interaction partners NEDD8 and APP as the first approach.

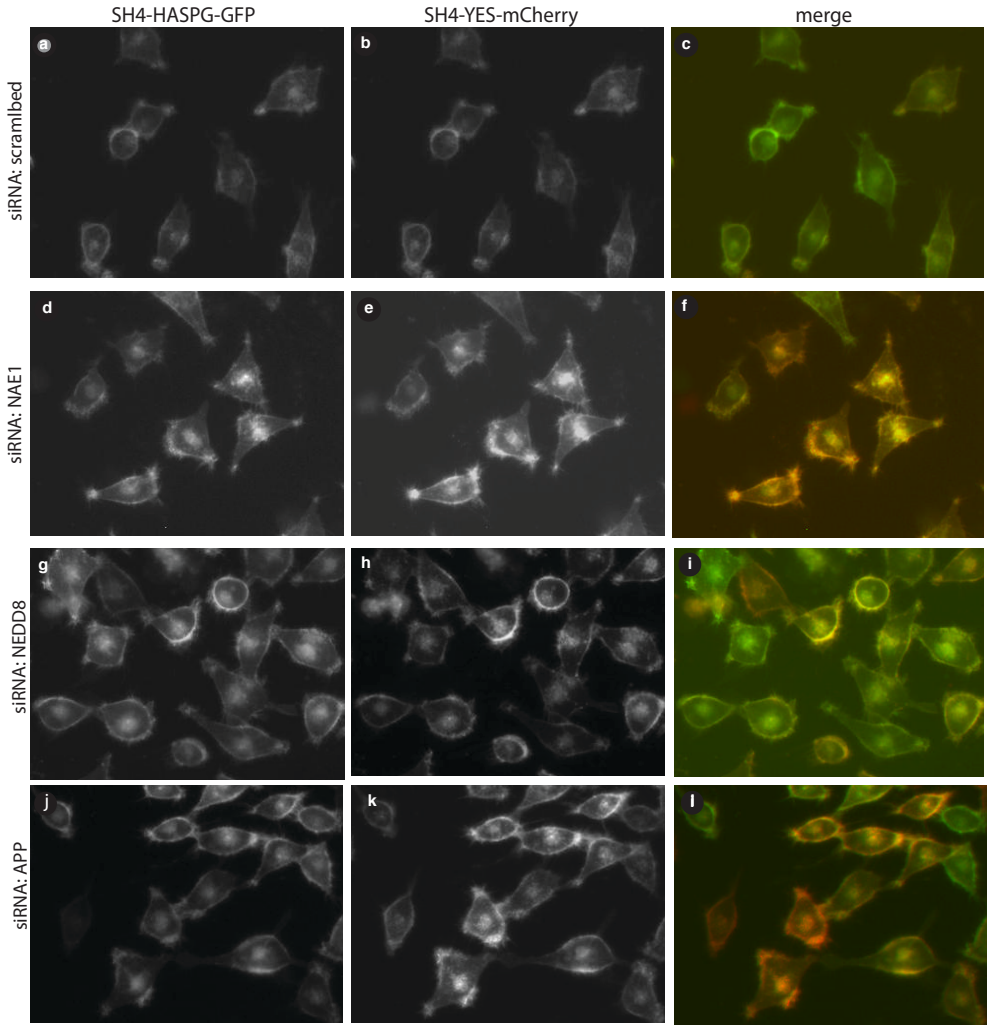

Figure 28 Characterization of NAE1, NEDD8 and APP as components in SH4-dependent protein transport. HeLa cells expressing SH4-HASPB-GFP and SH4-YES-mCherry were reverse transfected with a scrambled siRNA (a-c), a siRNA against NAE1 (b-f) and a siRNA against APP (j-i). 48 hours post siRNA transfection cells were subjected to live-cell wide-field microscopy to determine the localization of both SH4 fusion proteins (cutouts of 10X magnification images).

Figure 28 shows wide-field microscopy images of HeLa cells expressing SH4-HASPB-GFP and SH4-YES-mCherry, which were transfected with respective siRNAs against NAE1, NEDD8 and APP for 36 hours before protein expression was induced by doxycline for additional 12 hours. A moderate perinuclear retention of SH4 fusion proteins can be observed after siRNA treatments against NEDD8 and APP. siRNA treatment against NAE1 caused a pronounced intracellular accumulation of SH4 fusion proteins.

3.5.2 Determination of knockdown efficiencies of NAE1, NEDD8 and APP on mRNA level

As mentioned in the previous section, we employed siRNA mediated knockdown against NAE1, NEDD8 and APP to study the intracellular localization of SH4-proteins. Each siRNA was transfected for 48 hours followed by analysis of NAE1, NEDD8 and APP on mRNA level by RT-qPCR.

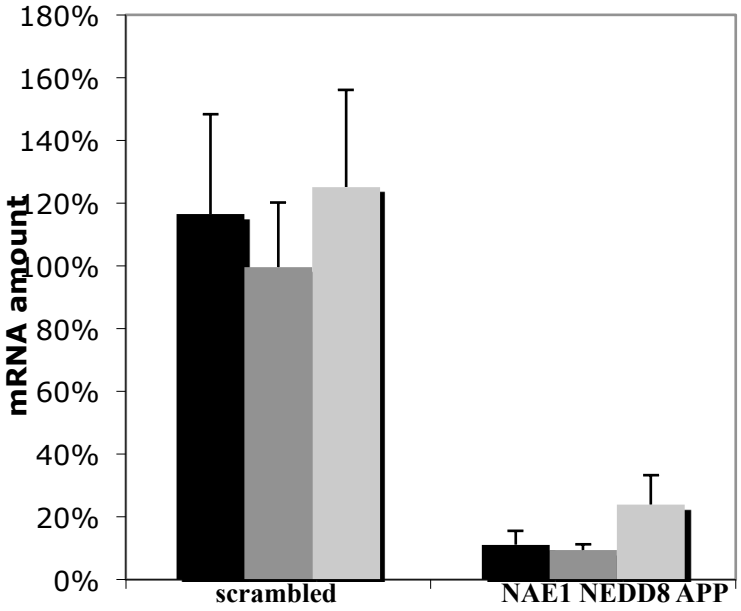

Figure 29 Determination of knockdown efficiencies of NAE1, NEDD8 and APP on mRNA level. The mRNA levels of NAE1, NEDD8 and APP were quantified by Realtime-qPCR in HeLa cells expressing SH4-HASPB-GFP and SH4-YES-mCherry. Graphs indicate relative mRNA levels after 48h in cells treated with various siRNAs.

The reduction on mRNA level is quantified by using Realtime-qPCR and as shown in Figure 29 around 15% of NAE1, 15% NEDD8 and 30% of APP mRNA remained in the cells 48 hours post transfection with respective siRNAs.

3.5.3 Analysis of wide field microscopy data with the automated image analysis tool

An automated image analysis tool was developed for the identification of phenotypic changes with regard to the localization of SH4-reporter proteins (Remmle et al., 2008). We used this automated image analysis tool to analyze the intracellular distribution of

SH4-reporter proteins after siRNA treatments against NAE1, NEDD8 and APP for 48 hours and 72 hours, respectively.

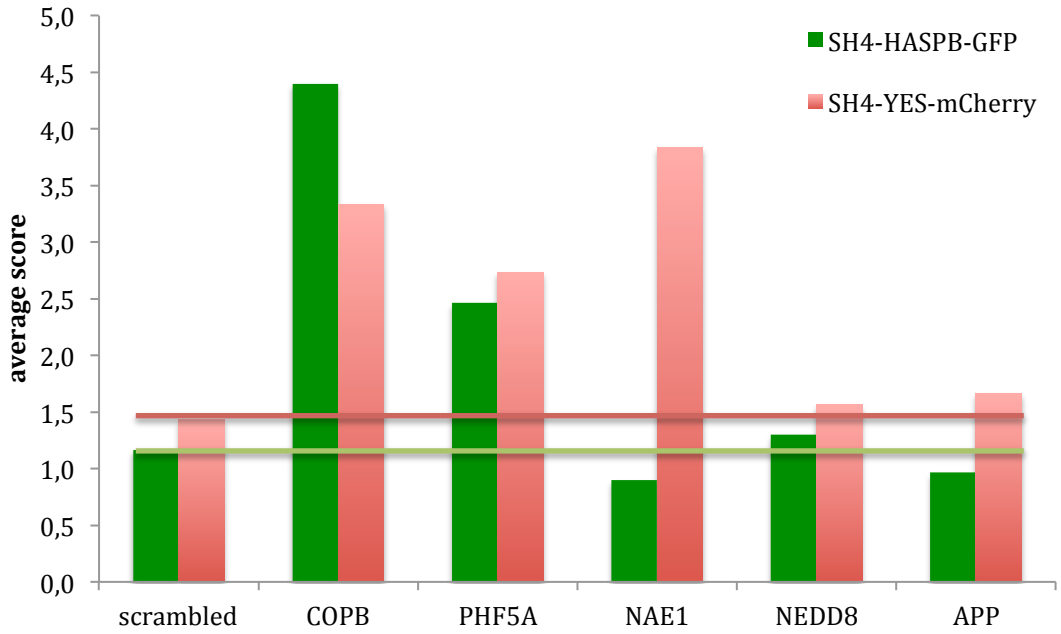

Figure 30 Hit scores of siRNA treatments against NAE1, NEDD8 and APP by an automated image analysis tool. 48 hours after transfection with scrambled siRNA and respective siRNAs against COPB, PHF5A, NAE1 and APP, live-cell wide-field microscopy data were analyzed by an automated image analysis tool to determine the hit scores. The green line indicates the average score of treatment with scrambled siRNA in SH4-HASPB-GFP. The red line indicates the average score of treatment with scrambled siRNA in SH4-YES-mCherry.

Figure 30 shows an automated image analysis result of HeLa cells expressing SH4-HASPB-GFP and SH4-YES-mCherry after respective RNAi treatments 48 hours post transfection. Treatment with siRNA against NAE1 in SH4-YES-mCherry resulted an average score of 4, which is higher than average scores caused by siRNAs against COPB and PHF5A as positive controls. In SH4-HASPB-GFP, treatment with siRNA against NAE1 resulted an average score above 2.0, which is close to the average score of PHF5A as a positive control. Treatments with siRNAs against NEDD8 and APP showed low scores in both SH4-reporter proteins. These results suggest that NAE1 might be required for the correct targeting of SH4-YES.

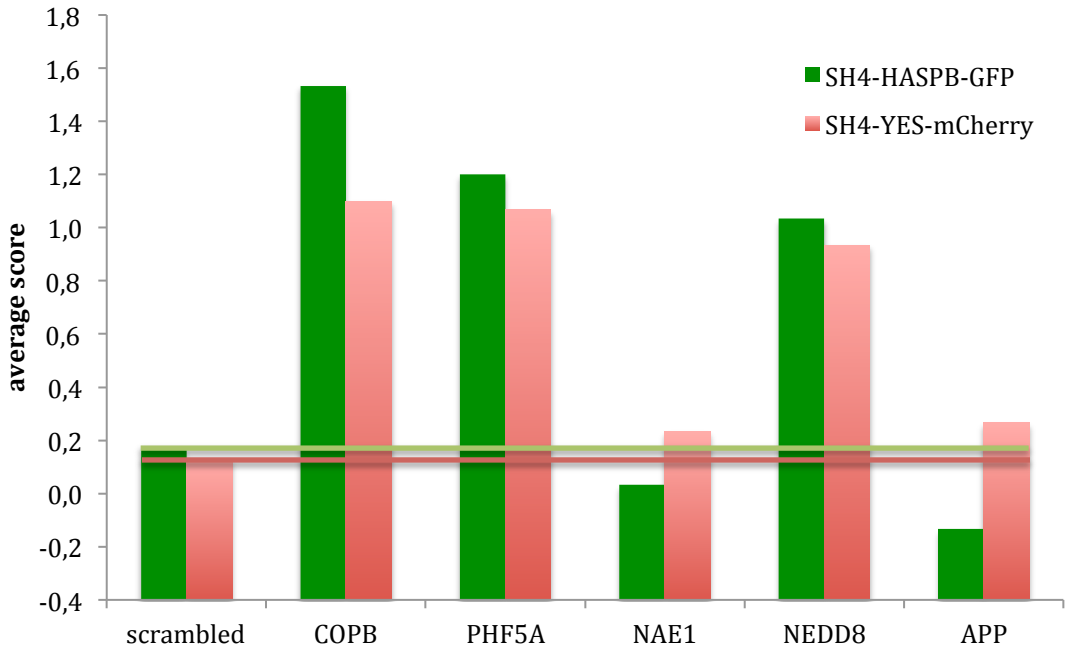

Figure 31 Hit scores of siRNA treatments against NAE1, NEDD8 and APP by an automated image analysis tool. 72 hours after transfection with scrambled siRNA and respective siRNAs against COPB, PHF5A, NAE1 and APP, live-cell wide-field microscopy data were analyzed by an automated image analysis tool to determine the hit scores. The green line indicates the average score of treatment with scrambled siRNA in SH4-HASPB-GFP. The red line indicates the average score of treatment with scrambled siRNA in SH4-YES-mCherry.

Figure 31 shows an automated image analysis result of HeLa cells expressing SH4-HASPB-GFP and SH4-YES-mCherry after respective RNAi treatments 72 hours post transfection. Treatment with siRNA against NAE1 did not result in a high score after 72 hours post transfection. Treatment with siRNA against NEDD8 resulted in the score of around 1,0 in SH4-HASPB-GFP and SH4-YES-mCherry, which are comparable to the scores gained by the positive controls. Treatment with siRNA against APP showed low scores in both SH4-reporter proteins. Scores for positive controls gained in this experiment are generally low due to the fact that cells might undergo apoptosis with extended knockdown time for 72 hours.

Taking together, transfection with respective siRNAs targeted against NAE1, NEDD8 and APP resulted in efficient reduction of the respective mRNA levels. Knockdown of NAE1 and NEDD8 resulted in an intracellular accumulation of SH4-YES-mCherry with 48h and 72h knockdown periods, respectively. In SH4-HASPB-GFP knockdown of NEDD8 for extended period of 72h also caused comparable scores as for positive

controls. It might be that NAE1 and NEDD8 affected more in the trafficking of SH4-YES than SH4-HASPB. This could indicate that the fact that SH4-YES and SH4-HASPB traffic along different routes. Finally, knockdown of APP resulted low scores for both 48h and 72h periods and in both SH4-reporter proteins.

3.5.4 DRM association of HASPB-N18-GFP after diverse siRNAs treatments with NAE1, NEDD8 and APP

Previous studies suggested that SH4 protein trafficking was dependent on cholesterol-dependent membrane microdomains (Brown and London 1998; Webb et al. 2000; Edidin 2003; Smotrys and Linder 2004; Linder and Deschenes 2007). In addition, it has been proposed lipid rafts are required as sorting and transport platforms for the correct targeting of SH4 proteins. Studies about NAE1 showed that NAE1 binds APP and colocalize with APP in lipid rafts, a cell surface protein with signal transducing properties (Chen et al., 2003). Combining these two facts, we hypothesize the colocalization of NAE1 and APP in lipid rafts could directly influence the DRM association of SH4-reporter proteins and thus influence raft-dependent transport to the plasma membrane. There is also a possibility that NAE1 might colocalize with SH4-proteins in lipid rafts and thus increase their affinity to lipid rafts. To answer these questions, we transfected the HeLa cells expressing SH4-HASPB-GFP and SH4-YES-mCherry with respective siRNAs against NAE1, NEDD8 and APP and observed the association of SH4-HASPB-GFP with DRMs.

A

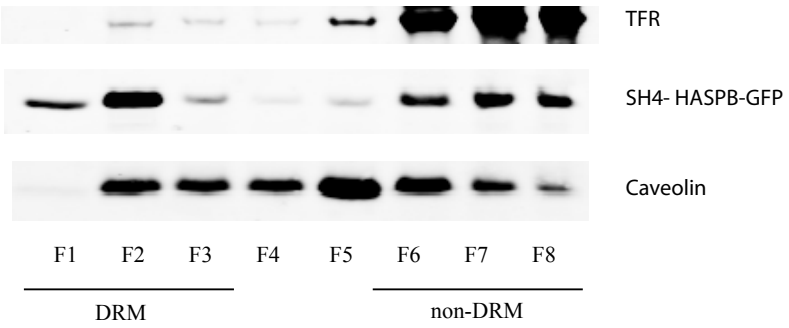

B

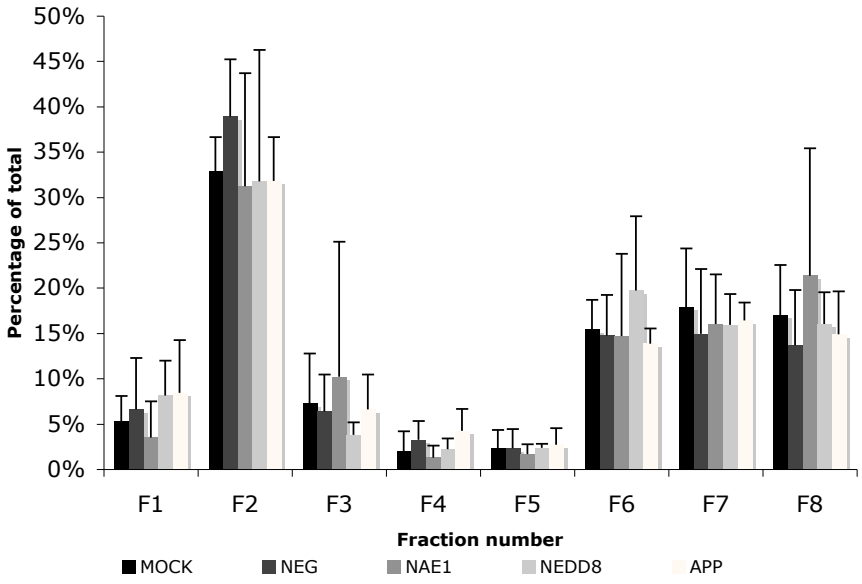

Figure 32 Plasma membrane versus intracellular localization of SH4-HASPB-GFP correlates with the degree of association with DRMs after respective siRNA treatments. (A) HeLa cells expressing SH4-HASPB-GFP and SH4-YES-mCherry were treated with respective siRNAs. Subsequently, floatation of cell material with Optiprep was performed. Eight fractions were collected and analyzed by SDS-PAGE. Caveolin-1 and Transferrin receptor were used as a DRM-marker and non-DRM marker, respectively. (B) Quantitative analysis of the relative distribution of the fusion protein indicated within the flotation gradient. Antibody signals in each fraction were quantified and further expressed as the percentage of the total material recovered from all fractions.

As shown in Figure 32 we did not observe a significant difference on DRM association of SH4-HASPB-GFP after respective siRNA treatments against NAE1, NEDD8 or APP compared to negative controls. These results suggest that presences of NAE1, NEDD8 and APP might be not required for the DRM association of SH4-HASPB-GFP.

3.5.5 Wide-field microscopy analysis under RNAi treatments with diverse siRNAs in SH4-YES-GFP

According to results by applying the automated image analysis tool, we could conclude the knockdown of NAE1 and NEDD8 have a stronger effect on trafficking of SH4-YES than SH4-HASPB. To further elucidate the requirements of NAE1 and its interaction partners for the plasma membrane targeting of SH4-YES, we further involved a cell line expressing SH4-YES-GPF for our study.

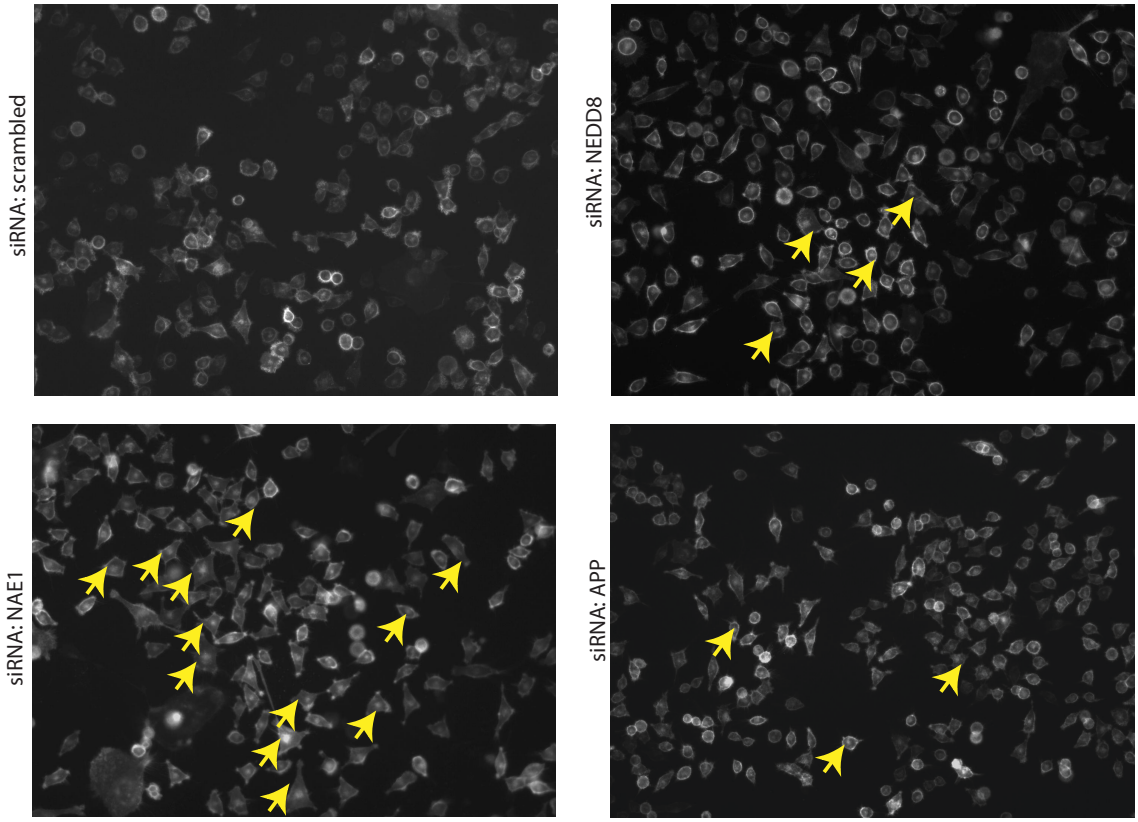

Figure 33 Characterization of NAE1, NEDD8 and APP as components in SH4-YES dependent protein transport. HeLa cells expressing SH4-YES-GFP were reverse transfected with a scrambled siRNA, a siRNA against NAE1 and a siRNA against APP. 48 hours post siRNA transfection cells were subjected to live-cell wide-field microscopy to determine the localization of SH4-YES-GFP.

Figure 33 shows wide field microscopy images of HeLa SH4-YES-GFP, which were transfected with respective siRNAs against NAE1, NEDD8 and APP for 36 hours before protein expression was induced for additional 12 hours. Significant perinuclear retention of SH4-YES-GFP can be observed after siRNA treatment against NAE1. Treatments with

siRNAs against NEDD8 and APP caused a moderate perinuclear accumulation of SH4-YES-GFP.

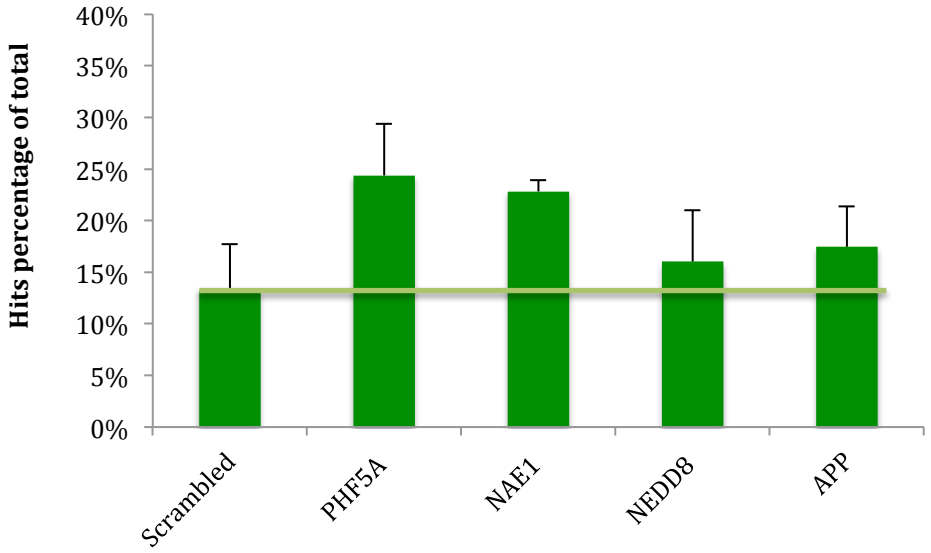

Figure 34 Hit percentages after siRNA treatments with PHF5A, NAE1, NEDD8 and APP by automated image analysis tool. 48 hours after transfection with scrambled siRNA and respective siRNAs against PHF5A, NAE1, NEDD8 and APP, live-cell wide-field microscopy data were analyzed by an automated image analysis tool to determine the hits percentage of total. The green line indicates the average score of treatment with scrambled siRNA in SH4-YES-GFP.

Figure 34 shows hit percentages of HeLa cells expressing SH4-YES-GFP after siRNA treatments with PHF5A, NAE1, NEDD8 and APP by automated image analysis tool. Around 13% of HeLa cells expressing SH4-YES-GFP treated by scrambled siRNA are identified as hits. As a positive control, around 25% of HeLa cells expressing SH4-YES-GFP after a treatment with siRNA against PHF5A are identified as hits. Around 23% of the HeLa cells expressing SH4-YES-GFP after siRNA treatment against NAE1 are regarded as hits, which is comparable to the positive control PHF5A. Around 15% and 17% of the HeLa cells expressing SH4-YES-GFP after siRNA treatment against NEDD8 and APP are identified as hits, respectively, which are close to the value of negative control.

Overall, results shown here are in accordance with the results by using HeLa cells expressing SH4-HASPB-GFP and SH4-YES-mCherry (Figure 30). It seems that NAE1 might be required in the trafficking of SH4-YES to the plasma membrane since the value

caused by siRNA treatment against NAE1 is comparable to the positive control in both experiments. However, we were not able to ascertain that APP or NEDD8 is required in the trafficking of both SH4-reporter proteins.

3.5.6 Rescue Experiment with mouse homolog NAE1

To address whether intracellular retention evoked by knockdown of NAE1 was indeed a result of depletion of NAE1 protein, we transiently transfected HeLa cells expressing SH4-YES-GFP with mouse homolog pIRES NAE1-dsRED before siRNA treatment against human NAE1 and subsequently monitored the intracellular localization of SH4-YES. The expression of dsRED visualized the transfected cells in red color.

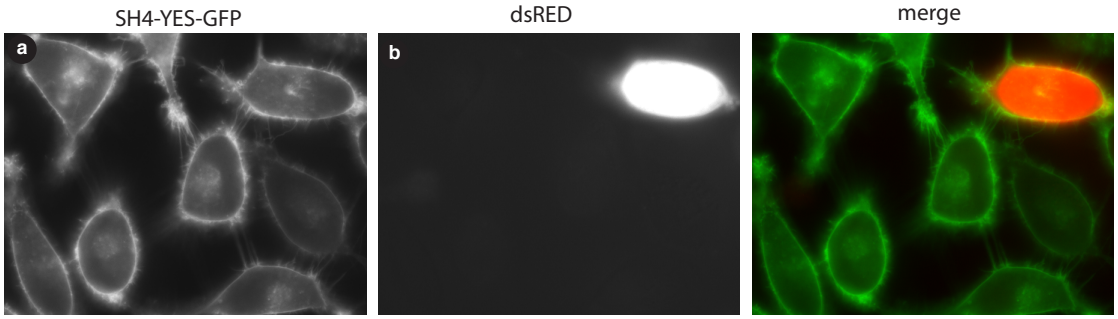

Figure 35 Rescue experiment by transient transfection of mouse homolog. NAE1 HeLa cells expressing SH4-YES-GFP were transfected with mouse-NAE-dsRED 12 hours before transfection with a siRNA against human NAE1. Post-transfection 36 hours, live-cell confocal microscopy was applied for the analysis of subcellular localization of the SH4 fusion protein.

As shown in Figure 35 intracellular accumulation of SH4-YES-GFP caused by silencing of NAE1 is prevented after the cells were transiently transfected with mouse homolog NAE1 dsRED. Non-transfected cells however still show a pronounced intracellular retention of SH4-YES-GFP. These results excluded the possibility of mistargeting of siNRA against NAE1 and thus indicated the requirement of NAE1 in correct targeting of SH4-YES to the plasma membrane. One challenge was the transient transfection efficiency. After optimization of the protocol, the transfection efficiency was low. We performed rescue experiments for other gene products involved in the neddylation pathway as well; however, we were not able to transfect the cells successfully with respective mouse or rat homolog constructs.

3.6 INVESTIGATION OF A POTENTIAL ROLE OF NEDDYLATION IN SH4-DEPENDENT PROTEIN TARGETING

Since knockdown of APP did not result in a pronounced intracellular retention of both SH4-proteins, we decided to focus our study on whether NAE1 as a component of neddylation or a functional neddylation pathway plays a role in the plasma-membrane targeting of SH4-YES. Neddylation, similar to ubiquitination, involves a three-step cascade to modify target proteins with ubiquitin-like protein NEDD8. In the first step, a NEDD8-specific E1-like enzyme, which is a NAE1/UBA3 heterodimer, activates NEDD8 by adenylating the carboxyl terminal glycine residue of NEDD8 followed by formation of high-energy thioester bond with a catalytic cysteine residue in UBA3. In the next step, NEDD8 is transferred from NAE1/UBA3 to the catalytic cysteine residue of the NEDD8-specific E2 enzyme UBC12 by formation of a thioester linkage. In the final step, active NEDD8 is subsequently transferred and conjugated to the substrates with the help of E3 ligases (Gong and Yeh, 1999).

3.6.1 Phenotype analysis under knockdown conditions of UBA3 and UBC12

To analyze the role of neddylation in intracellular targeting of SH4 proteins, we first used siRNAs directed against two other components UBA3 and UBC12 involved in the neddylation cascade pathway; further we applied dominant-negative mutants of such components and finally a pharmacological inhibitor against NAE1.

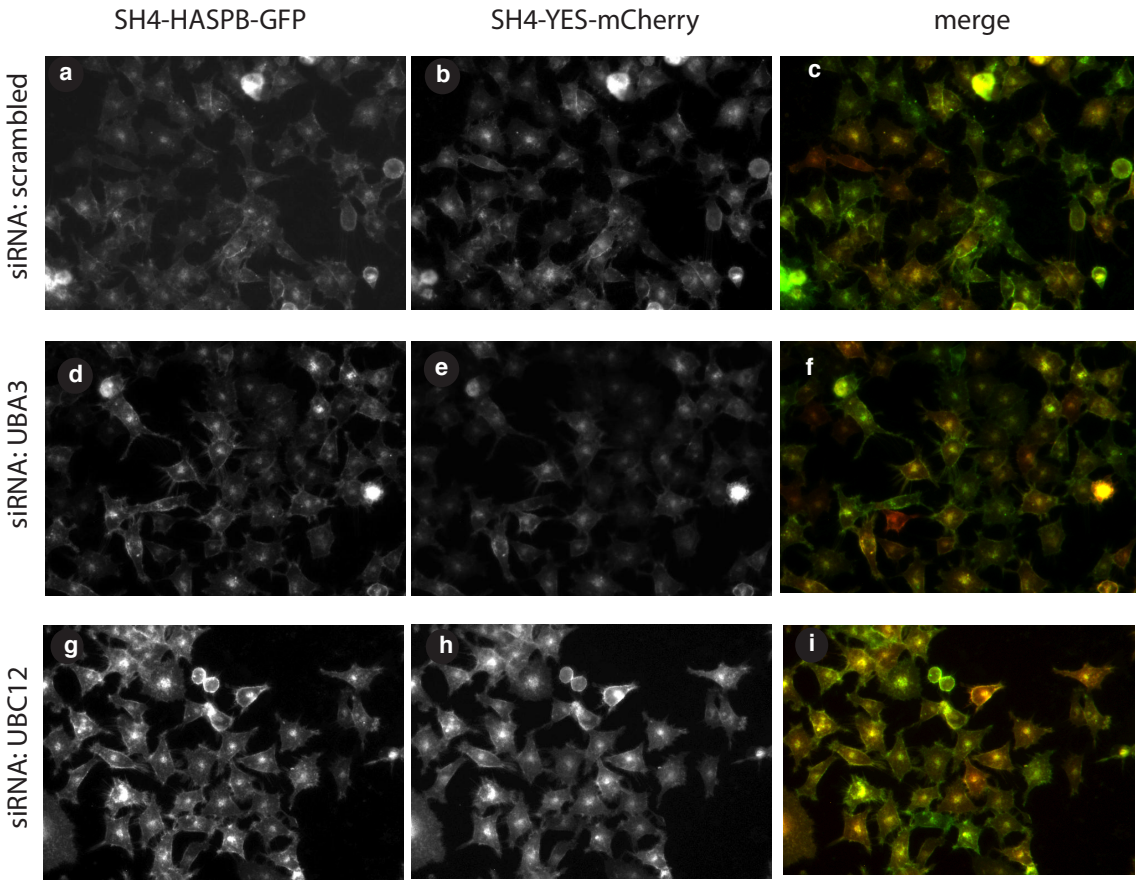

Figure 36 Wide field images of HeLa cells expressing SH4-HASPB-GFP and SH4-YES-mCherry treated with siRNAs against UBA3 and UBC12. HeLa cells expressing SH4-HASPB-GFP and SH4-YES-mCherry were transfected with siRNAs against UBA3 (d-f) and UBC12 (g-i) and subjected to live-cell wide field microscopy to determine the localization of both SH4 fusion proteins.

Figure 36 shows wide field microscopy images of HeLa cells expressing SH4-HASPB-GFP and SH4-YES-mCherry, which were transfected by respective siRNAs against UBA3 and UBC12 for 36 hours before protein expression was induced for additional 12 hours. siRNA treatments against UBA3 and UBC12 caused perinuclear accumulation of SH4-proteins.

3.6.2 Determination of knockdown efficiencies of UBA3 and UBC12 on mRNA level

As mentioned in the previous section, we employed siRNA mediated knockdown against UBA3 and UBC12 to study the intracellular localization of SH4-proteins. Each siRNA

was transfected for 48 hours followed by analysis of UBA3 and UBC12 on mRNA level by RT-qPCR.

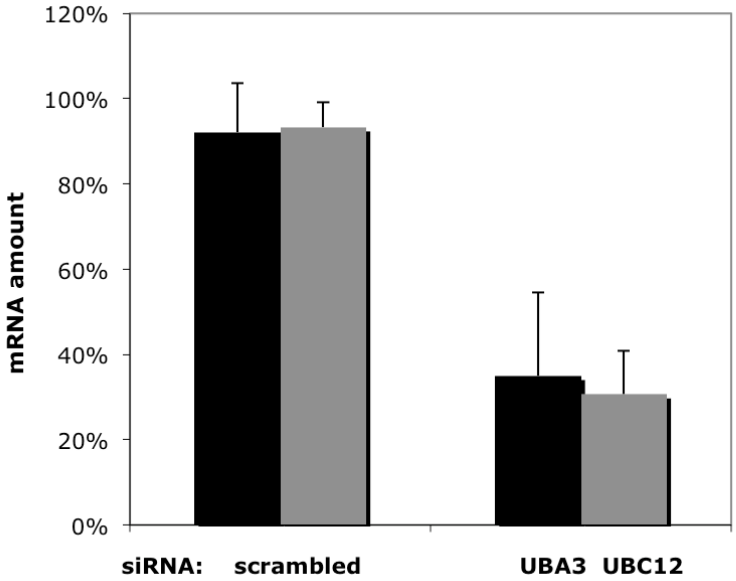

Figure 37 Determination of knockdown efficiencies of UBA3 and UBC12 on mRNA levels by RT-qPCR. The mRNA levels of UBA3 and UBC12 were quantified by Realtime-qPCR in HeLa cells expressing SH4-HASPB-GFP and SH4-YES-mCherry. Graphs indicate relative mRNA levels after 48h in cells treated with respective siRNAs.

Figure 37 shows that around 30% of UBA3 and 27% of UBC12 on mRNA levels remained in the cells expressing SH4-HASPB-GFP and SH4-YES-mCherry 48 hours after knockdown with siRNAs directed against UBA3 and UBC12, respectively.

3.6.3 Analysis of wide field microscopy data with automated image analysis tool

Respective siRNAs were immobilized on 384-well plates and subsequently cell lines expressing SH4-HASPG-GFP and SH4-YES-mCherry were cultured on siRNA arrays to be reverse transfected by respective siRNAs. We imaged the cells at two different time-points, 48h and 72 hours, post siRNA transfection. With the automatic software analysis tool, we determined the percentage of cells displaying hits on each position and determined hit scores using the standard deviation and also the median of the incidence rate of each hit phenotype of all 384 spots on the plate.

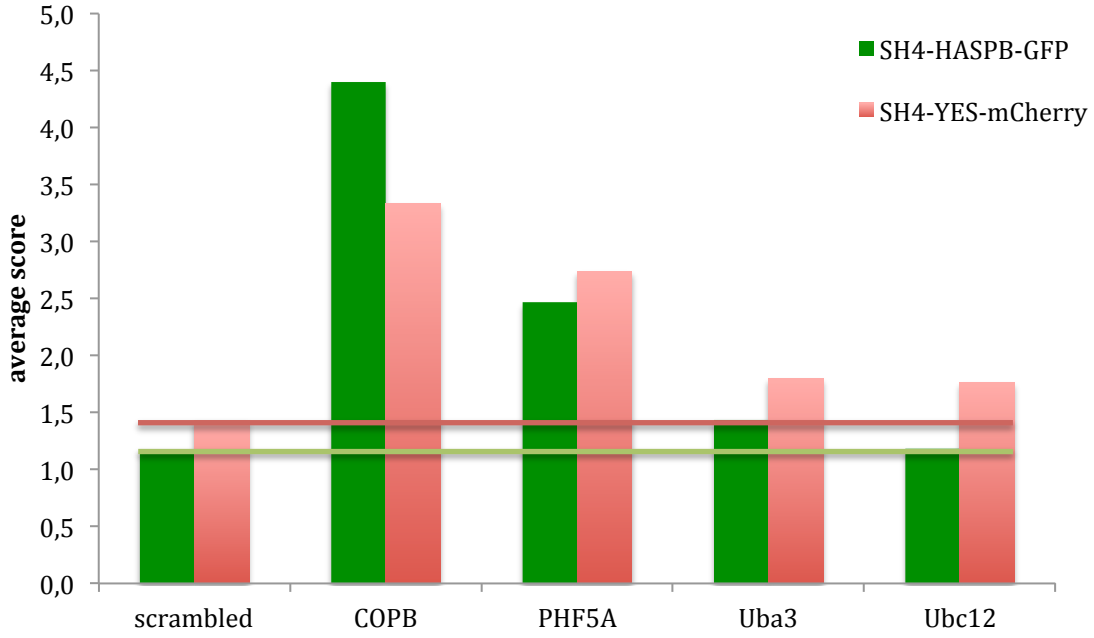

Figure 38 Hit scores of siRNA treatments against COPB, PHF5A, UBA3 and UBC12 by an automated image analysis tool. 48 hours after transfection with scrambled siRNA and respective siRNAs against COPB, PHF5A, UBA3 and UBC12, live-cell wide-field microscopy data were analyzed by an automated image analysis tool to determine the hit scores. The green line indicates the average score of treatment with scrambled siRNA in SH4-HASPB-GFP. The red line indicates the average score of treatment with scrambled siRNA in SH4-YES-mCherry.

Figure 38 shows an automated image analysis result of HeLa cells expressing SH4-HASPB-GFP and SH4-YES-mCherry after respective RNAi treatments 48 hours post transfection. Hit scores of knockdown UBA3 and UBC12 are higher than the negative control, however much lower than the hit scores of the positive controls by using siRNAs against COPB and PHF5A in both SH4-reporter proteins.

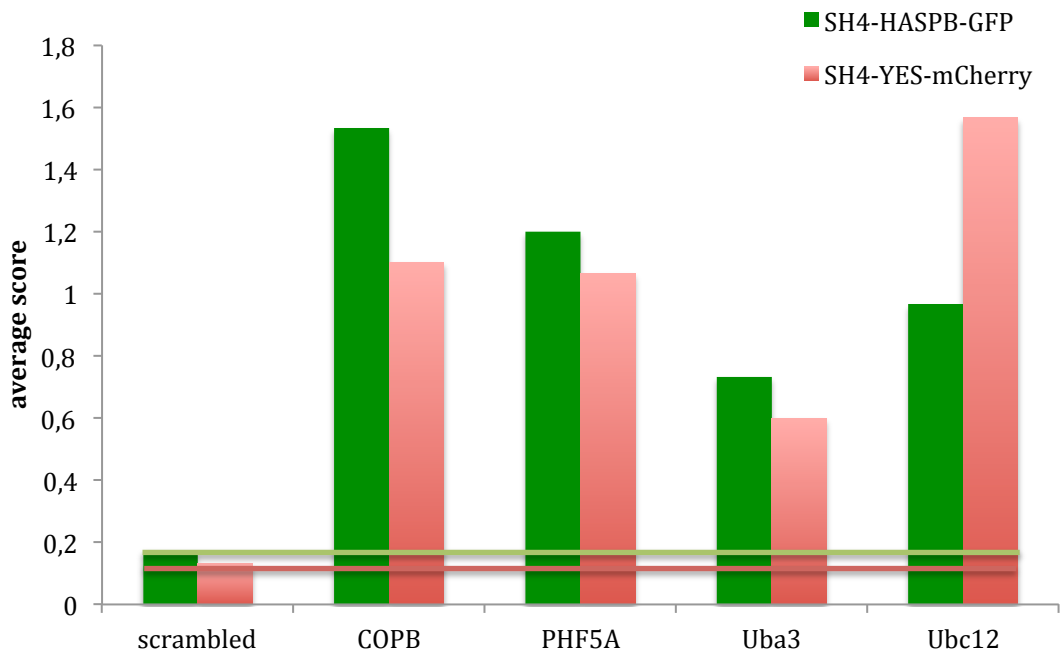

Figure 39 Hit scores of siRNA treatments against COPB, PHF5A, UBA3 and UBC12 by an automated image analysis tool. 72 hours after transfection with scrambled siRNA and respective siRNAs against COPB, PHF5A, UBA3 and UBC12, live-cell wide-field microscopy data were analyzed by an automated image analysis tool to determine the hit scores. The green line indicates the average score of treatment with scrambled siRNA in SH4-HASPB-GFP. The red line indicates the average score of treatment with scrambled siRNA in SH4-YES-mCherry.

Figure 39 shows an automated image analysis result of HeLa cells expressing SH4-HASPB-GFP and SH4-YES-mCherry after respective RNAi treatments 72 hours post transfection. siRNA treatment against UBC12 causes high scores in both SH4-reporter proteins and remarkably the highest score in SH4-YES-mCherry comparing to the positive controls COPB and PHF5A. Similar results were gained when we down-regulated NAE1 and NEDD8 in HeLa cells expressing SH4-HASPB-GFP and SH4-YES-mcherry (Figure 30; Figure 31). It seems that knockdown of NAE1, NEDD8 and UBC12 affect more the intracellular targeting of SH4-YES than SH4-GFP to the plasma membrane.

Knockdown of UBA3 also causes relative high scores in both SH4-reporter proteins compared to the scores of treatment with scrambled siRNAs, however lower than positive controls caused by siRNA treatments against PHF5A and COPB1. Scores of positive

controls gained in this experiment are general low due to the fact that cells might undergo apoptosis with the extended knockdown time for 72 hours.

Overall, knockdown of UBA3 and UBC12 did not cause intracellular retention of any SH4-reporter proteins after 48 hours; however, at the extended time of 72 hours, UBA3 and UBC12 caused comparable scores to the positive controls in both SH4-reporter proteins. We observed that 48 hours after siRNA transfection effects mildly on the localization of SH4 proteins, while extended knockdown period of 72 hours resulted a significant intracellular retention of both SH4-reporter proteins. These results suggest a requirement of UBA3 and UBC12 in the intracellular transport of SH4-reporter proteins and could further indicate a requirement for a functional neddylation pathway.

Taken together all the microscopy data under respective knockdown conditions and the results by applying automated analysis tool, we could conclude that:

1) Knockdown of NAE1 caused intracellular retention of SH4-YES with a time period of 48 hours post transfection.
2) Knockdown of NEDD8, UBA3 and UBC12 caused intracellular retention of both SH4-reporter proteins with an extended time period of 72 hours post transfection.
3) APP is probably not involved in the trafficking of both SH4-proteins to the plasma membrane.

In addition, we were able to confirm that the intracellular accumulation of SH4-YES was indeed caused by RNAi-mediated down-regulation of NAE1 by the rescue experiment.

3.6.4 Inhibition of neddylation pathway by using dominate negative constructs

We focused our study on the question whether a dysfunctional neddylation pathway affects on the localization of the acylated reporter proteins especially on SH4-YES. As a second independent approach, we used dominant-negative mutants of components involved in neddylation to inhibit the pathway. NAE1 443-479, first described in (Chen et al., 2000), is a 36-amino acid fragment of NAE1 to which UBA3 binds. With this construct, the function of endogenous NAE1 is supposed to be inhibited due to the

competition of NAE1 443-479 for binding to UBA3. UBC12C111S, in which the NEDD8 E2 active site a single cysteine is mutated to serine (Wada et al., 2000) binds NEDD8 covalently, forming a covalent oxyester bond with the free carboxyl group of the C-terminal glycine of NEDD8 that is stable and blocking the transfer of NEDD8 onto the substrate (Leck et al., 2010). Similar to UBC12C111S, UBA3C216S is supposed to bind NEDD8 and thus block the neddylation pathway in similar manner. We also designed construct NEDD8ΔGG, a conjugative-defective protein, which is supposed to compete against cellular NEDD8 and thus could be able to block the neddylation pathway.

3.6.5 Phenotype analysis by using dominant negative constructs

We transiently transfected the dominant negative constructs in pIRES vector containing dsRED in the second open reading frame in HeLa cells expressing SH4-YES-GFP and subsequently, subjected the cells to confocal microscopy for the determination of the subcellular localization of SH4-YES-GFP.

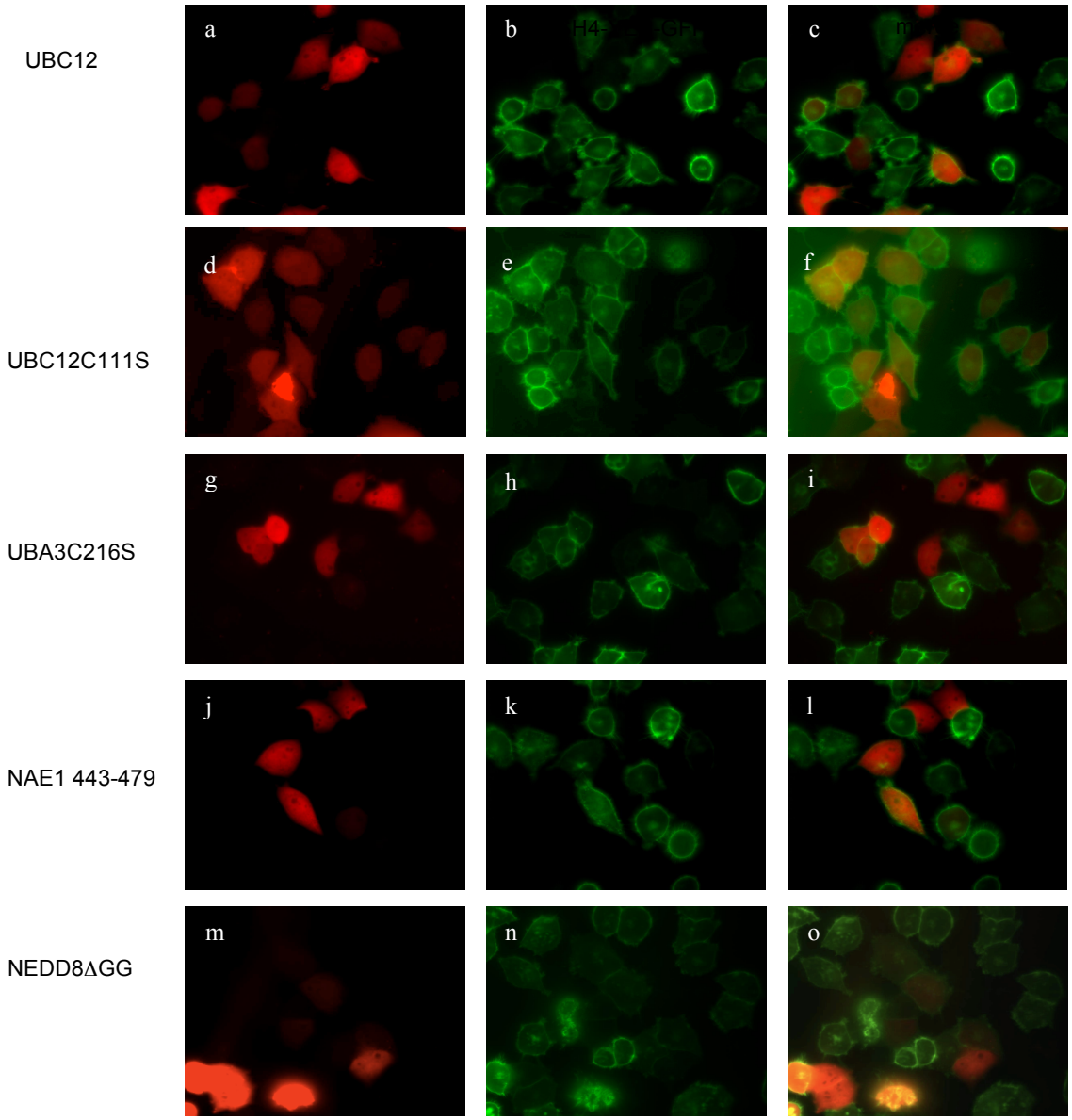

Figure 40 Confocal microscopy analysis of HeLa cells expressing SH4-YES-GFP after transient transfection of dominant negative constructs. HeLa cells were transient transfected with respective dominant negative constructs before SH4-YES-GFP expression was induced by cultivation in the presence of doxycycline for additional 12 hours. UBC12 (a-c), UBC12C111S (g-i), UBA3C216S (j-l), NAE1 443-479 (j-l), NEDD8ΔGG (m-o).

Wild-type UBC12 was used as a negative control while other 4 dominant negative constructs UBC12C111S, UBA3C216S and NAE1 443-479 as well as NEDD8ΔGG were used to block the neddylation pathway at different steps. Transfected cells were in red due to the overexpression of dsRED (Figure 40). A challenge for the experiment was the transient transfection efficiency. After optimization of transfection conditions, we were

able to transfect the cells with UBC12C111S with a transfection efficiency around 50% of the whole cell population, while transfection efficiencies of the other three DN constructs were below 15% of cell population. Compared to non-transfected cells, the overexpression of UBC12C111S or UBA3C216S as well as NAE1 443-479 and NEDDΔGG did not cause a significant intracellular accumulation of SH4-YES-GFP as shown in Figure 40.

3.6.6 Neddylation blocking assay after transfection of respective dominant negative constructs

We performed a neddylation-blocking assay to verify blocking efficiencies after transient transfection of respective dominant-negative constructs as described in Soucy et al., 2009.

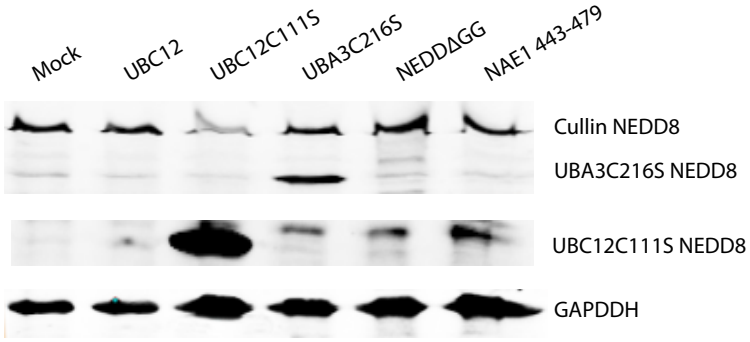

Figure 41 Determination the blocking efficiency of dominant negative constructs on cellular neddylation. HeLa cells expressing SH4-YES-GFP were transfected with respective dominant negative constructs UBC12C111S, UBA3C216S, NEDD8ΔGG and NAE1 443-479. UBC12 was used as a negative control. Cell lysates were collected and analyzed by Western blotting with anti NEDD8 and GPADH antibodies.

HeLa cells were harvested 20h post transiently transfection. Cellular levels of neddylated cullins were detected by using anti-NEDD8 antibody in Western Blot (Figure 41). Neddylated UBC12C111S (32kD) and UBA3C216S (62kD) were detected by anti-NEDD8 antibody as well. Protein amounts were normalized to GAPDH.

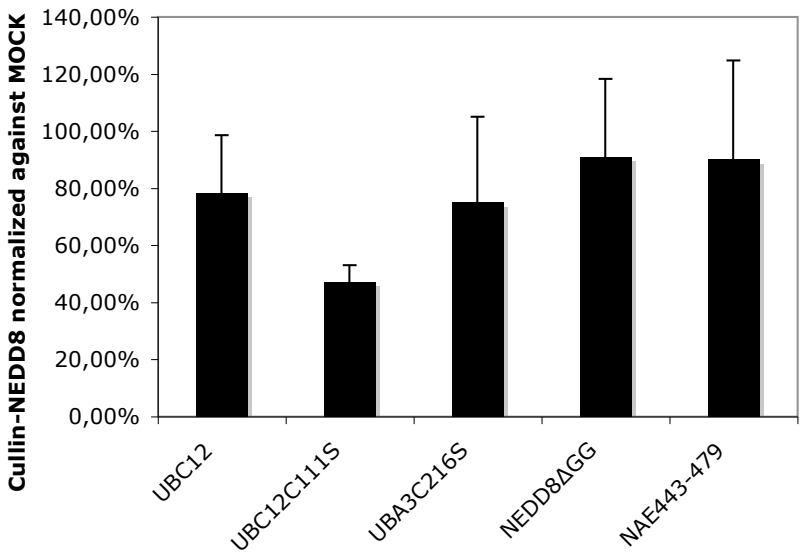

Figure 42 Quantification on protein level of neddylation blocking assay. HeLa cells expressing SH4-YES-GFP were transfected with respective dominant negative constructs. Neddylated cullins were detected using an anti-NEDD8 antibody. Signals were quantified by using a Odyssey imaging system

Figure 42 shows a quantification of the inhibition efficiencies of respective dominant negative constructs on neddylation. The inhibition efficiency on the formation of cullin-NEDD8 by the overexpression of dominant negative construct UBC12 C111S is around 50% and the corresponding transfection efficiency was around 60%, indicating a high inhibition efficiency in transfected cells. Similar to UBC12C111S, overexpression of the dominant negative constructs UBA3C216S, NEDD8ΔGG and NAE1 443-479 inhibited the neddylation of cullins at 25%, 10% and 10% corresponding the transfection efficiencies of around 15%, respectively. These results suggested the dominant negative construct UBC12C111S indeed blocked the neddylation pathway in the transfected cells. However, it is difficult to draw a conclusion about the other dominant negative constructs due to the low transfection efficiencies.

3.6.7 Inhibition of NAE1 with a pharmacological inhibitor MLN4924

Another way to probe the activity of an enzyme is to use pharmacological compounds with defined biochemical activities. To determine if neddylation is required for the correct targeting of SH4-proteins to the plasma membrane, we used MLN4924 as an inhibitor for NAE1, which is structurally related to adenosine 5´monophosphate (AMP)-

a tight binding product of the NAE reaction (Soucy et al., 2009). MLN4924 is reported and well characterized as a selective NAE1 inhibitor, which inhibits only NAE1 without affecting the function of ubiquitin-activating enzyme (UAE) and SUMO-activating enzyme (SAE).

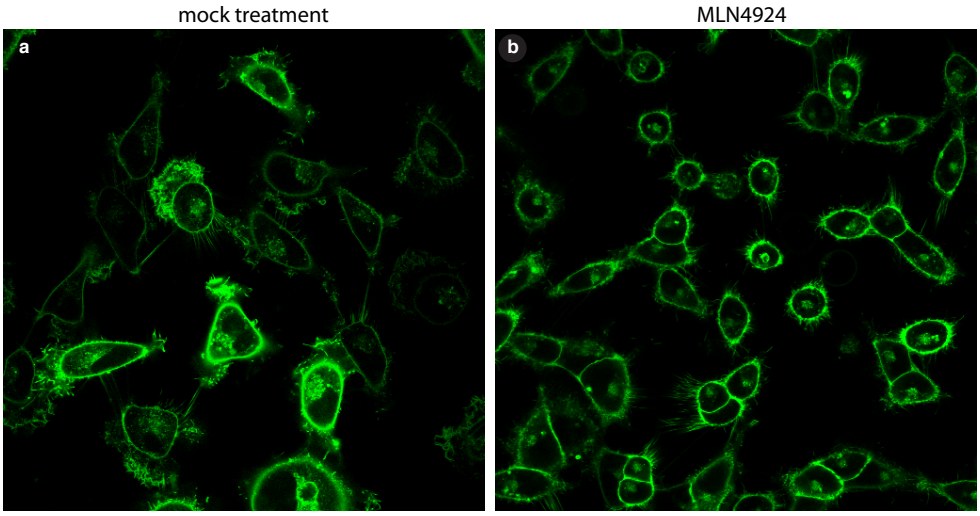

Figure 43 Confocal microscopy analysis of HeLa cells expressing SH4-YES-GFP treated with DMSO and MLN4924. HeLa cells expressing SH4-YES-GFP were subjected to mock with 1% DMSO (a) or 1 µM inhibitor MLN4924 for 6 hours (b).

HeLa cells expressing SH4-YES-GFP were treated with 1% DMSO as mock control and 1 µM MLN4924 for 6 hours. Subsequently, treated cells were subjected to confocal microscopy analysis. Figure 43 shows that the treatment with MLN4924 resulted in a mild intracellular retention of SH4-YES-GFP. In order to prove that cellular neddylation is indeed blocked by MLN4924, we performed the same neddylation blocking assay as for the transient transfection of dominant negative constructs.

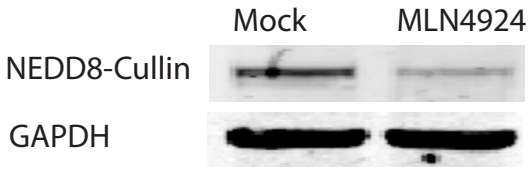

Figure 44 Determination the blocking efficiency of MLN4924 on cellular neddylation. HeLa cells expressing SH4-YES-GFP were incubated with 1% DMSO or 1 µM MLN4924 for 6 hours. Cell lysates were collected and analyzed by Western blotting with NEDD8 and GPADH antibodies.

HeLa cells expressing SH4-YES-GFP were incubated with 1 μM MLN4924 for 6 hours. Cell lysate were analyzed for the inhibition efficiency of MLN4924 on the formation of NEDD8-cullin conjugates by using an antibody against NEDD8 on Western Blot (Figure 44). Normalized to GAPDH protein level, about 13% of NEDD8-cullin remained in the cells after 6-hour incubation with MLN4924. These results suggest that neddylation was indeed blocked by MLN4924 at the time point for the confocal microscopy analysis; however, the blocking of neddylation solely resulted in a mild intracellular retention of SH4-YES-GFP.

3.6.8 Quantification of intracellular accumulation of SH4 proteins

A crucial step of microscopy image analysis is the segmentation of cells and classification of hit phenotypes. With the automated image analysis tool developed by S. Remmele used for the previous study so far, we are able to identify phenotypes with regard to the localization of SH4-reporter proteins. This tool represents a fast, reliable and unbiased system, especially suitable for high-content screening. However, a quantification of the intracellular retention of SH4- reporter proteins within one cell is not possible. Another limitation is that the software is solely able to quantify pictures taken by wide field microscopy at 10X magnification. A further challenge is to quantify phenotypes in a heterogeneous system, quite often e.g. when the transfection efficiency of the cells is not 100%. In this case, the automated image analysis tool failed to discriminate the untransfected cells. To overcome these limitations, we therefore established single cell assay by using of ImageJ as a quantification tool.

Previous studies showed that Bodipy-Cer are internalized and then localize mainly in the trans-Golgi and trans-Golgi network (Ladinsky et al., 1994). We used of Bodipy-Cer to identify the perinuclear area containing potential accumulation sites for SH4-reporter proteins. Further, we quantified the intracellular accumulation of SH4-reporter protein per cell. As described, Z-stacks of cells were taken under identical parameters and exposure time. Only the stacks containing potential accumulation sites for SH4-reporter proteins, which are marked by Bodipy-Cer in red, are considered for the calculation afterwards. For each stack, the intracellular accumulation site of SH4-reporter proteins was defined as Area of Interest (AOI). Integrated intensity of AOI and total signal of each

slice was then measured using ImageJ. Afterwards, both values were summed up respectively and the percent of intracellular accumulation of SH4-reporter protein was calculated by the value of AOI divided by the total signal value.

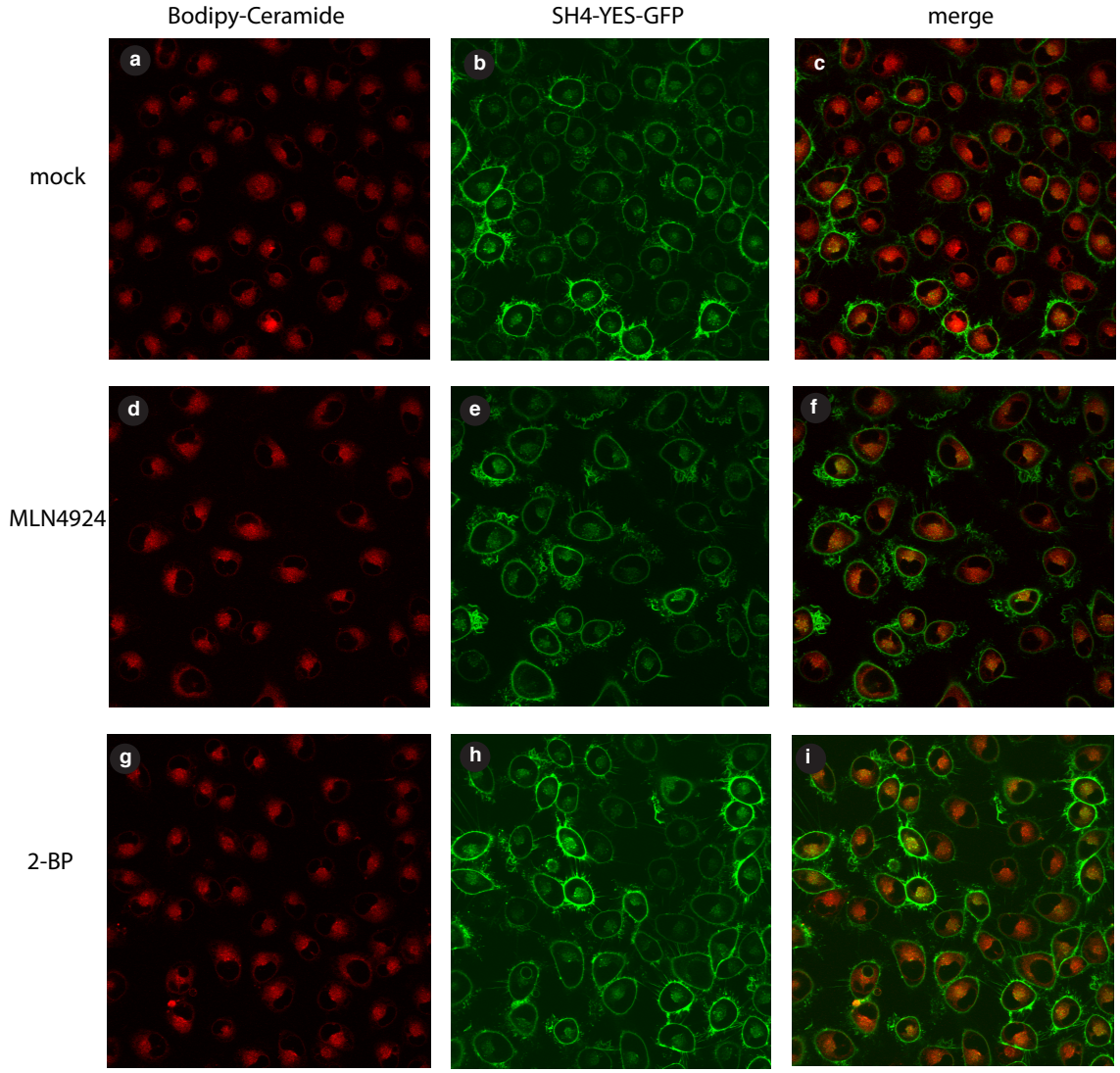

Figure 45 Confocal microscopy analysis of HeLa cells expressing SH4-YES-GFP after mock treatment and treatments with MLN4924 and 2-BP. HeLa cells expressing SH4-YES-GFP were incubated with MLN4924 for 6 hours. Bodipy Cer-Tx was applied directly into the medium. Subsequently, cells were stored at 4°C for 1 hour (2 hours after adding MLN4924) and further 3 hours incubation at 37°C. Mock treatment (a-c), MLN4924 treatment (d-f), 2-bromopalmitat treatment (2-BP) (g-i).

Figure 45 shows confocal microscopy images of HeLa cells expressing SH4-YES-GFP after treatment treated with 1% DMSO, 3 µM MLN4924 and 100 µM 2-bromopalmitat for 6 hours after protein expression was induced by adding doxycycline for 12 hours. The fifth layer of z-stacks is depicted where the area containing the potential accumulation

site for SH4-reporter proteins is red, marked by Bodipy Cer-TxRED (Invitrogen). A moderate intracellular accumulation of SH4-YES-GFP is observed after treatments with MLN4924 as well as 2-bromopalmitat as a positive control.

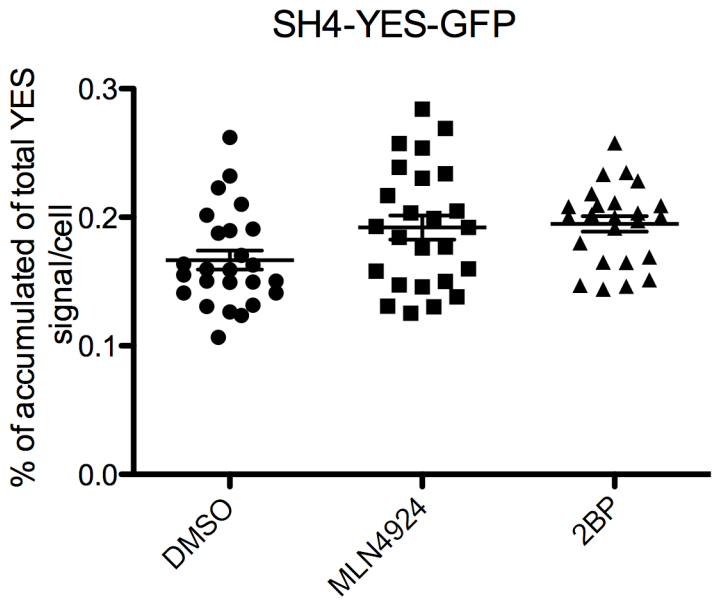

Figure 46 Quantification of intracellular accumulation of SH4-YES-GFP after respective treatments by using two-tailed unpaired student-t-test. HeLa cells expressing SH4-YES-GFP was treated with 1% DMSO, 3µM of MLN4924 for 6 hours and 100 µM of 2-BP for 24 hours.

As described in the previous paragraph, the obtained values of each treatment are presented in Figure 46. The difference between mock and MLN4924 or mock and 2-BP treatment is 3%, respectively, which are relative low however statistically significant by using two-tailed unpaired student´s t-test. These results indicate that the correct targeting of SH4-YES-GFP is affected by the treatment of MLN4924, suggesting a requirement of NAE1, which is in accordance with the results of studies by applying RNAi and dominant negative constructs as methods.

Although data from RNAi showed that downregulation of molecular components involved in neddylation pathway affected the intracellular transport of SH4-YES, experiments by using dominant negative construct UBC12C111S and NAE1 inhibitor MLN4924 demonstrated a relative moderate effect on the targeting of SH4-YES. We might conclude that the neddylation is required however not essential for correct targeting of SH4-YES.

4 Discussion

4.1 CLASSIFICATION OF GENE PRODUCTS IDENTIFIED IN MANUAL VALIDATION APPROACH

A genome-wide microscopy-based RNAi screen was carried out to identify cellular components involved in intracellular targeting of SH4-domain-containing proteins in a previous study. Generated microscopy data were analyzed by applying a software-based image analysis module, which can detect and quantify intracellular retention of SH4 fusion proteins. All together 286 genes were identified in the primary screen by application of suitable score thresholds. These 286 genes were further validated by automated and 12 genes were validated by manual screening approaches in the current study. We used two independent siRNAs targeting different regions of each mRNA and subjected doxycycline-inducible HeLa cells expressing SH4-HASPB-GFP and SH4-YES-mCherry directly to wide field microscopy. With a manual microscopy-based approach, we were able to image the cells at two different time-points, 48 hours and 60 hours post siRNA transfection. The manual microscopy-based approach reduced screening time which is an advantage compared to the complete validation screen of 286 gene products by using automated microscopy carried out in parallel. We validated and identified 5 gene products by manual inspection: NAE1, PHF5A, CCDC43 and GALTNL4 as well as MAK10 in manual validation approach. Stable HeLa cells expressing SH4-HASPB-GFP and SH4-YES-mCherry showed a pronounced intracellular accumulation of SH4-proteins after respective siRNA treatments.

4.1.1 Potential roles of PHF5A, GALTNL4 and MAK10 in SH4-domain-dependent protein transport

PHD finger protein 5A was a gene product identified in the manual microscopy-based validation approach. Microscopy analysis showed a pronounced intracellular retention of SH4 protein after siRNA treatment against PHF5A (Figure 12). PHF5A is a small nuclear protein containing a PHD domain, a subunit of the splicing factor 3b protein complex and

may act as a chromatin-associated protein. Most possibly, knockdown of PHF5A may affect indirectly the intracellular transport of SH4-proteins to the plasma membrane.

One gene product identified in the manual microsocopy-based approach was putative polypeptide N-acetylgalactosaminyltransferase-like protein 4 (GALNTL4) (Figure 13), which is an integral membrane protein and localizes to Golgi apparatus. According to sequence homology analysis, GALNTL4 may catalyze the initial reaction in O-linked oligosaccharide biosynthesis, the transfer of an N-acetyl-D-galactosamine residue to a serine or threonine residue on target proteins. Previous studies showed that both N- and O-glycosylation are critically important in the sorting of some membrane glycoproteins (Gut et al., 1998; Scheiffele et al., 1995; Spodsberg et al., 2001; Yeaman et al., 1997). siRNA mediated knockdown of GALNTL4 might abolish the glycosylation of membrane glycoproteins that are involved in the formation or stabilization of lipid rafts clusters at the Golgi apparatus, which is hypothesized as a prerequisite for the targeting of SH4 proteins to the plasma membrane, thus might affect the plasma-membrane targeting of SH4 proteins.

siRNA treatment against N-alpha-acetyltransferase 35, NatC auxiliary subunit (MAK10 homolog) results a pronounced intracellular retention of both SH4-proteins (Figure 14). Studies in yeast showed that MAK10 functions as a component of the N-terminal acetyltransferase C (NatC) complex catalyzing acetylation of N-terminal methionine residues. Recent work has suggested that acetylation of α-tubulin on lysine 40 is common and can be found on stable microtubules in most cell types (Hammond et al., 2008). Further, it was postulated that kinesin-1 has higher affinity to acetylated microtubulin *in vitro* and pharmacological treatments that increase microtubule acetylation cause a misdirection of kinesin-1 transport of its cargo to nearly all neurite tips *in vivo* (Reed et al., 2006). In addition, it was also shown that α-tubulin plays a positive role in motor-based trafficking in mammals (Janke et al., 2005; Reed et al., 2006; van Dijk et al., 2007). By using Mass spectrometry as a tool, cytoskeletal proteins are identified in the samples associated with SH4-HASPB-and SH4-YES-containing DRM fractions (unpublished data, Paulina Turcza, Nickel lab). Therefore, it might be that the trafficking

of SH4-proteins to the plasma membrane requires acetylated microtubules for the transport from TGN to the plasma membrane.

Since PHF5A is located in the nucleus and our limited knowledge on the putative functions of GALNTL4, MAK10 homolog and CCDC43, whose functions are unknown, we focused our study on the role of NAE1 and a potential requirement of the neddylation pathway in the intracellular targeting of SH4 proteins to the plasma membrane (discussed in the section 4.3).

4.2 CLASSIFICATION OF GENE PRODUCTS IDENTIFIED IN AUTOMATED VALIDATION APPROACH

286 hits identified during primary screening were validated by using automated microscopy platform in parallel to the manual validation approach. The list of validated gene products whose down-regulation causes intracellular retention of SH4 reporter molecules consists of 54 gene products. We validated the involvements and further characterized the involvement of 1) coatomer since several subunits like COPB1 and COPA were also validated in the automated microscopy-based screen; 2) MVD which is involved in the lipid metabolism; and 3) PKCα since reversible phosphorylation as a molecular switch regulates the plasma membrane targeting of SH4 proteins (Tournaviti et al., 2009).

4.2.1 Coatomer as a component of SH4-domain-dependent protein transport

COPB1 was the first gene product identified in the genome-wide RNAi screen to play a role in Sh4-domain-dependent protein transport. Microscopy analysis showed that downregulation of COPB1 caused a pronounced intracellular accumulation of SH4-domain proteins. Further, we also observed a similar effect after knock down of COPD, another subunit of heptameric coatomer complex (Figure 16). Analysis of knockdown efficiencies on the protein level showed that down-regulation of the coatomer subunit COPB1 resulted in decreased protein levels of other coatomer subunits such as COPD

and *vice versa* (Figure 17). This indicated that downregulation of one coatomer subunit probably resulted in destabilization of the heterooligomeric coatomer complex. Coatomer as the coat protein of COPI transport vesicles mediates retrograde transport from the Golgi to the ER and also bidirectional traffic between Golgi cisternae (Rothman, 1996). Using immuno-electron microscopy, it has been shown that coatomer not only localizes to the intermediate compartment and the Golgi, but also associates with membranes of the trans-Golgi-network (Griffiths et al., 1995). Moreover, *in vitro* generation of TGN-derived vesicles is dependent on Arf and PKC activity (Simon et al., 1996), two components involved in membrane recruitment of coatomer (De Matteis et al., 1993). The in vitro generated vesicles had a size of 50-80nm and, in the presence of GTPγS, retained a proteinaceous coat (Simon et al., 1996). Additionally, it was shown that coatomer was required for and present on *in vitro* generated TGN-derived vesicles (Simon et al., 1998). These data may suggest a role of coatomer in the formation of TGN-derived vesicles, which may play a role in SH4-dependent proteins transport to the plasma membrane. However, *in vitro* vesicle generation was significantly reduced by treatment with BFA (Simon et al., 1996), while transport of SH4-proteins to the plasma membrane appears to be BFA-insensitive (Paulina Turcza, unpublished results from our laboratory). Whether BFA-insensitive Arf guanine nucleotide exchange factors may play a role in this process remains a subject of further investigation in our laboratory.

Another explanation for our observation might be that downregulation of coatomer inhibits indirectly palmitoylation and thus perturbs the insertion of SH4-proteins into membrane microdomain. As a consequence, transport from Golgi to the cell surface could be blocked because the partitioning into membrane microdomains is hypothesized to play a role in further transport to the plasma membrane (Brown and London, 1998; Edidin, 2003; Linder and Deschenes, 2007; Smotrys and Linder, 2004; Webb et al., 2000). Although palmitoylation activity was assigned to several membrane compartments and DHHC palmitoyltransferasese associate with ER, Golgi and plasma membrane (Greaves et al., 2010; Ohno et al., 2006). Independent analyses of DHHC substrate pairs returned a high percentage of DHHC proteins located at Golgi as positive hits (Fernandez-Hernando et al., 2006; Fukata et al., 2004; Greaves et al., 2010; Greaves et al., 2008; Huang et al., 2004b; Tsutsumi et al., 2009) indicating that palmitoylation

occurs at the Golgi apparatus. Recently, Rocks et al., (2010) also stated that palmitoylation is detectable only on the Golgi apparatus. Taken together, whether coatomer is directly involved in formation of TGN-derived vesicles containing SH4 proteins or indirectly affects palmitoylation of SH4-domain at the Golgi apparatus requires further studies.

To further exclude off-target effects, we performed rescue experiments by microinjection of cells with recombinant coatomer. In previously microinjected cells, down-regulation of endogenous coatomer by RNAi did not cause intracellular accumulation of SH4-proteins any further (Figure 18). Therefore, using our experimental system, we were able to identify COPB1 and COPD as components of a multi-protein complex coatomer, which is required for the correct targeting of SH4 dependent protein to the plasma membrane.

4.2.2 PKCα as a component of SH4-domain-dependent protein transport

Another protein whose down-regulation caused a pronounced intracellular retention of SH4 dependent protein transport was a protein kinase C, alpha (PKCα) (Figure 19). Members of protein kinase C (PKC) family are serine/threonine kinases that play key regulatory roles in a multitude of cellular processes ranging from control of fundamental cell autonomous activities, such as proliferation to other cellular functions like memory (Mellor and Parker, 1998). PKCα is ubiquitously expressed and activated by stimuli such as tyrosine kinase receptors and also physical stresses like hypoxia and mechanical strain (Nakashima, 2002). Upon stimulation, PKCα redistributes from cytosol to the entire membrane in response to non-specific activator for PKCs such as phorbol myristate acetate (PMA). As shown in Figure 20, the reduction of PKCα protein levels to about 20% compared to the treatment with a scrambled siRNA caused significant perinuclear accumulation of SH4 fusion proteins. Further, to test whether PKC activity is required for the correct targeting of SH4-proteins, we applied a pharmacological inhibitor of protein kinase C to the cells and observed similar intracellular retention of SH4-proteins compared to the cells treated with the siRNA against PKCα (Figure 22). These results indicate a requirement of protein kinase C activity in the targeting of SH4 proteins to the plasma membrane. A possible explanation is that the abolishment of the phosphorylation caused the intracellular redistribution of SH4-proteins. Whether SH4 proteins are directly

or other targets involved in the transport of SH4 proteins are phosphorylated by PKCα is still not clear. However, a previous study showed that reversible phosphorylation and dephosphorylation of SH4-domains of HASPB and YES plays a role in the subcellular localization and further it was postulated that phosphorylation of SH4 proteins caused the perinuclear accumulation at Golgi and endosome and the dephosphorylation lead to the attachment to the plasma membrane (Tournaviti et al., 2009). Also in another previous study, Resh (1999) postulated the two-signal model for membrane binding of myristoylated proteins. As an example for this model, the myristoylated SH4 domain of Src contains phosphorylation sites by PKCα and the phosphorylation of SH4 domain produces a small shift in the distribution of the Src from the plasma membrane to the cytosol (Murray et al., 1998). This model and the study (Tournaviti et al., 2009) contradict our observation of intracellular retention of SH4 proteins when PKCα is downregulated by RNAi. However, translocation of Src from the membrane to the cytosol upon phosphorylation has not been consistently demonstrated (Murray et al., 1998; Walker et al., 1993). Notably, the possibility is not excluded that the PKCα might be more indirectly involved in the intracellular transport of acylated proteins. Therefore, further studies are required to obtain a precise role of PKCα in SH4 protein transport.

4.2.3 A role of lipid homeostasis in SH4-dependent protein transport

Previous studies postulated that the targeting of SH4-dependent protein transport requires cholesterol-dependent lipid rafts (Brown and London, 1998; Edidin, 2003; Linder and Deschenes, 2007; Smotrys and Linder, 2004; Webb et al., 2000). We identified and validated a gene product mevalonate decarboxylase (MVD) whose siRNA-mediated down-regulation caused intracellular retention of SH4 proteins (Figure 23). MVD is a cytosolic homodimer and plays a role in early steps of cholesterol biosynthesis where it catalyzes the conversion of mevalonate pyrophosphate into isopentenyl pyrophosphate (IPP) and dehydrates its substrate under the consumption of ATP (Hogenboom et al., 2002; Hogenboom et al., 2003; Toth and Huwyler, 1996). Inhibition of cholesterol synthesis by downregulation of the enzyme MVD may lead to a reduction of endogenous cholesterol and further interfere with the formation of cholesterol-enriched lipid microdomains.

To get a better understanding on the role of cholesterol of SH4-protein trafficking, we treated cells with methyl-β-cyclodextrin (MβCD) in delipidated medium to deplete cellular cholesterol. Unlike other cholesterol-binding agents that incorporate into membranes, cyclodextrin are strictly surface-acting and selectively extract membrane cholesterol by including it in a central, non-polar cavity of cyclic oligomers of glucopyranoside in α-1,4 glycosidic linkage (Pitha et al., 1988). β-cyclodextrins have been shown to be a specific cholesterol-binding agent that neither binds nor inserts into the plasma membrane (Ohtani et al., 1989). Later, it was found that cholesterol depletion of membranes by MβCD could result in tight packing of sphingolipids chains to form a rigid gel-like phase (Ilangumaran and Hoessli, 1998). It was also suggested that MβCD preferentially extract cholesterol from outside rather than within the sphingolipid microdomain and this partly solubilized GPI-anchored and transmembrane proteins from microdomains and releases microdomains in both vesicular and non-vesicular form (Ilangumaran and Hoessli, 1998).

Remarkably, a pronounced intracellular retention of SH4-proteins was observed after one-hour incubation with MβCD (Figure 26). If cholesterol is indeed required for the correct targeting of SH4-proteins to the plasma membrane, then addition of exogenous cholesterol to the delipidated media should be able to rescue the phenotype caused by cholesterol depletion. We indeed observed a pronounced re-localization of SH4-proteins to the plasma membrane (Figure 26).

Meanwhile, we measured the cellular cholesterol levels by using nano-elecrospray ionization mass spectrometry using phosphatidylcholine (PC) as a bulk lipid to normalize data. Compared to treatments with siRNAs against MVD and MβCD, we found a reduction of cellular cholesterol concomitantly by 30% and 50% relative to PC, respectively (Figure 27). Previous study showed that a reduction of cholesterol levels by 30-50% affected cholesterol-dependent processes such as shedding of the type XIII collagen ectodomain (Vaisanen et al., 2006). To test whether stress potentially exerted by MβCD causes a pleiotropic effect on the targeting of SH4 proteins to the plasma membrane, we treated cells with ouabain, an unrelated Na^+/K^+ ATPase inhibitor. We

observed a mild effect on overall cell morphology by incubation of ouabain however it did not result in perinuclear accumulation of SH4 proteins (Figure 26). Our results indicate that interference with cellular cholesterol levels causes a significant intracellular retention of SH4-proteins and further corroborate the role of cholesterol-dependent lipid rafts in the targeting of SH4 proteins to plasma membrane. They are further in accordance with other study suggesting that RNAi-mediated down-regulation of MVD affects cholesterol-dependent processes such as Dengue virus replication (Rothwell et al., 2009). However, studies also showed that cyclodextrin treatment led to serious side effects such as lateral protein immobilization (Kenworthy, 2008). As plasma membranes can contain up to 40 mol% cholesterol (Zidovetzki and Levitan, 2007), cholesterol depletion can perturb cellular functions: for example the plasma membrane can depolarize and Ca^{2+} can be induced to empty (Pizzo et al., 2002) leading to global cellular effects (Simons and Gerl, 2010) and indirectly affect the transport of SH4 proteins.

4.3 A ROLE OF NAE1 AS A COMPONENT OF NEDDYLATION IN SH4-DOMAIN-DEPENDENT PROTEIN TRANSPORT

One gene product identified in the manual validation approach was Neddylation-Activating-Enzyme 1 (NAE1). NAE1 was first identified as a novel binding partner of the cytoplasmic domain of amyloid precursor protein (APP) and was thus called as APP binding protein 1 (APP-BP1) (Chow et al., 1996). Further, NAE1 is involved in activation of the ubiquitin-like protein NEDD8 and participates in the neddylation pathway (Gong and Yeh, 1999). Similar to ubiquitination, ATP-dependent NEDD8 activation is initiated by NEDD8 E1 enzyme NAE1-UBA3, which creates a high-energy intermediate. This heterodimer of NAE1 and UBA3 is homologous to the amino- and C-terminal domains of ubiquitin-activating enzyme, respectively (Liakopoulos et al., 1998; Osaka et al., 1998; Walden et al., 2003). siRNA mediated down-regulation of NAE1 caused a significant intracellular accumulation of SH4-YES (Figure 28). Further, we were able to confirm the phenotype was not caused by off-target effects by RNAi but indeed by downregulation of NAE1 by the rescue experiment with mouse homolog

NAE1. In order to get a better understanding of the requirement of NAE1 in the targeting of SH4-proteins to the plasma membrane, we further downregulated NEDD8 and APP, which functionally interact with NAE1; finally UBA3 and UBC12, which are involved in the neddylation pathway. With extended time period, siRNA mediated downregulation of NEDD8, UBA3 and UBC12 but not APP caused intracellular retention of SH4-YES and SH4-HASPB (Figure 31; Figure 39). These results indicate that neddylation may be required in the correct targeting of SH4 proteins. It might be that factors required for the localization of SH4 proteins at the plasma membrane could be regulated by NAE1 or by covalent attachment of NEDD8. Neddylation of these factors could be required for efficient surface delivery of SH4 proteins or might prevent their reinternalization.

Hence, we further focused our study on the question whether an intact neddylation pathway is required for the correct targeting of SH4 proteins to the plasma membrane. As a second independent approach we used dominant-negative mutants of components involved in neddylation to inhibit the pathway. Dominant negative UBC12C111S binds NEDD8 covalently by forming an oxyester bond with the free carboxyl group off the C-terminal of NEDD8 (Leck et al., 2010). Therefore overexpression of UBC12C11S is able to block the transfer of NEDD8 onto the substrates, which was confirmed in the neddylation blocking assay (Figure 41; Figure 42). However, a pronounced intracellular accumulation of SH4-YES is not observed in the cells transfected by UBC12C111S compared to untransfected cells (Figure 40). Finally, we applied a pharmacological compound to determine if neddylation is indeed required for the correct targeting of SH4-proteins to the plasma membrane. MLN4924 was identified as a cell-permeable inhibitor targeting the E1 for neddylation (Soucy et al., 2009). Further it was shown that MLN4924 effectively inhibits NAE1 activity and as a result inhibits downstream activities such as activation of the UBC12 and cullin neddylation (Soucy et al., 2009). Our data showed that blocking neddylation by incubation with MLN4924 (Figure 44) resulted in a mild intracellular retention of SH4-YES (Figure 43). We quantified the intracellular accumulation of SH4-proteins per cell (Figure 46). The difference between mock and MLN4924 treatments is minor, however it is comparable to the difference between mock and the positive control 2-BP which is a palmitoylation inhibitor (Resh,

2006) and 2-BP treated cells showed a pronounced intracellular accumulation of SH4-proteins (Ritzerfeld et al., 2011). Both values are statistically significant by using two-tail unpaired student´s T-test. Whether the redistribution of SH4-proteins from the plasma membrane to perinuclear region is a direct effect of the abolishment of cullin neddylation is not clear. This abolishment or deficiency of cullin neddylation would ultimately lead to the accumulation of cullin-RING ubiquitin ligases (CRLs) substrates that are normally targeted for degradation by the 26 S proteasome. This accumulation of CRLs substrates might indirectly affect the surface delivery of SH4-proteins and explain their intracellular redistribution.

Overall, our data suggest that correct targeting of SH4 proteins to the plasma membrane may not essentially require a functional neddylation pathway. NAE1 may affect the transport of SH4 proteins in neddylation-independent ways. A recent study showed the interaction of APP and NAE1 activated Rab5-dependent endocytosis in a neddylation-independent manner (Laifenfeld et al., 2007). Hence, NAE1 may have a distinct function other than neddylation in the transport of SH4 proteins. However, the precise role of NAE1 in the targeting of SH4-proteins to the plasma membrane could not be revealed in the course of the this study.

4.4 CONCLUSION AND FUTURE PERSPECTIVES

In the current study we validated gene products identified during primary screening by applying independent siRNAs. We confirmed COPB1 and PRCα as necessary components for the correct targeting of SH4 proteins to the plasma membrane. Results obtained on MVD and cholesterol corroborates the role of cholesterol-dependent membrane microdomains in SH4 proteins trafficking (McCabe and Berthiaume, 1999; McCabe and Berthiaume, 2001; Tournaviti et al., 2009; Webb et al., 2000). Another observation of this study was the role of NAE1 and neddylation pathway in the targeting of SH4 proteins. Our data suggest the correct targeting of SH4 proteins to the plasma membrane may not essentially require a functional neddylation pathway, however, down-

regulation of NAE1 causes intracellular retention of SH4-YES suggesting additional functions of NAE1.

Further investigations on the lipid and protein composition of SH4 proteins containing lipid rafts will help to have a close sight on the putative interacting partners of SH4 proteins. In addition, a microscopy independent readout of the distribution of SH4 protein might help to confirm the intracellular accumulation of SH4 proteins. Recent studies on another dually acylated Src-family tyrosine kinase Lyn showed that the requirement of the tyrosine-kinase domains but not the kinase activity of Lyn for its biosynthetic targeting to caveolin-positive Golgi membrane (Ikeda et al., 2009) and further Nadolski and Linder et al., (2009) suggested that an SH4 domain is not sufficient to confer the specificity for a DHHC protein. It might be interesting to study the full-length form of YES with its kinase domain. Finally, the putative roles of the identified gene products in SH4-domain dependent transport will be interesting aspects of future studies.

5 Abbreviations

2-BP	2-bromopalmitate
APT	acyl protein thioesterase
ATP	adenosine triphosphate
ARF	ADP-ribosylation factor
COPA	alpha-COP
N-terminal	amino-terminal
APP	amyloid precursor protein
APP-BP1	amyloid precursor protein binding protein 1
CCDC43	coiled-coil domain containing 43
COPB	beta-COP
BFA	brefeldin A
C-terminal	carboxy-terminal
COP	coat protein
DNA	desoxyribonucleic acid
dNTP	desoxyribonucleotid triphosphate
DRM	detergent-resistant membrane
dsRNA	double-stranded RNA
D-MEM	Dulbecco´s modified eagle medium
ER	endoplasmic reticulum
ERGIC	ER/Golgi intermediate compartment
E.coli	Escherichia coli
FCS	fetal calf serium
FGF	fibroblast growth factor
GALNTL4	putative ppolypeptide N-acetylgalactosaminyltransferase-like protein 4
GPI	glycosylphosphatidylinositol
GPF	green fluorescent protein
GAP	growth associated protein
GTP	guanosine triphosphate

HSPG	heparin sulfate progeoglycan
mRNA	messenger RNA
MAK10	N-alpha-acetyltransferase 35, Natc auxiliary subunit
MVD	Mevalonate (diphospho) dehydrogenase
MARCKS	myristoylated alanine-rich C kinase substrate
NAE1	nedd-activating enzyme1
NEDD8	neural precursor cell expressed, developmentally downregulated8
PBS	phosphate buffered saline
PE	phosphatidylethanolamine
PI	phosphatidylinositol
PI(4,5)P2	phsophatidylinositol-4,5-bisphosphate
PM	plasma membrane
PCR	polymerase chain reaction
PAT	protein acyltransferase
PKC	protein kinase C
PRKCA	protein kinase C alpha
PTP	protein tyrosine phosphatase
RNA	ribonucleic acid
RNAi	RNA interference
Rpm	rounds per minute
siRNA	short interfering RNA
SRP	signal recognition paticle
SNARE	SNAP receptor
SNAP	soluble NSF attachment protein
TGN	trans-Golgi network
UBA3	ubiquitin-like modifier activating enzyme 3
UBC12	ubiquitin-conjugating enzyme E2M

6 References

Ahearn, I.M., F.D. Tsai, H. Court, M. Zhou, B.C. Jennings, M. Ahmed, N. Fehrenbacher, M.E. Linder, and M.R. Philips. 2011. FKBP12 binds to acylated H-ras and promotes depalmitoylation. *Mol Cell*. 41:173-185.

Barlowe, C. 1998. COPII and selective export from the endoplasmic reticulum. *Biochim Biophys Acta*. 1404:67-76.

Bartels, D.J., D.A. Mitchell, X. Dong, and R.J. Deschenes. 1999. Erf2, a novel gene product that affects the localization and palmitoylation of Ras2 in Saccharomyces cerevisiae. *Molecular and cellular biology*. 19:6775-6787.

Beck, R., M. Rawet, F.T. Wieland, and D. Cassel. 2009. The COPI system: molecular mechanisms and function. *FEBS Lett*. 583:2701-2709.

Blenis, J., and M.D. Resh. 1993. Subcellular localization specified by protein acylation and phosphorylation. *Curr Opin Cell Biol*. 5:984-989.

Blobel, G., and B. Dobberstein. 1975a. Transfer of proteins across membranes. I. Presence of proteolytically processed and unproce ssed nascent immunoglobulin light chains on membrane-bound ribosomes of murine myeloma. *J Cell Biol*. 67:835-851.

Blobel, G., and B. Dobberstein. 1975b. Transfer of proteins across membranes. II. Reconstitution of functional rough microsomes from heterologous components. *J Cell Biol*. 67:852-862.

Bock, J.B., H.T. Matern, A.A. Peden, and R.H. Scheller. 2001. A genomic perspective on membrane compartment organization. *Nature*. 409:839-841.

Bolen, J.B., and J.S. Brugge. 1997. Leukocyte protein tyrosine kinases: potential targets for drug discovery. *Annu Rev Immunol*. 15:371-404.

Bonifacino, J.S. 2004. The GGA proteins: adaptors on the move. *Nat Rev Mol Cell Biol*. 5:23-32.

Borgese, N., W. Mok, G. Kreibich, and D.D. Sabatini. 1974. Ribosomal-membrane interaction: in vitro binding of ribosomes to microsomal membranes. *J Mol Biol*. 88:559-580.

Brown, D.A., and E. London. 1998. Functions of lipid rafts in biological membranes. *Annu Rev Cell Dev Biol*. 14:111-136.

Brown, M.T., and J.A. Cooper. 1996. Regulation, substrates and functions of src. *Biochim Biophys Acta*. 1287:121-149.

Carrabino, S., E. Carminati, D. Talarico, R. Pardi, and E. Bianchi. 2004. Expression pattern of the JAB1/CSN5 gene during murine embryogenesis: colocalization with NEDD8. *Gene Expr Patterns*. 4:423-431.

Chairatvit, K., and C. Ngamkitidechakul. 2007. Control of cell proliferation via elevated NEDD8 conjugation in oral squamous cell carcinoma. *Mol Cell Biochem*. 306:163-169.

Chen, Y., W. Liu, D.L. McPhie, L. Hassinger, and R.L. Neve. 2003. APP-BP1 mediates APP-induced apoptosis and DNA synthesis and is increased in Alzheimer's disease brain. *The Journal of cell biology*. 163:27-33.

Chen, Y., D.L. McPhie, J. Hirschberg, and R.L. Neve. 2000. The amyloid precursor protein-binding protein APP-BP1 drives the cell cycle through the S-M checkpoint and causes apoptosis in neurons. *J Biol Chem*. 275:8929-8935.

Chow, N., J.R. Korenberg, X.N. Chen, and R.L. Neve. 1996. APP-BP1, a novel protein that binds to the carboxyl-terminal region of the amyloid precursor protein. *J Biol Chem*. 271:11339-11346.

Ciechanover, A., H. Heller, R. Katz-Etzion, and A. Hershko. 1981. Activation of the heat-stable polypeptide of the ATP-dependent proteolytic system. *Proc Natl Acad Sci U S A*. 78:761-765.

Clague, M.J. 1999. Membrane transport: Take your fusion partners. *Curr Biol*. 9:R258-260.

Conner, S.D., and S.L. Schmid. 2003. Regulated portals of entry into the cell. *Nature*. 422:37-44.

Cope, G.A., and R.J. Deshaies. 2003. COP9 signalosome: a multifunctional regulator of SCF and other cullin-based ubiquitin ligases. *Cell*. 114:663-671.

Corsi, A.K., and R. Schekman. 1996. Mechanism of polypeptide translocation into the endoplasmic reticulum. *J Biol Chem*. 271:30299-30302.

Cosson, P., and F. Letourneur. 1994. Coatomer interaction with di-lysine endoplasmic reticulum retention motifs. *Science*. 263:1629-1631.

Dalbey, R.E., and G. Von Heijne. 1992. Signal peptidases in prokaryotes and eukaryotes--a new protease family. *Trends Biochem Sci*. 17:474-478.

De Matteis, M.A., and A. Luini. 2008. Exiting the Golgi complex. *Nat Rev Mol Cell Biol*. 9:273-284.

De Matteis, M.A., G. Santini, R.A. Kahn, G. Di Tullio, and A. Luini. 1993. Receptor and protein kinase C-mediated regulation of ARF binding to the Golgi complex. *Nature*. 364:818-821.

Deichaite, I., L.P. Casson, H.P. Ling, and M.D. Resh. 1988. In vitro synthesis of pp60v-src: myristylation in a cell-free system. *Molecular and cellular biology*. 8:4295-4301.

Dekker, F.J., O. Rocks, N. Vartak, S. Menninger, C. Hedberg, R. Balamurugan, S. Wetzel, S. Renner, M. Gerauer, B. Scholermann, M. Rusch, J.W. Kramer, D. Rauh, G.W. Coates, L. Brunsveld, P.I. Bastiaens, and H. Waldmann. 2010. Small-molecule inhibition of APT1 affects Ras localization and signaling. *Nat Chem Biol*. 6:449-456.

Denny, P.W., S. Gokool, D.G. Russell, M.C. Field, and D.F. Smith. 2000. Acylation-dependent protein export in Leishmania. *J Biol Chem*. 275:11017-11025.

Duda, D.M., L.A. Borg, D.C. Scott, H.W. Hunt, M. Hammel, and B.A. Schulman. 2008. Structural insights into NEDD8 activation of cullin-RING ligases: conformational control of conjugation. *Cell*. 134:995-1006.

Duncan, J.A., and A.G. Gilman. 1998. A cytoplasmic acyl-protein thioesterase that removes palmitate from G protein alpha subunits and p21(RAS). *J Biol Chem*. 273:15830-15837.

Edidin, M. 2003. Lipids on the frontier: a century of cell-membrane bilayers. *Nat Rev Mol Cell Biol*. 4:414-418.

Elsasser, S., R.R. Gali, M. Schwickart, C.N. Larsen, D.S. Leggett, B. Muller, M.T. Feng, F. Tubing, G.A. Dittmar, and D. Finley. 2002. Proteasome subunit Rpn1 binds ubiquitin-like protein domains. *Nat Cell Biol*. 4:725-730.

Fang, C., L. Deng, C.A. Keller, M. Fukata, Y. Fukata, G. Chen, and B. Luscher. 2006. GODZ-mediated palmitoylation of GABA(A) receptors is required for normal assembly and function of GABAergic inhibitory synapses. *J Neurosci*. 26:12758-12768.

Fernandez-Hernando, C., M. Fukata, P.N. Bernatchez, Y. Fukata, M.I. Lin, D.S. Bredt, and W.C. Sessa. 2006. Identification of Golgi-localized acyl transferases that palmitoylate and regulate endothelial nitric oxide synthase. *J Cell Biol*. 174:369-377.

Fukata, M., Y. Fukata, H. Adesnik, R.A. Nicoll, and D.S. Bredt. 2004. Identification of PSD-95 palmitoylating enzymes. *Neuron*. 44:987-996.

Gilmore, R., P. Walter, and G. Blobel. 1982. Protein translocation across the endoplasmic reticulum. II. Isolation and characterization of the signal recognition particle receptor. *J Cell Biol*. 95:470-477.

Glick, B.S. 2000. Organization of the Golgi apparatus. *Curr Opin Cell Biol*. 12:450-456.

Glickman, M.H., and A. Ciechanover. 2002. The ubiquitin-proteasome proteolytic pathway: destruction for the sake of construction. *Physiol Rev*. 82:373-428.

Goldberg, J. 1998. Structural basis for activation of ARF GTPase: mechanisms of guanine nucleotide exchange and GTP-myristoyl switching. *Cell*. 95:237-248.

Goldberg, J. 1999. Structural and functional analysis of the ARF1-ARFGAP complex reveals a role for coatomer in GTP hydrolysis. *Cell*. 96:893-902.

Gong, L., and E.T. Yeh. 1999. Identification of the activating and conjugating enzymes of the NEDD8 conjugation pathway. *J Biol Chem*. 274:12036-12042.

Goodwin, J.S., K.R. Drake, C. Rogers, L. Wright, J. Lippincott-Schwartz, M.R. Philips, and A.K. Kenworthy. 2005. Depalmitoylated Ras traffics to and from the Golgi complex via a nonvesicular pathway. *J Cell Biol*. 170:261-272.

Gorlich, D., S. Prehn, E. Hartmann, K.U. Kalies, and T.A. Rapoport. 1992. A mammalian homolog of SEC61p and SECYp is associated with ribosomes and nascent polypeptides during translocation. *Cell*. 71:489-503.

Greaves, J., O.A. Gorleku, C. Salaun, and L.H. Chamberlain. 2010. Palmitoylation of the SNAP25 protein family: specificity and regulation by DHHC palmitoyl transferases. *J Biol Chem*. 285:24629-24638.

Greaves, J., G.R. Prescott, Y. Fukata, M. Fukata, C. Salaun, and L.H. Chamberlain. 2009a. The hydrophobic cysteine-rich domain of SNAP25 couples with downstream residues to mediate membrane interactions and recognition by DHHC palmitoyl transferases. *Mol Biol Cell*. 20:1845-1854.

Greaves, J., G.R. Prescott, O.A. Gorleku, and L.H. Chamberlain. 2009b. The fat controller: roles of palmitoylation in intracellular protein trafficking and targeting to membrane microdomains (Review). *Mol Membr Biol*. 26:67-79.

Greaves, J., C. Salaun, Y. Fukata, M. Fukata, and L.H. Chamberlain. 2008. Palmitoylation and membrane interactions of the neuroprotective chaperone cysteine-string protein. *J Biol Chem*. 283:25014-25026.

Griffiths, G., R. Pepperkok, J.K. Locker, and T.E. Kreis. 1995. Immunocytochemical localization of beta-COP to the ER-Golgi boundary and the TGN. *J Cell Sci*. 108 (Pt 8):2839-2856.

Gu, Y., H. Misonou, T. Sato, N. Dohmae, K. Takio, and Y. Ihara. 2001. Distinct intramembrane cleavage of the beta-amyloid precursor protein family resembling gamma-secretase-like cleavage of Notch. *J Biol Chem*. 276:35235-35238.

Gut, A., F. Kappeler, N. Hyka, M.S. Balda, H.P. Hauri, and K. Matter. 1998. Carbohydrate-mediated Golgi to cell surface transport and apical targeting of membrane proteins. *Embo J*. 17:1919-1929.

Haas, A.L., J.V. Warms, A. Hershko, and I.A. Rose. 1982. Ubiquitin-activating enzyme. Mechanism and role in protein-ubiquitin conjugation. *J Biol Chem*. 257:2543-2548.

Haglund, K., and I. Dikic. 2005. Ubiquitylation and cell signaling. *Embo J*. 24:3353-3359.

Hammond, J.W., D. Cai, and K.J. Verhey. 2008. Tubulin modifications and their cellular functions. *Curr Opin Cell Biol*. 20:71-76.

Hancock, J.F. 2006. Lipid rafts: contentious only from simplistic standpoints. *Nat Rev Mol Cell Biol*. 7:456-462.

Hancock, J.F., H. Paterson, and C.J. Marshall. 1990. A polybasic domain or palmitoylation is required in addition to the CAAX motif to localize p21ras to the plasma membrane. *Cell*. 63:133-139.

Hanson, P.I., R. Roth, H. Morisaki, R. Jahn, and J.E. Heuser. 1997. Structure and conformational changes in NSF and its membrane receptor complexes visualized by quick-freeze/deep-etch electron microscopy. *Cell*. 90:523-535.

Harder, T., P. Scheiffele, P. Verkade, and K. Simons. 1998. Lipid domain structure of the plasma membrane revealed by patching of membrane components. *J Cell Biol*. 141:929-942.

Hayashi, T., G. Rumbaugh, and R.L. Huganir. 2005. Differential regulation of AMPA receptor subunit trafficking by palmitoylation of two distinct sites. *Neuron*. 47:709-723.

Hicke, L. 2001. A new ticket for entry into budding vesicles-ubiquitin. *Cell*. 106:527-530.

Hicke, L., and H. Riezman. 1996. Ubiquitination of a yeast plasma membrane receptor signals its ligand-stimulated endocytosis. *Cell*. 84:277-287.

Hochstrasser, M. 2006. Lingering mysteries of ubiquitin-chain assembly. *Cell*. 124:27-34.

Hochstrasser, M. 2009. Origin and function of ubiquitin-like proteins. *Nature*. 458:422-429.

Hogenboom, S., G.J. Romeijn, S.M. Houten, M. Baes, R.J. Wanders, and H.R. Waterham. 2002. Absence of functional peroxisomes does not lead to deficiency of enzymes involved in cholesterol biosynthesis. *J Lipid Res*. 43:90-98.

Hogenboom, S., G.J. Romeijn, S.M. Houten, M. Baes, R.J. Wanders, and H.R. Waterham. 2003. Peroxisome deficiency does not result in deficiency of enzymes involved in cholesterol biosynthesis. *Adv Exp Med Biol*. 544:329-330.

Hori, T., F. Osaka, T. Chiba, C. Miyamoto, K. Okabayashi, N. Shimbara, S. Kato, and K. Tanaka. 1999. Covalent modification of all members of human cullin family proteins by NEDD8. *Oncogene*. 18:6829-6834.

Huang, D.T., H.W. Hunt, M. Zhuang, M.D. Ohi, J.M. Holton, and B.A. Schulman. 2007. Basis for a ubiquitin-like protein thioester switch toggling E1-E2 affinity. *Nature*. 445:394-398.

Huang, D.T., D.W. Miller, R. Mathew, R. Cassell, J.M. Holton, M.F. Roussel, and B.A. Schulman. 2004a. A unique E1-E2 interaction required for optimal conjugation of the ubiquitin-like protein NEDD8. *Nat Struct Mol Biol*. 11:927-935.

Huang, K., S. Sanders, R. Singaraja, P. Orban, T. Cijsouw, P. Arstikaitis, A. Yanai, M.R. Hayden, and A. El-Husseini. 2009. Neuronal palmitoyl acyl transferases exhibit distinct substrate specificity. *Faseb J*. 23:2605-2615.

Huang, K., A. Yanai, R. Kang, P. Arstikaitis, R.R. Singaraja, M. Metzler, A. Mullard, B. Haigh, C. Gauthier-Campbell, C.A. Gutekunst, M.R. Hayden, and A. El-Husseini. 2004b. Huntingtin-interacting protein HIP14 is a palmitoyl transferase involved in palmitoylation and trafficking of multiple neuronal proteins. *Neuron*. 44:977-986.

Huttner, W.B., and J. Zimmerberg. 2001. Implications of lipid microdomains for membrane curvature, budding and fission. *Curr Opin Cell Biol*. 13:478-484.

Ikeda, K., Y. Nakayama, M. Ishii, Y. Obata, K. Kasahara, Y. Fukumoto, and N. Yamaguchi. 2009. Requirement of the SH4 and tyrosine-kinase domains but not the kinase activity of Lyn for its biosynthetic targeting to caveolin-positive Golgi membranes. *Biochim Biophys Acta*. 1790:1345-1352.

Ilangumaran, S., and D.C. Hoessli. 1998. Effects of cholesterol depletion by cyclodextrin on the sphingolipid microdomains of the plasma membrane. *Biochem J*. 335 (Pt 2):433-440.

Jacobson, K., O.G. Mouritsen, and R.G. Anderson. 2007. Lipid rafts: at a crossroad between cell biology and physics. *Nat Cell Biol*. 9:7-14.

Janke, C., K. Rogowski, D. Wloga, C. Regnard, A.V. Kajava, J.M. Strub, N. Temurak, J. van Dijk, D. Boucher, A. van Dorsselaer, S. Suryavanshi, J. Gaertig, and B. Edde. 2005. Tubulin polyglutamylase enzymes are members of the TTL domain protein family. *Science*. 308:1758-1762.

Jones, A.L., and D.W. Fawcett. 1966. Hypertrophy of the agranular endoplasmic reticulum in hamster liver induced by phenobarbital (with a review on the functions of this organelle in liver). *J Histochem Cytochem*. 14:215-232.

Jones, J., K. Wu, Y. Yang, C. Guerrero, N. Nillegoda, Z.Q. Pan, and L. Huang. 2008. A targeted proteomic analysis of the ubiquitin-like modifier nedd8 and associated proteins. *J Proteome Res*. 7:1274-1287.

Kaplan, K.B., J.R. Swedlow, H.E. Varmus, and D.O. Morgan. 1992. Association of p60c-src with endosomal membranes in mammalian fibroblasts. *J Cell Biol*. 118:321-333.

Kasahara, K., Y. Nakayama, K. Ikeda, Y. Fukushima, D. Matsuda, S. Horimoto, and N. Yamaguchi. 2004. Trafficking of Lyn through the Golgi caveolin involves the charged residues on alphaE and alphaI helices in the kinase domain. *J Cell Biol*. 165:641-652.

Keenan, R.J., D.M. Freymann, R.M. Stroud, and P. Walter. 2001. The signal recognition particle. *Annu Rev Biochem*. 70:755-775.

Kenworthy, A.K. 2008. Have we become overly reliant on lipid rafts? Talking Point on the involvement of lipid rafts in T-cell activation. *EMBO Rep*. 9:531-535.

Kerr, M.L., and D.H. Small. 2005. Cytoplasmic domain of the beta-amyloid protein precursor of Alzheimer's disease: function, regulation of proteolysis, and implications for drug development. *J Neurosci Res*. 80:151-159.

Kerscher, O., R. Felberbaum, and M. Hochstrasser. 2006. Modification of proteins by ubiquitin and ubiquitin-like proteins. *Annu Rev Cell Dev Biol*. 22:159-180.

Kirchhausen, T. 2000. Clathrin. *Annu Rev Biochem*. 69:699-727.

Klemm, R.W., C.S. Ejsing, M.A. Surma, H.J. Kaiser, M.J. Gerl, J.L. Sampaio, Q. de Robillard, C. Ferguson, T.J. Proszynski, A. Shevchenko, and K. Simons. 2009. Segregation of sphingolipids and sterols during formation of secretory vesicles at the trans-Golgi network. *J Cell Biol*. 185:601-612.

Koegl, M., P. Zlatkine, S.C. Ley, S.A. Courtneidge, and A.I. Magee. 1994. Palmitoylation of multiple Src-family kinases at a homologous N-terminal motif. *Biochem J*. 303 (Pt 3):749-753.

Kolling, R., and C.P. Hollenberg. 1994. The ABC-transporter Ste6 accumulates in the plasma membrane in a ubiquitinated form in endocytosis mutants. *Embo J*. 13:3261-3271.

Kumar, S., Y. Tomooka, and M. Noda. 1992. Identification of a set of genes with developmentally down-regulated expression in the mouse brain. *Biochem Biophys Res Commun*. 185:1155-1161.

Kusumi, A., I. Koyama-Honda, and K. Suzuki. 2004. Molecular dynamics and interactions for creation of stimulation-induced stabilized rafts from small unstable steady-state rafts. *Traffic*. 5:213-230.

Ladinsky, M.S., J.R. Kremer, P.S. Furcinitti, J.R. McIntosh, and K.E. Howell. 1994. HVEM tomography of the trans-Golgi network: structural insights and identification of a lace-like vesicle coat. *The Journal of cell biology*. 127:29-38.

Laifenfeld, D., L.J. Patzek, D.L. McPhie, Y. Chen, Y. Levites, A.M. Cataldo, and R.L. Neve. 2007. Rab5 mediates an amyloid precursor protein signaling pathway that leads to apoptosis. *J Neurosci*. 27:7141-7153.

Lammer, D., N. Mathias, J.M. Laplaza, W. Jiang, Y. Liu, J. Callis, M. Goebl, and M. Estelle. 1998. Modification of yeast Cdc53p by the ubiquitin-related protein rub1p affects function of the SCFCdc4 complex. *Genes Dev*. 12:914-926.

Le Borgne, R., and B. Hoflack. 1998a. Mechanisms of protein sorting and coat assembly: insights from the clathrin-coated vesicle pathway. *Curr Opin Cell Biol*. 10:499-503.

Le Borgne, R., and B. Hoflack. 1998b. Protein transport from the secretory to the endocytic pathway in mammalian cells. *Biochim Biophys Acta*. 1404:195-209.

Leck, Y.C., Y.Y. Choo, C.Y. Tan, P.G. Smith, and T. Hagen. 2010. Biochemical and cellular effects of inhibiting Nedd8 conjugation. *Biochem Biophys Res Commun*. 398:588-593.

Lee, M.C., E.A. Miller, J. Goldberg, L. Orci, and R. Schekman. 2004. Bi-directional protein transport between the ER and Golgi. *Annu Rev Cell Dev Biol*. 20:87-123.

Lee, M.R., D. Lee, S.K. Shin, Y.H. Kim, and C.Y. Choi. 2008. Inhibition of APP intracellular domain (AICD) transcriptional activity via covalent conjugation with Nedd8. *Biochem Biophys Res Commun*. 366:976-981.

Letourneur, F., E.C. Gaynor, S. Hennecke, C. Demolliere, R. Duden, S.D. Emr, H. Riezman, and P. Cosson. 1994. Coatomer is essential for retrieval of dilysine-tagged proteins to the endoplasmic reticulum. *Cell*. 79:1199-1207.

Levental, I., M. Grzybek, and K. Simons. 2010a. Greasing their way: lipid modifications determine protein association with membrane rafts. *Biochemistry*. 49:6305-6316.

Levental, I., D. Lingwood, M. Grzybek, U. Coskun, and K. Simons. 2010b. Palmitoylation regulates raft affinity for the majority of integral raft proteins. *Proceedings of the National Academy of Sciences of the United States of America*. 107:22050-22054.

Li, T., R. Santockyte, R.F. Shen, E. Tekle, G. Wang, D.C. Yang, and P.B. Chock. 2006. A general approach for investigating enzymatic pathways and substrates for ubiquitin-like modifiers. *Arch Biochem Biophys*. 453:70-74.

Liakopoulos, D., G. Doenges, K. Matuschewski, and S. Jentsch. 1998. A novel protein modification pathway related to the ubiquitin system. *Embo J*. 17:2208-2214.

Lin, D.T., Y. Makino, K. Sharma, T. Hayashi, R. Neve, K. Takamiya, and R.L. Huganir. 2009. Regulation of AMPA receptor extrasynaptic insertion by 4.1N, phosphorylation and palmitoylation. *Nat Neurosci*. 12:879-887.

Linder, M.E., and R.J. Deschenes. 2007. Palmitoylation: policing protein stability and traffic. *Nat Rev Mol Cell Biol*. 8:74-84.

Linder, M.E., P. Middleton, J.R. Hepler, R. Taussig, A.G. Gilman, and S.M. Mumby. 1993. Lipid modifications of G proteins: alpha subunits are palmitoylated. *Proc Natl Acad Sci U S A*. 90:3675-3679.

Lingwood, D., and K. Simons. 2007. Detergent resistance as a tool in membrane research. *Nat Protoc*. 2:2159-2165.

Lingwood, D., and K. Simons. 2010. Lipid rafts as a membrane-organizing principle. *Science*. 327:46-50.

Luini, A., A. Ragnini-Wilson, R.S. Polishchuck, and M.A. De Matteis. 2005. Large pleiomorphic traffic intermediates in the secretory pathway. *Curr Opin Cell Biol*. 17:353-361.

Ma, Y., and L.M. Hendershot. 2004. ER chaperone functions during normal and stress conditions. *J Chem Neuroanat*. 28:51-65.

Malsam, J., S. Kreye, and T.H. Sollner. 2008. Membrane fusion: SNAREs and regulation. *Cell Mol Life Sci*. 65:2814-2832.

Matsuoka, K., L. Orci, M. Amherdt, S.Y. Bednarek, S. Hamamoto, R. Schekman, and T. Yeung. 1998. COPII-coated vesicle formation reconstituted with purified coat proteins and chemically defined liposomes. *Cell*. 93:263-275.

Maxfield, F.R., and T.E. McGraw. 2004. Endocytic recycling. *Nat Rev Mol Cell Biol*. 5:121-132.

Maxfield, F.R., and I. Tabas. 2005. Role of cholesterol and lipid organization in disease. *Nature*. 438:612-621.

McCabe, J.B., and L.G. Berthiaume. 1999. Functional roles for fatty acylated amino-terminal domains in subcellular localization. *Mol Biol Cell*. 10:3771-3786.

McCabe, J.B., and L.G. Berthiaume. 2001. N-terminal protein acylation confers localization to cholesterol, sphingolipid-enriched membranes but not to lipid rafts/caveolae. *Mol Biol Cell*. 12:3601-3617.

McKean, P.G., P.W. Denny, E. Knuepfer, J.K. Keen, and D.F. Smith. 2001. Phenotypic changes associated with deletion and overexpression of a stage-regulated gene family in Leishmania. *Cell Microbiol*. 3:511-523.

McLaughlin, S., and A. Aderem. 1995. The myristoyl-electrostatic switch: a modulator of reversible protein-membrane interactions. *Trends Biochem Sci*. 20:272-276.

Melkonian, K.A., A.G. Ostermeyer, J.Z. Chen, M.G. Roth, and D.A. Brown. 1999. Role of lipid modifications in targeting proteins to detergent-resistant membrane rafts. Many raft proteins are acylated, while few are prenylated. *J Biol Chem*. 274:3910-3917.

Mellman, I., and K. Simons. 1992. The Golgi complex: in vitro veritas? *Cell*. 68:829-840.

Mellor, H., and P.J. Parker. 1998. The extended protein kinase C superfamily. *Biochem J*. 332 (Pt 2):281-292.

Mironov, A.A., G.V. Beznoussenko, R.S. Polishchuk, and A. Trucco. 2005. Intra-Golgi transport: a way to a new paradigm? *Biochim Biophys Acta*. 1744:340-350.

Mohn, H., V. Le Cabec, S. Fischer, and I. Maridonneau-Parini. 1995. The src-family protein-tyrosine kinase p59hck is located on the secretory granules in human neutrophils and translocates towards the phagosome during cell activation. *Biochem J*. 309 (Pt 2):657-665.

Mossessova, E., R.A. Corpina, and J. Goldberg. 2003. Crystal structure of ARF1*Sec7 complexed with Brefeldin A and its implications for the guanine nucleotide exchange mechanism. *Mol Cell*. 12:1403-1411.

Mousavi, S.A., L. Malerod, T. Berg, and R. Kjeken. 2004. Clathrin-dependent endocytosis. *Biochem J*. 377:1-16.

Mukhopadhyay, D., and H. Riezman. 2007. Proteasome-independent functions of ubiquitin in endocytosis and signaling. *Science*. 315:201-205.

Muller, U., and S. Kins. 2002. APP on the move. *Trends Mol Med*. 8:152-155.

Munro, S. 2003. Lipid rafts: elusive or illusive? *Cell*. 115:377-388.

Murray, D., L. Hermida-Matsumoto, C.A. Buser, J. Tsang, C.T. Sigal, N. Ben-Tal, B. Honig, M.D. Resh, and S. McLaughlin. 1998. Electrostatics and the membrane association of Src: theory and experiment. *Biochemistry*. 37:2145-2159.

Nadolski, M.J., and M.E. Linder. 2009. Molecular recognition of the palmitoylation substrate Vac8 by its palmitoyltransferase Pfa3. *J Biol Chem*. 284:17720-17730.

Nakashima, S. 2002. Protein kinase C alpha (PKC alpha): regulation and biological function. *J Biochem*. 132:669-675.

Nickel, W., B. Brugger, and F.T. Wieland. 2002. Vesicular transport: the core machinery of COPI recruitment and budding. *J Cell Sci*. 115:3235-3240.

Nishikawa, S., J.L. Brodsky, and K. Nakatsukasa. 2005. Roles of molecular chaperones in endoplasmic reticulum (ER) quality control and ER-associated degradation (ERAD). *J Biochem*. 137:551-555.

Norman, J.A., and R. Shiekhattar. 2006. Analysis of Nedd8-associated polypeptides: a model for deciphering the pathway for ubiquitin-like modifications. *Biochemistry*. 45:3014-3019.

Novick, P., and M. Zerial. 1997. The diversity of Rab proteins in vesicle transport. *Curr Opin Cell Biol*. 9:496-504.

Obata, Y., Y. Fukumoto, Y. Nakayama, T. Kuga, N. Dohmae, and N. Yamaguchi. 2010. The Lyn kinase C-lobe mediates Golgi export of Lyn through conformation-dependent ACSL3 association. *J Cell Sci*. 123:2649-2662.

Ohno, Y., A. Kihara, T. Sano, and Y. Igarashi. 2006. Intracellular localization and tissue-specific distribution of human and yeast DHHC cysteine-rich domain-containing proteins. *Biochim Biophys Acta*. 1761:474-483.

Ohtani, Y., T. Irie, K. Uekama, K. Fukunaga, and J. Pitha. 1989. Differential effects of alpha-, beta- and gamma-cyclodextrins on human erythrocytes. *Eur J Biochem*. 186:17-22.

Orci, L., M. Stamnes, M. Ravazzola, M. Amherdt, A. Perrelet, T.H. Sollner, and J.E. Rothman. 1997. Bidirectional transport by distinct populations of COPI-coated vesicles. *Cell*. 90:335-349.

Osaka, F., H. Kawasaki, N. Aida, M. Saeki, T. Chiba, S. Kawashima, K. Tanaka, and S. Kato. 1998. A new NEDD8-ligating system for cullin-4A. *Genes Dev*. 12:2263-2268.

Oved, S., Y. Mosesson, Y. Zwang, E. Santonico, K. Shtiegman, M.D. Marmor, B.S. Kochupurakkal, M. Katz, S. Lavi, G. Cesareni, and Y. Yarden. 2006. Conjugation to Nedd8 instigates ubiquitylation and down-regulation of activated receptor tyrosine kinases. *J Biol Chem*. 281:21640-21651.

Paladino, S., D. Sarnataro, R. Pillich, S. Tivodar, L. Nitsch, and C. Zurzolo. 2004. Protein oligomerization modulates raft partitioning and apical sorting of GPI-anchored proteins. *J Cell Biol*. 167:699-709.

Parenti, M., M.A. Vigano, C.M. Newman, G. Milligan, and A.I. Magee. 1993. A novel N-terminal motif for palmitoylation of G-protein alpha subunits. *Biochem J*. 291 (Pt 2):349-353.

Patterson, G.H., K. Hirschberg, R.S. Polishchuk, D. Gerlich, R.D. Phair, and J. Lippincott-Schwartz. 2008. Transport through the Golgi apparatus by rapid partitioning within a two-phase membrane system. *Cell*. 133:1055-1067.

Pavel, J., C. Harter, and F.T. Wieland. 1998. Reversible dissociation of coatomer: functional characterization of a beta/delta-coat protein subcomplex. *Proc Natl Acad Sci U S A*. 95:2140-2145.

Petroski, M.D., and R.J. Deshaies. 2005. Mechanism of lysine 48-linked ubiquitin-chain synthesis by the cullin-RING ubiquitin-ligase complex SCF-Cdc34. *Cell*. 123:1107-1120.

Peyroche, A., S. Paris, and C.L. Jackson. 1996. Nucleotide exchange on ARF mediated by yeast Gea1 protein. *Nature*. 384:479-481.

Pickart, C.M., and M.J. Eddins. 2004. Ubiquitin: structures, functions, mechanisms. *Biochim Biophys Acta*. 1695:55-72.

Pickart, C.M., and D. Fushman. 2004. Polyubiquitin chains: polymeric protein signals. *Curr Opin Chem Biol*. 8:610-616.

Pimenta, P.F., P. Pinto da Silva, D. Rangarajan, D.F. Smith, and D.L. Sacks. 1994. Leishmania major: association of the differentially expressed gene B protein and the surface lipophosphoglycan as revealed by membrane capping. *Exp Parasitol*. 79:468-479.

Pitha, J., T. Irie, P.B. Sklar, and J.S. Nye. 1988. Drug solubilizers to aid pharmacologists: amorphous cyclodextrin derivatives. *Life Sci*. 43:493-502.

Pizzo, P., E. Giurisato, M. Tassi, A. Benedetti, T. Pozzan, and A. Viola. 2002. Lipid rafts and T cell receptor signaling: a critical re-evaluation. *Eur J Immunol*. 32:3082-3091.

Pralle, A., P. Keller, E.L. Florin, K. Simons, and J.K. Horber. 2000. Sphingolipid-cholesterol rafts diffuse as small entities in the plasma membrane of mammalian cells. *J Cell Biol*. 148:997-1008.

Prior, I.A., C. Muncke, R.G. Parton, and J.F. Hancock. 2003. Direct visualization of Ras proteins in spatially distinct cell surface microdomains. *J Cell Biol*. 160:165-170.

Rabut, G., and M. Peter. 2008. Function and regulation of protein neddylation. 'Protein modifications: beyond the usual suspects' review series. *EMBO Rep*. 9:969-976.

Rapoport, T.A. 1992. Transport of proteins across the endoplasmic reticulum membrane. *Science*. 258:931-936.

Reed, N.A., D. Cai, T.L. Blasius, G.T. Jih, E. Meyhofer, J. Gaertig, and K.J. Verhey. 2006. Microtubule acetylation promotes kinesin-1 binding and transport. *Curr Biol*. 16:2166-2172.

Resh, M.D. 1993. Interaction of tyrosine kinase oncoproteins with cellular membranes. *Biochim Biophys Acta*. 1155:307-322.

Resh, M.D. 1994. Myristylation and palmitylation of Src family members: the fats of the matter. *Cell*. 76:411-413.

Resh, M.D. 1999. Fatty acylation of proteins: new insights into membrane targeting of myristoylated and palmitoylated proteins. *Biochim Biophys Acta*. 1451:1-16.

Resh, M.D. 2006. Use of analogs and inhibitors to study the functional significance of protein palmitoylation. *Methods*. 40:191-197.

Robineau, S., M. Chabre, and B. Antonny. 2000. Binding site of brefeldin A at the interface between the small G protein ADP-ribosylation factor 1 (ARF1) and the nucleotide-exchange factor Sec7 domain. *Proc Natl Acad Sci U S A*. 97:9913-9918.

Rocks, O., M. Gerauer, N. Vartak, S. Koch, Z.P. Huang, M. Pechlivanis, J. Kuhlmann, L. Brunsveld, A. Chandra, B. Ellinger, H. Waldmann, and P.I. Bastiaens. 2010. The palmitoylation machinery is a spatially organizing system for peripheral membrane proteins. *Cell*. 141:458-471.

Rocks, O., A. Peyker, M. Kahms, P.J. Verveer, C. Koerner, M. Lumbierres, J. Kuhlmann, H. Waldmann, A. Wittinghofer, and P.I. Bastiaens. 2005. An acylation cycle regulates localization and activity of palmitoylated Ras isoforms. *Science*. 307:1746-1752.

Roth, A.F., J. Wan, A.O. Bailey, B. Sun, J.A. Kuchar, W.N. Green, B.S. Phinney, J.R. Yates, 3rd, and N.G. Davis. 2006. Global analysis of protein palmitoylation in yeast. *Cell*. 125:1003-1013.

Rothman, J.E. 1996. The protein machinery of vesicle budding and fusion. *Protein Sci*. 5:185-194.

Rothman, J.E., and L. Orci. 1992. Molecular dissection of the secretory pathway. *Nature*. 355:409-415.

Rothman, J.E., and G. Warren. 1994. Implications of the SNARE hypothesis for intracellular membrane topology and dynamics. *Curr Biol*. 4:220-233.

Rothwell, C., A. Lebreton, C. Young Ng, J.Y. Lim, W. Liu, S. Vasudevan, M. Labow, F. Gu, and L.A. Gaither. 2009. Cholesterol biosynthesis modulation regulates dengue viral replication. *Virology*. 389:8-19.

Roy, S., S. Plowman, B. Rotblat, I.A. Prior, C. Muncke, S. Grainger, R.G. Parton, Y.I. Henis, Y. Kloog, and J.F. Hancock. 2005. Individual palmitoyl residues serve distinct roles in H-ras trafficking, microlocalization, and signaling. *Mol Cell Biol*. 25:6722-6733.

Salaun, C., J. Greaves, and L.H. Chamberlain. 2010. The intracellular dynamic of protein palmitoylation. *J Cell Biol*. 191:1229-1238.

Salon, C., E. Brambilla, C. Brambilla, S. Lantuejoul, S. Gazzeri, and B. Eymin. 2007. Altered pattern of Cul-1 protein expression and neddylation in human lung tumours: relationships with CAND1 and cyclin E protein levels. *J Pathol*. 213:303-310.

Sandilands, E., V.G. Brunton, and M.C. Frame. 2007. The membrane targeting and spatial activation of Src, Yes and Fyn is influenced by palmitoylation and distinct RhoB/RhoD endosome requirements. *J Cell Sci*. 120:2555-2564.

Sandilands, E., C. Cans, V.J. Fincham, V.G. Brunton, H. Mellor, G.C. Prendergast, J.C. Norman, G. Superti-Furga, and M.C. Frame. 2004. RhoB and actin polymerization coordinate Src activation with endosome-mediated delivery to the membrane. *Dev Cell*. 7:855-869.

Sandilands, E., and M.C. Frame. 2008. Endosomal trafficking of Src tyrosine kinase. *Trends Cell Biol*. 18:322-329.

Sato, I., Y. Obata, K. Kasahara, Y. Nakayama, Y. Fukumoto, T. Yamasaki, K.K. Yokoyama, T. Saito, and N. Yamaguchi. 2009. Differential trafficking of Src, Lyn, Yes and Fyn is specified by the state of palmitoylation in the SH4 domain. *J Cell Sci*. 122:965-975.

Scheiffele, P., J. Peranen, and K. Simons. 1995. N-glycans as apical sorting signals in epithelial cells. *Nature*. 378:96-98.

Schekman, R., and L. Orci. 1996. Coat proteins and vesicle budding. *Science*. 271:1526-1533.

Schimmoller, F., I. Simon, and S.R. Pfeffer. 1998a. Rab GTPases, directors of vesicle docking. *J Biol Chem*. 273:22161-22164.

Schimmoller, F., I. Simon, and S.R. Pfeffer. 1998b. Rab GTPases, directors of vesicle docking. *J Biol Chem*. 273:22161-22164.

Schmid, S.L. 1997. Clathrin-coated vesicle formation and protein sorting: an integrated process. *Annu Rev Biochem*. 66:511-548.

Schuck, S., and K. Simons. 2004. Polarized sorting in epithelial cells: raft clustering and the biogenesis of the apical membrane. *J Cell Sci*. 117:5955-5964.

Schwechheimer, C. 2004. The COP9 signalosome (CSN): an evolutionary conserved proteolysis regulator in eukaryotic development. *Biochim Biophys Acta*. 1695:45-54.

Seol, J.H., R.M. Feldman, W. Zachariae, A. Shevchenko, C.C. Correll, S. Lyapina, Y. Chi, M. Galova, J. Claypool, S. Sandmeyer, K. Nasmyth, and R.J. Deshaies. 1999. Cdc53/cullin and the essential Hrt1 RING-H2 subunit of SCF define a ubiquitin ligase module that activates the E2 enzyme Cdc34. *Genes Dev*. 13:1614-1626.

Shahinian, S., and J.R. Silvius. 1995. Doubly-lipid-modified protein sequence motifs exhibit long-lived anchorage to lipid bilayer membranes. *Biochemistry*. 34:3813-3822.

Shaw, A.S. 2006. Lipid rafts: now you see them, now you don't. *Nat Immunol*. 7:1139-1142.

Shenoy-Scaria, A.M., D.J. Dietzen, J. Kwong, D.C. Link, and D.M. Lublin. 1994. Cysteine3 of Src family protein tyrosine kinase determines palmitoylation and localization in caveolae. *J Cell Biol*. 126:353-363.

Shmueli, A., M. Segal, T. Sapir, R. Tsutsumi, J. Noritake, A. Bar, S. Sapoznik, Y. Fukata, I. Orr, M. Fukata, and O. Reiner. 2010. Ndel1 palmitoylation: a new mean to regulate cytoplasmic dynein activity. *Embo J*. 29:107-119.

Silverman, L., and M.D. Resh. 1992. Lysine residues form an integral component of a novel NH2-terminal membrane targeting motif for myristylated pp60v-src. *The Journal of cell biology*. 119:415-425.

Silverman, L., M. Sudol, and M.D. Resh. 1993. Members of the src family of nonreceptor tyrosine kinases share a common mechanism for membrane binding. *Cell Growth Differ*. 4:475-482.

Simon, J.P., I.E. Ivanov, B. Shopsin, D. Hersh, M. Adesnik, and D.D. Sabatini. 1996. The in vitro generation of post-Golgi vesicles carrying viral envelope glycoproteins requires an ARF-like GTP-binding protein and a protein kinase C associated with the Golgi apparatus. *J Biol Chem*. 271:16952-16961.

Simons, K., and M.J. Gerl. 2010. Revitalizing membrane rafts: new tools and insights. *Nat Rev Mol Cell Biol*. 11:688-699.

Simons, K., and E. Ikonen. 1997. Functional rafts in cell membranes. *Nature*. 387:569-572.

Simons, K., and D. Toomre. 2000. Lipid rafts and signal transduction. *Nat Rev Mol Cell Biol*. 1:31-39.

Simons, K., and G. van Meer. 1988. Lipid sorting in epithelial cells. *Biochemistry*. 27:6197-6202.

Simons, K., and W.L. Vaz. 2004. Model systems, lipid rafts, and cell membranes. *Annu Rev Biophys Biomol Struct*. 33:269-295.

Smotrys, J.E., and M.E. Linder. 2004. Palmitoylation of intracellular signaling proteins: regulation and function. *Annu Rev Biochem*. 73:559-587.

Sollner, T., M.K. Bennett, S.W. Whiteheart, R.H. Scheller, and J.E. Rothman. 1993. A protein assembly-disassembly pathway in vitro that may correspond to sequential steps of synaptic vesicle docking, activation, and fusion. *Cell*. 75:409-418.

Sollner, T.H., and J.E. Rothman. 1996. Molecular machinery mediating vesicle budding, docking and fusion. *Experientia*. 52:1021-1025.

Somsel Rodman, J., and A. Wandinger-Ness. 2000. Rab GTPases coordinate endocytosis. *J Cell Sci*. 113 Pt 2:183-192.

Sonnichsen, B., S. De Renzis, E. Nielsen, J. Rietdorf, and M. Zerial. 2000. Distinct membrane domains on endosomes in the recycling pathway visualized by multicolor imaging of Rab4, Rab5, and Rab11. *J Cell Biol*. 149:901-914.

Sonnichsen, B., R. Watson, H. Clausen, T. Misteli, and G. Warren. 1996. Sorting by COP I-coated vesicles under interphase and mitotic conditions. *J Cell Biol*. 134:1411-1425.

Soucy, T.A., P.G. Smith, M.A. Milhollen, A.J. Berger, J.M. Gavin, S. Adhikari, J.E. Brownell, K.E. Burke, D.P. Cardin, S. Critchley, C.A. Cullis, A. Doucette, J.J. Garnsey, J.L. Gaulin, R.E. Gershman, A.R. Lublinsky, A. McDonald, H. Mizutani, U. Narayanan, E.J. Olhava, S. Peluso, M. Rezaei, M.D. Sintchak, T. Talreja, M.P. Thomas, T. Traore, S. Vyskocil, G.S. Weatherhead, J. Yu, J. Zhang, L.R. Dick, C.F. Claiborne, M. Rolfe, J.B. Bolen, and S.P. Langston. 2009. An inhibitor of NEDD8-activating enzyme as a new approach to treat cancer. *Nature*. 458:732-736.

Spodsberg, N., M. Alfalah, and H.Y. Naim. 2001. Characteristics and structural requirements of apical sorting of the rat growth hormone through the O-glycosylated stalk region of intestinal sucrase-isomaltase. *J Biol Chem*. 276:46597-46604.

Stegmayer, C., A. Kehlenbach, S. Tournaviti, S. Wegehingel, C. Zehe, P. Denny, D.F. Smith, B. Schwappach, and W. Nickel. 2005. Direct transport across the plasma membrane of mammalian cells of Leishmania HASPB as revealed by a CHO export mutant. *J Cell Sci*. 118:517-527.

Tanigawa, G., L. Orci, M. Amherdt, M. Ravazzola, J.B. Helms, and J.E. Rothman. 1993. Hydrolysis of bound GTP by ARF protein triggers uncoating of Golgi-derived COP-coated vesicles. *J Cell Biol*. 123:1365-1371.

Terrell, J., S. Shih, R. Dunn, and L. Hicke. 1998. A function for monoubiquitination in the internalization of a G protein-coupled receptor. *Mol Cell*. 1:193-202.

Thomas, S.M., and J.S. Brugge. 1997. Cellular functions regulated by Src family kinases. *Annu Rev Cell Dev Biol*. 13:513-609.

Toth, M.J., and L. Huwyler. 1996. Molecular cloning and expression of the cDNAs encoding human and yeast mevalonate pyrophosphate decarboxylase. *J Biol Chem*. 271:7895-7898.

Tournaviti, S., S. Hannemann, S. Terjung, T.M. Kitzing, C. Stegmayer, J. Ritzerfeld, P. Walther, R. Grosse, W. Nickel, and O.T. Fackler. 2007. SH4-domain-induced plasma membrane dynamization promotes bleb-associated cell motility. *J Cell Sci*. 120:3820-3829.

Tournaviti, S., E.S. Pietro, S. Terjung, T. Schafmeier, S. Wegehingel, J. Ritzerfeld, J. Schulz, D.F. Smith, R. Pepperkok, and W. Nickel. 2009. Reversible phosphorylation as a molecular switch to regulate plasma membrane targeting of acylated SH4 domain proteins. *Traffic*. 10:1047-1060.

Tsukita, S., K. Oishi, T. Akiyama, Y. Yamanashi, and T. Yamamoto. 1991. Specific proto-oncogenic tyrosine kinases of src family are enriched in cell-to-cell adherens junctions where the level of tyrosine phosphorylation is elevated. *J Cell Biol*. 113:867-879.

Tsutsumi, R., Y. Fukata, J. Noritake, T. Iwanaga, F. Perez, and M. Fukata. 2009. Identification of G protein alpha subunit-palmitoylating enzyme. *Mol Cell Biol*. 29:435-447.

Vaisanen, T., M.R. Vaisanen, and T. Pihlajaniemi. 2006. Modulation of the cellular cholesterol level affects shedding of the type XIII collagen ectodomain. *J Biol Chem*. 281:33352-33362.

Valdez-Taubas, J., and H. Pelham. 2005. Swf1-dependent palmitoylation of the SNARE Tlg1 prevents its ubiquitination and degradation. *Embo J*. 24:2524-2532.

van Dijk, J., K. Rogowski, J. Miro, B. Lacroix, B. Edde, and C. Janke. 2007. A targeted multienzyme mechanism for selective microtubule polyglutamylation. *Mol Cell*. 26:437-448.

van Zanten, T.S., A. Cambi, M. Koopman, B. Joosten, C.G. Figdor, and M.F. Garcia-Parajo. 2009. Hotspots of GPI-anchored proteins and integrin nanoclusters function as nucleation sites for cell adhesion. *Proc Natl Acad Sci U S A*. 106:18557-18562.

van't Hof, W., and M.D. Resh. 1997. Rapid plasma membrane anchoring of newly synthesized p59fyn: selective requirement for NH2-terminal myristoylation and palmitoylation at cysteine-3. *J Cell Biol*. 136:1023-1035.

Wada, H., E.T. Yeh, and T. Kamitani. 2000. A dominant-negative UBC12 mutant sequesters NEDD8 and inhibits NEDD8 conjugation in vivo. *J Biol Chem*. 275:17008-17015.

Walden, H., M.S. Podgorski, D.T. Huang, D.W. Miller, R.J. Howard, D.L. Minor, Jr., J.M. Holton, and B.A. Schulman. 2003. The structure of the APPBP1-UBA3-NEDD8-ATP complex reveals the basis for selective ubiquitin-like protein activation by an E1. *Mol Cell*. 12:1427-1437.

Walker, F., J. deBlaquiere, and A.W. Burgess. 1993. Translocation of pp60c-src from the plasma membrane to the cytosol after stimulation by platelet-derived growth factor. *J Biol Chem*. 268:19552-19558.

Walter, P., R. Gilmore, and G. Blobel. 1984. Protein translocation across the endoplasmic reticulum. *Cell*. 38:5-8.

Warren, G., and V. Malhotra. 1998. The organisation of the Golgi apparatus. *Curr Opin Cell Biol*. 10:493-498.

Webb, Y., L. Hermida-Matsumoto, and M.D. Resh. 2000. Inhibition of protein palmitoylation, raft localization, and T cell signaling by 2-bromopalmitate and polyunsaturated fatty acids. *J Biol Chem*. 275:261-270.

Wei, J., and L.M. Hendershot. 1996. Protein folding and assembly in the endoplasmic reticulum. *Exs*. 77:41-55.

Wei, N., and X.W. Deng. 2003. The COP9 signalosome. *Annu Rev Cell Dev Biol*. 19:261-286.

Weissman, A.M. 2001. Themes and variations on ubiquitylation. *Nat Rev Mol Cell Biol*. 2:169-178.

Whyte, J.R., and S. Munro. 2002. Vesicle tethering complexes in membrane traffic. *J Cell Sci*. 115:2627-2637.

Wolven, A., H. Okamura, Y. Rosenblatt, and M.D. Resh. 1997. Palmitoylation of p59fyn is reversible and sufficient for plasma membrane association. *Mol Biol Cell*. 8:1159-1173.

Xirodimas, D.P., A. Sundqvist, A. Nakamura, L. Shen, C. Botting, and R.T. Hay. 2008. Ribosomal proteins are targets for the NEDD8 pathway. *EMBO Rep*. 9:280-286.

Yeaman, C., A.H. Le Gall, A.N. Baldwin, L. Monlauzeur, A. Le Bivic, and E. Rodriguez-Boulan. 1997. The O-glycosylated stalk domain is required for apical sorting of neurotrophin receptors in polarized MDCK cells. *J Cell Biol*. 139:929-940.

Yeh, D.C., J.A. Duncan, S. Yamashita, and T. Michel. 1999. Depalmitoylation of endothelial nitric-oxide synthase by acyl-protein thioesterase 1 is potentiated by Ca(2+)-calmodulin. *J Biol Chem*. 274:33148-33154.

Young, P., Q. Deveraux, R.E. Beal, C.M. Pickart, and M. Rechsteiner. 1998. Characterization of two polyubiquitin binding sites in the 26 S protease subunit 5a. *J Biol Chem*. 273:5461-5467.

Zerial, M., and H. McBride. 2001a. Rab proteins as membrane organizers. *Nat Rev Mol Cell Biol*. 2:107-117.

Zerial, M., and H. McBride. 2001b. Rab proteins as membrane organizers. *Nat Rev Mol Cell Biol*. 2:107-117.

Zhao, C., J.T. Slevin, and S.W. Whiteheart. 2007. Cellular functions of NSF: not just SNAPs and SNAREs. *FEBS Lett*. 581:2140-2149.

Zhao, L., J.B. Helms, J. Brunner, and F.T. Wieland. 1999. GTP-dependent binding of ADP-ribosylation factor to coatomer in close proximity to the binding site for dilysine retrieval motifs and p23. *J Biol Chem*. 274:14198-14203.

Zheng, N., B.A. Schulman, L. Song, J.J. Miller, P.D. Jeffrey, P. Wang, C. Chu, D.M. Koepp, S.J. Elledge, M. Pagano, R.C. Conaway, J.W. Conaway, J.W. Harper, and N.P. Pavletich. 2002. Structure of the Cul1-Rbx1-Skp1-F boxSkp2 SCF ubiquitin ligase complex. *Nature*. 416:703-709.

Zidovetzki, R., and I. Levitan. 2007. Use of cyclodextrins to manipulate plasma membrane cholesterol content: evidence, misconceptions and control strategies. *Biochim Biophys Acta*. 1768:1311-1324.

Acknowledgements

I am heartily thankful to Prof. Dr. Walter Nickel, who gave me the chance to study on such an interesting project in his lab, whose encouragement, guidance and support from the initial to the final level enabled me to develop a deep understanding of the subject.

I gratefully thank Prof. Dr. Thomas Söllner for being in my TAC committee giving me a lot of ideas along my Ph.D study and now being the second reviewer for my thesis.

I would like to thank all the members of the Nickel lab for a pleasant atmosphere: Dr. Hans Michael Müller, Giuseppe La Venuta, Helena Andreas, Sonja Zacherl, Mareike Laußmann, Julia Steringer, Georg Weidmann, Paulina Turcza and Sabine Wegehingel.

I thank very much Sabine Wegehingel, for your support not only on experiments but also for listening and encouraging me through the writing.

I am grateful to Sonja Zacherl, Paulina Turcza, Mareike Laußmann and Julia Steringer and Georg Weidmann. Thank you for holding me and cheering me up. Paulina, it is so much fun simply being childish together. Sonja, thank you for just being my friend, being there for me whenever I need you.

This thesis would not have been possible without Dr. Julia Ritzerfeld, my supervisor. Thank you for your brilliant ideas and knowledge. Many thanks for your encouragements, patience and helping me through my scientific life. Thank you for the critical discussions and reading my thesis.

I owe my deepest gratitude to my parents Zhang Jinying, Wang Peixin and my godparents Peter Luft, Erika Keidel. You are the reasons for everything. 我最亲爱的爸爸妈妈， 感谢生我，养我，教育我。感谢你们的爱。没有你们，不会有今天的我。